Chem Soc Rev

Azaphosphinines and their derivatives

Journal:	*Chemical Society Reviews*
Manuscript ID	CS-REV-09-2023-000737.R1
Article Type:	Review Article
Date Submitted by the Author:	05-Nov-2023
Complete List of Authors:	McNeill, J; University of Oregon, Department of Chemistry Bard, Jeremy; University of Oregon, Department of Chemistry and Biochemistry Johnson, Darren; University of Oregon, Department of Chemistry and Biochemistry Haley, Michael; University of Oregon, Department of Chemistry

Azaphosphinines and their derivatives

J. Nolan McNeill,[a] Jeremy P. Bard,[b]* Darren W. Johnson[a]* and Michael M. Haley[a]*

[a]*Department of Chemistry & Biochemistry and the Materials Science Institute, University of Oregon, Eugene, OR 97403-1253, USA. E-mail: haley@uoregon.edu, dwj@uoregon.edu*

[b]*Department of Chemistry, Washington College, Chestertown, MD 21620-1438, USA. E-mail: jbard2@washcoll.edu*

Abstract

Six-membered heterocycles containing one phosphorus and one nitrogen atom, known as azaphosphinines, have existed in the shadows of their single heteroatom-containing analogues for almost 150 years. Despite this, recent chemistry has seen a rapid increase in publications concerning this uncommon scaffold. Azaphosphinines exist in one of six isomers—there are three possible orientations of the pnictogen atoms and in each of these, the phosphorus is in one of two valences (P^{III} vs. P^{V}). This review aims to outline and inform on the synthesis and applications of all six isomers. P^{V}-oxo azaphosphinines are of particular interest to this review as many of the discussed heterocycles either form as the pentavalent species directly or oxidize to this over time. In very recent years the published applications of azaphosphinines have blossomed into subjects spanning several fields of chemistry such as asymmetric catalysis, supramolecular association, cellular imaging, and medicinal chemistry.

Introduction

Historically, heterocycle chemistry is inseparable from organic chemistry. The first isolated heterocyclic species, alloxan, discovered by Gaspare Brugnatelli in 1818,[1] predates the Kekulé model of benzene by roughly 50 years. These humble beginnings of a small nitrogenous poison isolated from uric acid kicked off an intense interest that has yet to subside. In the last 200 years, heterocycles have spread and flourished into every facet of chemistry—organic, medicinal, metal coordination, and otherwise. Much of the heavy lifting done in the field of heterocycles is done by pnictogen-based species. Simple five- and six-membered nitrogen-containing ring systems such as pyrrole, piperidine, and pyridine commonly act as solvents and/or bases in synthetic processes as well as fundamental building blocks to all manner of pharmaceuticals, dyes, ligands, and pesticides.[2–12] In comparison to their 2nd row counterparts, phosphorus heterocycles are considerably less common in the literature. However, this is not to say that these molecules do not find important uses in the modern world. A few specific examples include the use of phospholes in optoelectronic applications and phosphinines in catalysis and photophysical applications.[13–21] Nitrogen and phosphorus together serve as an interesting pair in heterocycles as well. In particular, the nature of the P^{V}=N bond has been a hotly researched phenomenon.

This review will reference phosphorus-specific nomenclature extensively. Many of the functional groups have alternative common names that have risen and fallen out of popularity in the last few decades or even centuries. For the sake of consistency, the nomenclature applied in the review will adhere to the following guide (Fig. 1). This

is not an exhaustive list of phosphorus nomenclature but rather establishes the naming for the functional groups referred to frequently in this review. More elaborate descriptions of azaphosphinine nomenclature are found below (Figs. 3 and 4). It should be noted that the term phosphine is generally used interchangeably with phosphane in the current literature; however, over a decade ago IUPAC decided that phosphane is the preferential term for the PR_3 functional group. For the sake of standardizing phosphorus nomenclature in this review, phosphane naming is used exclusively. This also extends to the pentavalent $P(O)R_3$, dubbed phosphane oxides.

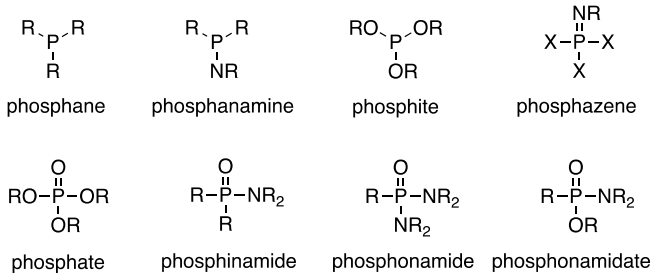

Fig 1. Phosphorus nomenclature commonly referred to in this article.

An intriguing example of what makes the P^V=N bond so unique are cyclophosphazenes.[22–24] They are cyclic species with the chemical formula $(X_2PN)_n$ (Fig. 2, top), that at first glance, present the qualities one would expect in an aromatic ring. Prepared by Liebig et al. in 1834, hexachlorophosphazene is one of the best examples, with the ring being totally planar, containing 6π electrons, and all ring bond-lengths being uniform.[25] For many years following its discovery, it was assumed that these qualities resulted from true delocalization of π-electrons from the nitrogen atoms into the participating 3d orbitals of the adjacent phosphorus atoms. However, it has become well understood in recent decades that a pentavalent phosphorus species has little-to-no participation of the 3d orbitals in its bonding. Instead, the nature of the P^V=N bond can be better described as highly polarized, bordering on ionic. The electronegativity difference in nitrogen and phosphorus atoms results in a transfer of the π electron to the nitrogen atom which can then participate in negative hyperconjugation. Popularized by Schleyer and Kos in 1983, negative hyperconjugation is the donation of π orbitals into adjacent σ* orbitals. This ultimately results in a stabilizing effect for the π-bond and a weakening of the σ-bond.[26] In the context of cyclophosphazenes, the lone pair orbitals of the nitrogen donate back into the $\sigma^*_{P–N}$ and $\sigma^*_{P–X}$. In total, this ionic character of each P^V=N bond and the consistent negative hyperconjugation from each nitrogen into each adjacent σ* creates a facsimile of aromaticity despite there being no delocalization through the phosphorus center (Fig 2, top). However, the heterocycles discussed in this review are not the inorganic cyclophosphazenes but are rather azaphosphinines containing just one nitrogen and phosphorus atom each. This difference adds two levels of complexity that must be addressed. While it would be appropriate to translate the cyclophosphazene example to 1,2λ^5-azaphosphinines with a P^V=N bond, we must also consider the other isomers.

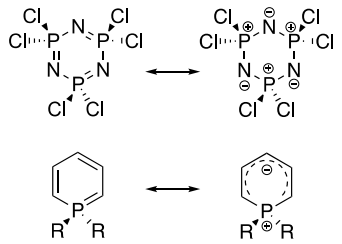

Fig. 2 Examples of (top) ionic nature in hexachlorophosphazene and (bottom) ylidic nature in P^V phosphinine.

It is commonly recognized that P^{III} phosphinines are aromatic heterocycles in the same vein as pyridine. However, P^V phosphinines are just as commonly understood to be nonaromatic. Several publications[27–29] have addressed the cyclic-phosphonium ylide nature of P^V phosphinines (Fig. 2, bottom), describing the partial negative charge buildup on the 2-, 4-, and 6-carbons with corresponding positive charge on the phosphorus. The result is a nonaromatic system that does not delocalize through the phosphorus like cyclophosphazenes. This situation would apply directly to the 1,4λ^5-azaphosphinines discussed in this review as there is no direct bond between the phosphorus and nitrogen in these cases, yet the electronegative nitrogen atom would be even more accepting of the negative character of the ylide. In this case it would be appropriate to conclude that the isolated 1,4λ^5-azaphosphinine ring could not be aromatic.

The last consideration to address is the phosphonyl (P^V=O) bond found in many of the heterocycles discussed in this review. Like the P^V=N bond, the phosphonyl bond is known to be extremely polarized[30] and exhibits negative hyperconjugation from the oxygen lone pairs back into the adjacent σ* of the other phosphorus bonds. While there are no thorough computational investigations into the electronics of azaphosphinines with exocyclic P^V=O bonds, we can imagine the resultant heterocycle shares the combined properties of phosphinines and phosphane oxides in which all the bonds to the phosphorus exhibit a high degree of ionic character while simultaneously being stabilized by negative hyperconjugation from not only the oxygen but also the nitrogen atom. The conclusion of these considerations being that ultimately no P^V azaphosphinine ring of any form could truly be considered aromatic because of the consistent lack of π-delocalization through the phosphorus atom. Despite this, many of the species discussed in this review have aromatic rings fused to the azaphosphinine rings, which result in an overall aromatic structure.

Azaphosphinines have a history that spans back 135 years, yet for much of their existence they have remained little more than a synthetic curiosity (e.g., Scheme 1).[31] Early work on these molecules was generally fueled by a desire to explore the definition of aromaticity and its existence in unusual heteroaromatic environments. However, the initial synthetic pathways that were developed by the likes of Campbell, Dewar, Märkl, and more provided the necessary groundwork for translating azaphosphinines into modern heterocyclic chemistry.[32–36] Since the start of the 21st century, azaphosphinines have begun to find increasingly diverse uses in the fields of asymmetric catalysis, supramolecular association, cellular imaging, and even medicinal chemistry.[37–39]

The primary goal of this review is to shed light on where the science of azaphosphinines originated, illustrate both older fundamental studies and numerous recent advances, and offer insights of what is yet to come. Most of the research done on this class of molecules comes from the last 25-30 years. The compounds surveyed in this review will contain at least one six-membered ring with no more than one endocyclic phosphorus and nitrogen atom. Only compounds with high degrees of unsaturation in the PN ring will be considered. Heterocycles with partial saturation will be included as necessary to give useful counterpoints and context when discussing reactivities or properties of the heterocycles such as aromaticity. Despite the propensity for P^V-azaphosphinines to be *P*-stereogenic, stereochemistry will typically only be shown for chiral centers (i.e., non-identical P-substituents) generated by asymmetric reactions where the enantiomeric or diastereomeric excess can be determined.

A secondary goal of this review is to provide a standardized nomenclature for azaphosphinines. While several names have been used to describe the same general system, it is the opinion of the authors that the terminology of azaphosphinine should be used to describe any six-membered ring containing one phosphorus and one nitrogen atom. This can be further divided into the isomers of 1,2-, 1,3-, and 1,4-azaphosphinine **1a-c** (Fig. 3, top), where the "1-" is in reference to the position of the nitrogen atom and the second number refers to the position of the phosphorus atom. The commonly observed *benzo* fusion aptly results in the name benzo[*x*]azaphosphinines **2a-b** (Fig. 3, bottom). The bracketed letter refers to the bond (Fig. 3, top) on which ring fusion occurs, with the N–X bond being "a", where x is either the phosphorus atom or the closest carbon to it. In the case of naming fused ring systems, Hantzch-Widman nomenclature rules should be used.[40] Further π-extension via ring fusion will continue appropriately. The phosphorus atom in every compound discussed will exist in one of two valences, either P^{III} or P^V. This is denoted by the superscript number on the λ inserted into the chemical name. Examples of this nomenclature system are given below (Fig. 4) for compounds **3** and **4**. As apparent, while these naming conventions are accurate, they rapidly become encumbered with substituents and substitution patterns. As such, when referring to libraries of synthesized azaphosphinines, the authors of this review will typically refer to them as azaphosphinines or benzo[*x*]azaphosphinines with key substituents as appropriate.

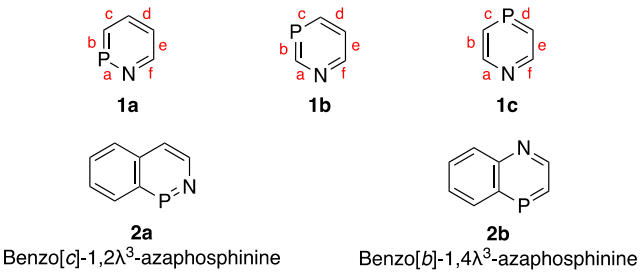

Fig. 3 Examples of (top) 1,2- (**1a**), 1,3- (**1b**) and 1,4-azaphosphinines (**1c**) and (bottom) benzo[*c*]- (**2a**) and benzo[*b*]azaphosphinine (**2b**) isomers.

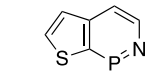

3
thieno[2,3-*c*]-1,2λ^3-azaphosphinine

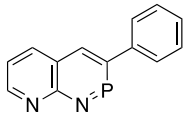

4
pyrido[2,3-*e*]-3-phenyl-1,2λ^3-azaphosphinine

Fig. 4 Examples of nomenclature rules applied to more complex azaphosphinine derivatives such as **3** and **4**.

This review is divided primarily into three sections concerned with the three isomeric forms of azaphosphinine. The 1,2-isomer is by far the most studied of the three, likely because of the wealth of reactions that have been developed to afford this scaffold. The inherent difference in electronegativities between the phosphorus and nitrogen atoms increases their electrophilicity and nucleophilicity, respectively. This increased reactivity aids reactions such as heteroannulation and C–H activation. These factors could help explain why there are several more publications for the 1,4-isomer than 1,3-isomers, with the latter being quite rare in the current literature. For the purposes of organization, each isomer's section will be divided into subcategories to distinguish between the different methods of synthesis applied to form the azaphosphinine ring.

Azaphosphinine origins

The first published example of a six-membered PN-heterocycle dates to 1888 with the work of Schenk and Michaelis on what are commonly referred to as dihydrophenophosphazines (Scheme 1).[31] This heterocyclic scaffold could also be classified as dibenzo[*b,e*]-1,4-dihydro-1,4λ^5-azaphosphinine under the naming scheme used in this review. The synthesis proceeds through an addition of PCl_3 to diphenylamine at elevated temperatures. This reaction yields the *P*-chloro species **5**, which can be subsequently hydrolyzed/oxidized into the corresponding 1,4λ^5-azaphosphinine 4-oxide **6**. Due to technological constraints, the structure of **6** was not definitively confirmed until nearly a century later thanks to the work of Häring.[41] The dihydrophenophosphazine scaffold stands somewhat alone among azaphosphinine derivatives, as the 1970s and 1980s saw three excellent review articles detailing the chemistry of these species, which we encourage those with further interest to read.[42–44] Since then, the literature has been extremely sparse on publications concerning these chemicals.[45,46] Due to the wealth of previously compiled research and a dearth of recent studies, dihydrophenphosphazines will be excluded from the remainder of this review.

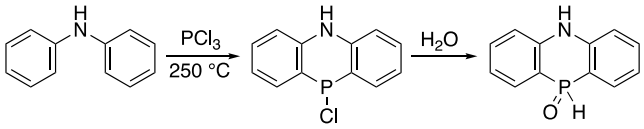

5 **6**

Scheme 1 Schenk and Michaelis' first reported synthesis of a PN-heterocycle scaffold, dibenzo[*b,e*]1,4-dihydro-1,4λ^5-azaphosphinine 4-oxide.

The oldest example of a 1,2-azaphosphinine comes from Dewar and Kubba in 1960.[47] Their synthesis follows a similar pathway to that laid out by Schenk and Michaelis nearly a century before.[31] This team had released a publication two years earlier describing aromatic resonance forms in boron-containing **7** and were interested in developing analogous PN species.[48] The work was aimed at trying to develop a phenanthrene-like dibenzo[*c,e*]-1,2-dihydro-1,2λ^3-azaphosphinine **9a** with hypothetical resonance structure **9a'**, in which the lone pair of the nitrogen atom would resonate through phosphorus to give some additional π-delocalization through the hypervalent P resonance structure **9a'** (Scheme 2). Starting from 2-aminobiphenyl, the authors generated an acyclic intermediate by reacting with phosphorus trichloride in benzene. This was then cyclized crude with $AlCl_3$ at elevated temperatures to furnish **8a**. Finally, replacement of the chlorine with PhMgBr resulted in the desired compound **9a**.

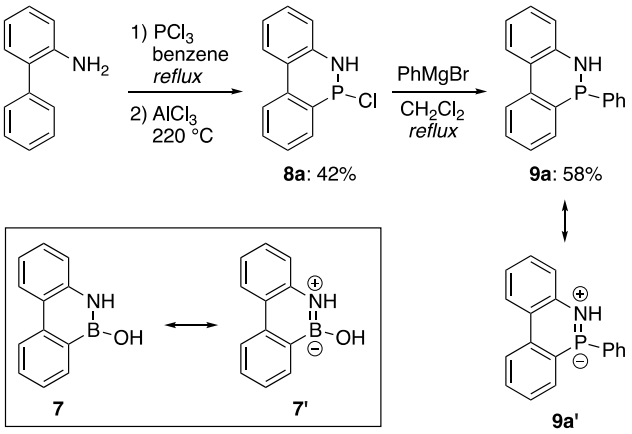

Scheme 2 Synthesis of Dewar and Kubba's early dibenzo[*c,e*]-1,2-dihydro-1,2λ^3-azaphosphinine **9** and comparison to the previously prepared boron-containing species **7**.

Comparison of UV-Vis spectra of **7** and **9a** indicated that while the electronic structures of the two species were similar, they were not identical. However, the authors noted that when left exposed to air for extended periods of time, two oxidation products (**10** and **11a**) were generated from **9a** (Scheme 3). Interestingly, the spectra of these oxidation products were nearly identical when compared to that of **7**. This emergent electron delocalization was rationalized by Dewar and Kubba through proposed resonance structures **10'** and **11a'**. By convention, P^V-oxo compounds are represented as P=O double bonds; however, due to the nature of the hypervalent bonding of these atoms, it can be argued that the phosphonyl moiety exists as P$^+$–O$^-$ in most cases. As discussed previously, it is unlikely any true aromaticity is occurring in these P^V heterocycles, but rather electron delocalization from the lone pairs of the oxygen and nitrogen to adjacent bonds via negative hyperconjugation. Further consideration of aromaticity in different azaphosphinine isomers is discussed at the end of the review. A majority of the azaphosphinines discussed in this review will feature this negative hyperconjugation phenomenon.

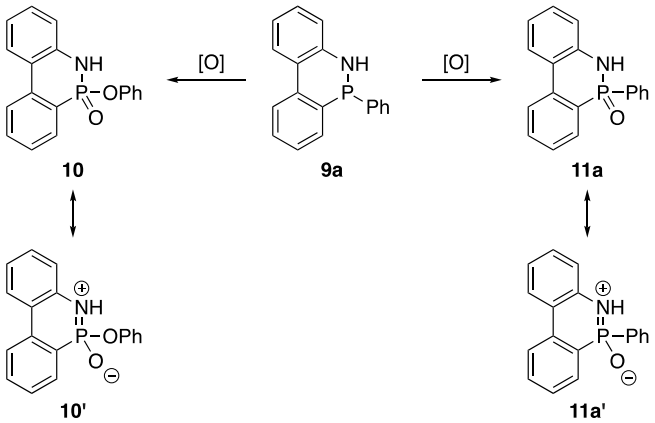

Scheme 3 Oxidation products of Dewar and Kubba's azaphosphinine **9** with aromatic resonance structures.

That same year, Campbell and Way significantly expanded upon the previous work laid out by Dewar and Kubba.[49] Starting from one of two *P*-chloro species **8** (R=H or Me), they arylated the system directly with several different aryl lithiates to furnish a family of corresponding azaphosphinines **9**. The authors found that they could induce the oxidation observed by Dewar and Kubba by exposing the heterocycles to a mixture of H_2O_2 and EtOH at room temperature (Scheme 4). No yields were reported for the final oxidation to furnish **11**.

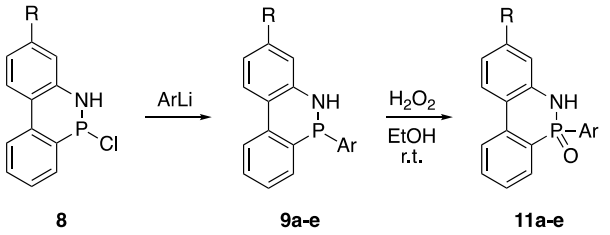

9a: R = H, Ar = Ph, 11%
9b: R = Me, Ar = Ph, 25%
9c: R = H, Ar = *p*-MeC_6H_4, 5%
9d: R = H, Ar = *p*-BrC_6H_4, 9%
9e: R = H, Ar = *p*-$(NMe_2)C_6H_4$, 23%

11a: R = H, Ar = Ph
11b: R = Me, Ar = Ph
11c: R = H, Ar = *p*-MeC_6H_4
11d: R = H, Ar = *p*-BrC_6H_4
11e: R = H, Ar = *p*-$(NMe_2)C_6H_4$

Scheme 4 Campbell and Way's synthesis of early azaphosphinines **9** and oxidation to **11**.

1,2-Azaphosphinines

Reactivity with Alkynes

Pericyclic / Cycloadditions

When considering the different synthetic approaches used in the development of 1,2-azaphosphinines, few are as prevalent in the early literature as the [4 + 2] cycloaddition, more commonly known as the Diels-Alder reaction. The earliest example of this reaction being applied to the 1,2-isomer of azaphosphinine is from Kobayashi and Nitta in 1985 to furnish three 1,2λ^5-azaphosphinine derivatives.[34] While not the first reported synthesis of this family of heterocycle, it did lay the groundwork for what would become a very typical method. The researchers used an *N*-vinyl-phosphazene (**13**) as their diene (Scheme 5), which was generated through the Staudinger reaction of

azidostyrene **12** and trimethyl phosphite. The Diels-Alder reaction was then carried out using various substituted alkynes to yield 2,2-dimethoxy-1,2λ^5-azaphosphinines **14** in modest to good yields. The observed regioselectivity of **14b** is ascribed to the ylidic nature of the phosphazene diene and the comparatively electrophilic β-carbon of the ester dienophiles. When heated to high temperatures, azaphosphinines **14a-b** underwent a methyl shift to yield the corresponding dihydro derivatives **15** in excellent yields.

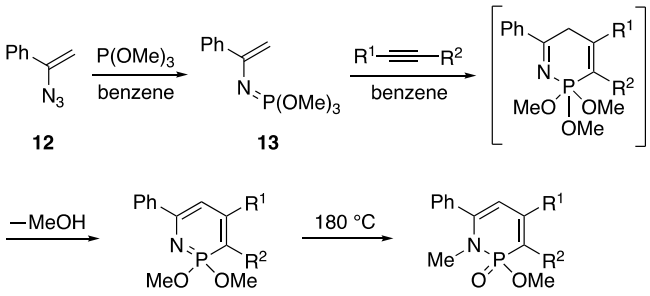

12 **13** **14a-c** **15a-b**

14a: $R^1 = R^2 = CO_2Me$, 58% **15a**: $R^1 = R^2 = CO_2Me$, 85%
14b: $R^1 = H$, $R^2 = CO_2Me$, 57% **15b**: $R^1 = H$, $R^2 = CO_2Me$, 87%
14c: $R^1 = R^2 = COPh$, 17%

Scheme 5 Synthesis of 1,2-azaphosphinine **14** using the Staudinger reaction and subsequent Diels-Alder cycloaddition.

Over a decade later, Nitta and coworkers returned to their work on the cycloadditions of *N*-vinyl-phosphazenes and substituted alkynes to explore further modifications.[50] They synthesized a similar series of 2,2-diphenyl-1,2λ^5-azaphosphinines **16** in modest yields by using phosphazene **17** as the phosphorus source for diene preparation (Scheme 6). Besides the new azaphosphinines, this paper also served to demonstrate potential post-synthetic modifications to these heterocycles. Unlike **14**, azaphosphinines **16** did not rearrange but instead could be reversibly protonated to give the corresponding azaphosphininium tetrafluoroborate salts **18**.

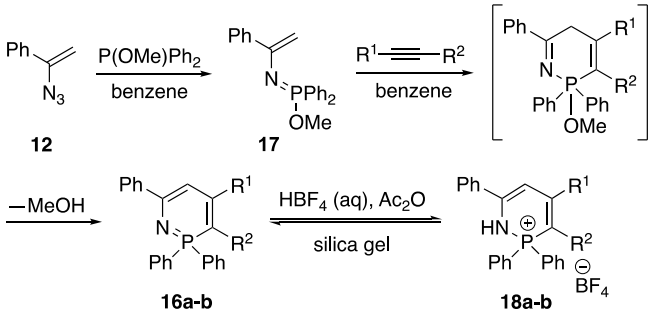

12 **17** **16a-b** **18a-b**

16a: $R^1 = R^2 = CO_2Me$, 36% **18a**: $R^1 = R^2 = CO_2Me$, 92%
16b: $R^1 = H$, $R^2 = CO_2Me$, 27% **18b**: $R^1 = H$, $R^2 = CO_2Me$, 97%

Scheme 6 Preparation of heterocycles **16** using phosphazene **17** and formation of azaphosphininium salts **18**.

In 1996, López-Ortiz and coworkers published an interesting alternative pathway to the 2,2-diphenyl-1,2λ^5-azaphosphinine scaffold by using *N*-methoxycarbonyl alkyldiphenylphosphazenes **19** as the pnictogen source in the

cycloaddition.[51] The key difference in this procedure from previous work was the generation of a stable ylide by deprotonation of the phosphazene with *n*-BuLi. The ylide then cyclized with dimethyl acetylenedicarboxylate (DMAD) to form the corresponding 2,2-diphenyl-1,2λ^5-azaphosphinin-6-one **20** in very good to excellent yields (Scheme 7). The authors concluded that only alkyldiphenylphosphazenes will react accordingly, as the substitution of a hydrogen inhibits the process. The authors noted that they had no explanation for the lack of reactivity in their system when R = H.

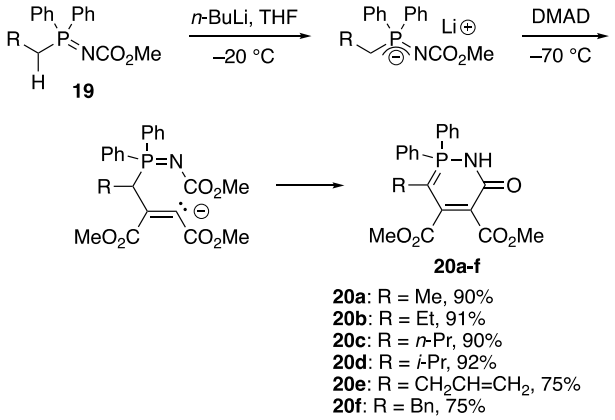

Scheme 7 Synthesis of 2,2-diphenyl-1,2λ^5-azaphosphinin-6-ones **20** through cycloaddition with DMAD.

Following this work from López-Ortiz, the chemistry of 1,2λ^3-azaphosphinines began to flourish with the seminal 1996 publication from Mathey and coworkers in which 1,3,2-diazatitana-cyclohexa-3,6-dienes **21** were reacted with an equivalent of PCl_3 at low temperature to furnish the corresponding 1,3,2-diazaphosphinines **22** (Scheme 8, top).[52] These diazaphosphinines can then be subjected to [4 + 2] cycloaddition conditions to yield a diazaphosphabarrelene intermediate **23**, which undergoes a subsequent [4 + 2] cycloreversion to extrude an equivalent of *t*-BuCN to yield 1,2λ^3-azaphosphinines **24**. Interestingly, this reaction can be repeated through the same conditions and extrude another equivalent of *t*-BuCN and furnish the corresponding phosphinine. This finding was similar to that of Märkl several years earlier who observed similar nitrile-extrusion properties in 1,3λ^3-azaphosphinines, as will be discussed in a later section of this review.[53] This mild synthesis offered several distinct advantages in the forms of regioselectivity, functional group tolerance, and high yields.

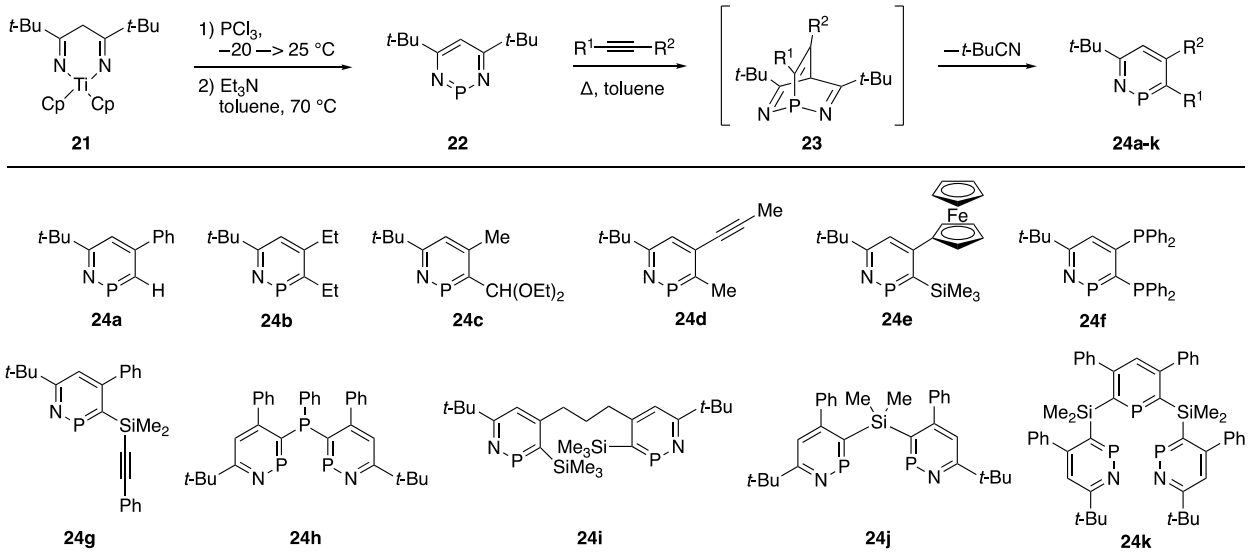

Scheme 8 (top) Synthesis of 1,2-azaphosphinines **24** through the formation and cycloaddition of a 1,3,2-diazaphosphinine. (bottom) Substrate scope of the heterocycles prepared in this way.

In 1997, Mathey and coworkers released a follow-up publication that dramatically expanded the substrate scope.[54] Despite demonstrating how titanocenes with either diphenyl or di-*t*-butyl substitution could be applied to the initial cycloaddition-cycloreversion reaction, the authors only used the di-*t*-butyl substituted derivative for the sake of purification. This resulted in a library of diverse 6-*t*-butyl-1,2λ^3-azaphosphinine derivatives **24**, highlighting the benefits of this synthetic approach (Scheme 8, bottom). The previously inaccessible derivatives include ferrocene, exocyclic phosphane, and silane-containing species. An interesting facet of the synthesis was discovered when comparing conjugated vs. nonconjugated diynes in the reaction. The authors found that use of conjugated diynes such as 2,4-butadiyne only facilitated a reaction from one of the triple bonds, leading to a 4-ethynyl azaphosphinine. Conversely, by using nonconjugated diynes, the reaction occurs at both alkyne sites resulting in bisazaphosphines (**24h-k**). It should be noted that every azaphosphinine generated through this method can be further transformed into the corresponding phosphinine as described above. Unfortunately, only the yields of the terminal phosphinines are reported. Application of this cycloaddition-cycloreversion strategy with nonconjugated diynes to generate more complex bisazaphosphinine heterocycles begged the question as to whether it could be extended to higher order systems. In 2000, Le Floch and coworkers provided the answer by performing the same reaction on tripodal species **25** and **26** to generate 1,2λ^3-azaphosphinine heterocycles **27** and **28** (Scheme 9).[55]

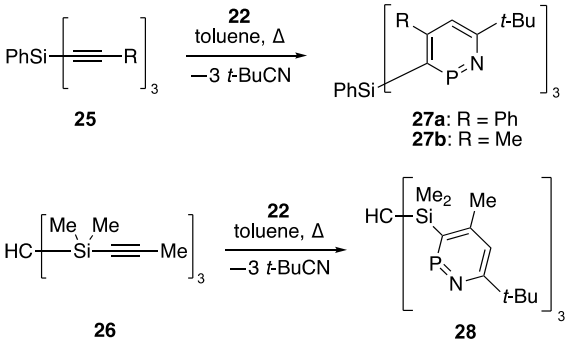

Scheme 9 Preparation of tripodal 1,2λ^3-azaphosphinine heterocycles (top) **27** and (bottom) **28**.

Transition Metal-Catalyzed C–H Activation

While the preparation of azaphosphinines via cycloaddition reactions was the most popular method in the 1980s and 1990s, this route has been supplanted by more modern techniques in recent years. One of the biggest synthetic advances across all of organic chemistry has been the advent and popularization of transition metal-mediated reactions stemming from pioneering works of Heck, Suzuki, Sonogashira, and more. One popular recent advance is transition-metal based C–H activation. A common technique for such reactions is the use of *ortho*-directing groups in aryl systems. By having an appropriate functional handle, specific aryl C–H bonds can be selected and reacted upon. In 2013, Glorius and coworkers published their work using phosphoryl-related directing groups in Rh^{III}-catalyzed C–H activation.[56] They reasoned that because there was a plethora of carbonyl-based directing groups for C–H activation, phosphonyl-based systems may work as well. After screening conditions, the authors found that the catalyst RhCp*(MeCN)$_3$(SbF$_6$)$_2$ was able to effect C–H activation reactions directed by different aryl phosphonamides. Within the scope of this review, when this reaction was performed on phosphonamide **29** and various bis-functionalized alkynes, the corresponding benzo[*c*]-1,2-dihydro-1,2λ^5-azaphosphinines **30** were furnished in good yields (Scheme 10). There was no apparent preference in electronic character of the alkyne. While the authors note that the desire to synthesize **30** was fueled by the biological relevance of the analogous isoquinolinone, this paper served more as a foray into phosphonyl-directed C–H activation and was not focused on the azaphosphinines outside of their application in reaction scope.

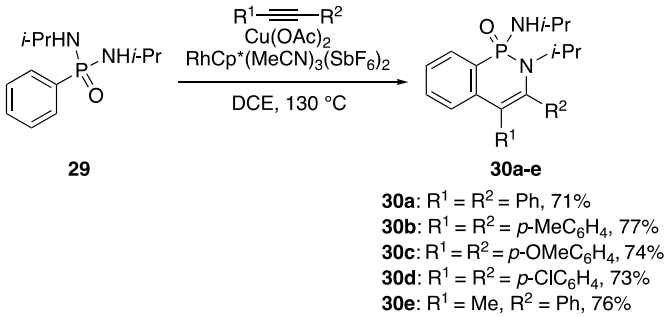

Scheme 10 Aryl phosphonamide directed C–H activation to furnish **30**.

In the same year as the work from Glorius, Lee and coworkers sought to use phosphinamides for C–H activation and heteroannulation using a different Rh catalyst.[57] Unlike the work from Glorius and coworkers, this publication was entirely focused on the construction of azaphosphinines. The goal was to use the lone pair of the phosphinamide as a directing group for the heteroannulated benzo[*c*]-1,2-dihydro-1,2λ^5-azaphosphinine 2-oxides. After optimizing the reaction conditions, Lee and coworkers examined a variety of phosphinamide substrates **31** (Scheme 11) and generated several derivatives of azaphosphinine **32** in good to excellent yields. There was no apparent preference for electron density or steric bulk in the alkyne coupling partner, and they observed excellent functional group tolerance. In several instances, they obtained heterocycles containing aryl chlorides and bromides that are available for further manipulation. They also proceeded to show how more complex, heterocyclic phosphinamides tolerate the reaction as with *P*-thiophene derivatives **32o** and **32p**.

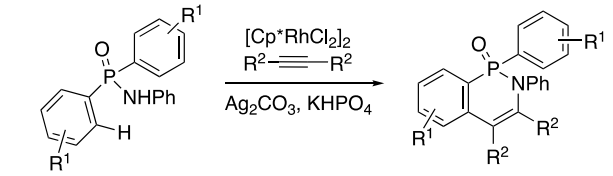

31 **32a-p**

32a-h: R^1 = H
32a: R^2 = Et, 71%
32b: R^2 = *n*-Bu, 68%
32c: R^2 = Ph, 81%
32d: R^2 = *m*-MeC_6H_4, 83%
32e: R^2 = *p*-MeC_6H_4, 79%
32f: R^2 = *p*-$OMeC_6H_4$, 99%
32g: R^2 = *m*-ClC_6H_4, 69%
32h: R^2 = *p*-BrC_6H_4, 87%

32i: R^1 = *o*-Me, R^2 = *p*-$OMeC_6H_4$, 87%
32j: R^1 = *p*-OMe, R^2 = *p*-$OMeC_6H_4$, 83%
32k: R^1 = *p*-OMe, R^2 = *p*-BrC_6H_4, 84%
32l: R^1 = *p*-F, R^2 = *p*-$OMeC_6H_4$, 89%
32m: R^1 = *p*-CF_3, R^2 = *p*-$OMeC_6H_4$, 74%
32n: R^1 = 3,5-$(Me)_2$, R^2 = *p*-$OMeC_6H_4$, 60%

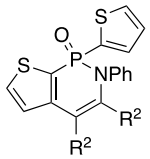

32o: R^2 = *p*-$OMeC_6H_4$, 93%
32p: R^2 = *p*-BrC_6H_4, 58%

Scheme 11 Formation of [*c*]-fused 1,2-dihydro-1,2λ^5-azaphosphinine-2-oxide **32**.

Electron lone pairs, particularly those on pnictogen atom centers, are commonly used to effect ligation. However, while many pnictogen-based ligands exist, the phosphinamide motif is rarely accessed for this purpose. Despite underutilization, the propensity of P^V to form chiral centers combines well with an adjacent directing lone pair. In 2017, Cramer and coworkers aimed to take the previous work from Lee and use it to develop a new class of benzo[*c*]-1,2-dihydro-1,2λ^5-azaphosphinine 2-oxide based *P*-stereogenic ligands.[58] To accomplish this, Cramer took advantage of prochiral molecule **33** to carry out the transition metal-catalyzed heteroannulation reaction. By using the nitrogen to direct the chiral catalyst to one of the two ortho aryl C–H bonds **34**, chiral intermediate **35** is formed, which is then carried through the reaction to give chiral benzo[*c*]-1,2-dihydro-1,2λ^5-azaphosphinine 2-oxide **36** (Scheme 12).

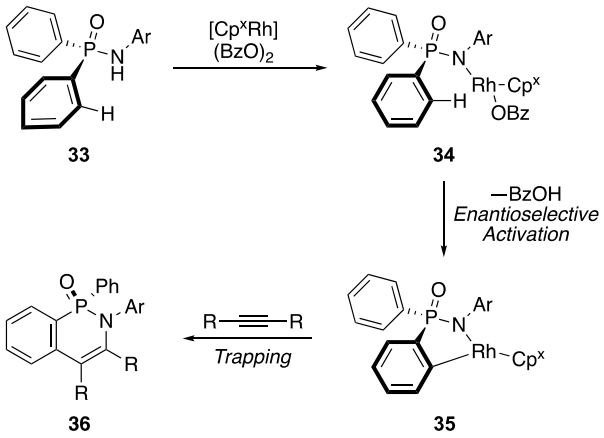

Scheme 12 Proposed mechanism for chiral C–H activation heteroannulation of achiral phosphinamide.

Optimization experiments determined that **Rh1** was the most appropriate catalyst for good enantioselectivity of the products, and thus a wide substrate scope was examined (Scheme 13). From the results of the synthetic trials, there does not seem to be a large electronic preference of substrate. Regardless, the high enantioselectivity of the reaction is undeniable, with enantiomeric excess being greater than 10:1 (*S:R*) for every derivative of **36** synthesized.

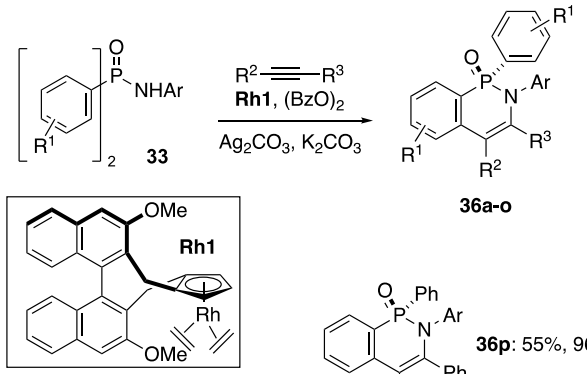

Ar = 3,5-$(CF_3)_2C_6H_3$
36a-g: $R^2 = R^3$ = Ph
36a: R^1 = *m*-Me, 80%, 96:4 e.r.
36b: R^1 = *o*-Me, 76%, 94:6 e.r.
36c: R^1 = *p*-Me, 85%, 93:7 e.r.
36d: R^1 = *p*-*t*-Bu, 45%, 94:6 e.r.
36e: R^1 = *p*-OMe, 81%, 95:5 e.r.
36f: R^1 = *p*-F, 60%, 96:4 e.r.
36g: R^1 = *m*-Br, 40%, 95:5 e.r.
36h-r: R^1 = H
36h: $R^2 = R^3$ = *p*-$OMeC_6H_4$, 86%, 94:6 e.r.
36i: $R^2 = R^3$ = *p*-ClC_6H_4, 50%, 92:8 e.r.
36j: $R^2 = R^3$ = *n*-Pr, 55%, 96:4 e.r.
36k: R^2 = *n*-Bu, R^3 = *p*-$CF_3C_6H_4$, 37%, 95:5 e.r.
36l: R^2 = *n*-Bu, R^3 = *p*-$OMeC_6H_4$, 75%, 95:5 e.r.
36m: $R^2 = CH_2OMe$, R^3 = *p*-$OMeC_6H_4$, 60%, 95:5 e.r.
36n: R^2 = *i*-Pr, R^3 = *p*-$OMeC_6H_4$, 78%, 95:5 e.r.
36o: R^2 = cyclopropyl, R^3 = *p*-$OMeC_6H_4$, 44%, 96:4 e.r.

36p: 55%, 96:4 e.r.

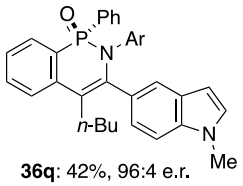

36q: 42%, 96:4 e.r.

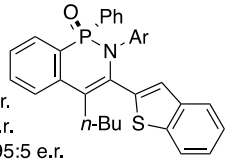

36r: 42%, 96:4 e.r.

Scheme 13 Chiral C–H activation heteroannulation to afford **36**. For every entry, Ar = 3,5-$(CF_3)_2C_6H_3$.

Because the primary aim of the Cramer paper was to generate useful chiral phosphinamide ligands for further chemistry, they also reported reducing the benzo[*c*]azaphosphinine from P^{V} to P^{III}. Although the authors found that the heterocycles were prone to racemization under certain conditions, the optimal method (Scheme 14) used 1,8-diazabicyclo[5.4.0]undec-7-ene (DBU) and trichlorosilane, resulting in 92% yield of P^{III} product and 97% retention of the initial configuration. The authors concluded this is a feasible pathway to enantiospecific benzo[*c*]-1,2-dihydro-1,2λ^3-azaphosphinines ligands **36'**; however, they have not reported additional studies on this system to date.

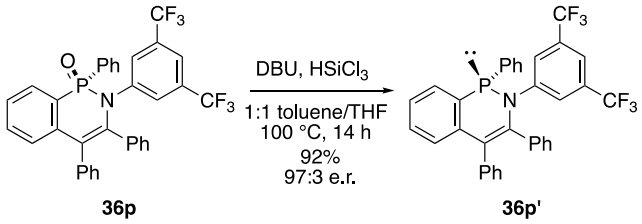

Scheme 14 Enantiospecific reduction to chiral azaphosphinine **36p'**.

In 2018, Cramer and Sun published a follow-up study that revealed a promising application for their system.[38] Previously, the syntheses of chiral azaphosphinines **36** via this method were limited to the desymmetrization of achiral phosphinamides with two identical aryl *P*-substituents **33**. The authors hypothesized that if the selectivity for the reactive enantiomer could be great enough, then one would be able to take a racemic mixture of chiral phosphinamide and generate two enantiomerically-pure materials, the heteroannulated reactive enantiomer **37** and the purified unreactive enantiomer of the starting racemate **38** (Table 1). In this study the chiral catalyst **Rh1** did not give sufficient selectivity, so Rh complexes with bulky trisubstituted Cp^x ligands (to deactivate reactivity on the mismatched substrate) were screened, with **Rh2** proving to be the most effective.

Table 1 Experimental details for reactions of *rac*-**36** with various internal alkynes. Ar = 3,5-$(CF_3)_2C_6H_3$.

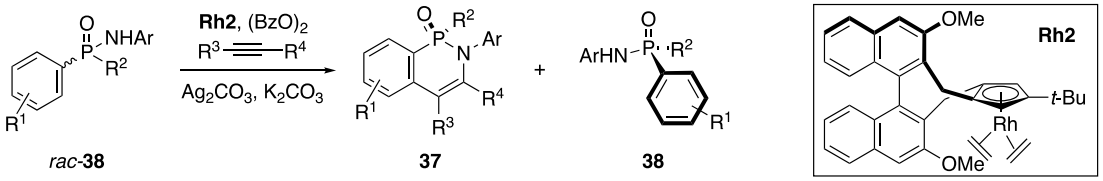

rac-**38**	R^1	R^2	R^3	R^4	Time [h]	Conv. [%]	e.r **37** (% yield)	e.r. **38** (% yield)
rac-**38a**	H	Me	Ph	Ph	8.5	51	93:7 (46)	95:5 (46)
rac-**38b**	*p*-Me	Me	Ph	Ph	10.5	55	89:11 (50)	98:2 (42)
rac-**38c**	*p*-F	Me	Ph	Ph	10.5	55	90:10 (48)	98:2 (40)
rac-**38d**	*p*-Cl	Me	Ph	Ph	10.5	55	89:11 (45)	97:3 (40)
rac-**38e**	*p*-OMe	Me	Ph	Ph	8.5	54	91:9 (48)	99:1 (42)
rac-**38f**	*p*-NMe_2	Me	Ph	Ph	9.5	42	95:5 (36)	83:17 (50)
rac-**38g**	*m*-Me	Me	Ph	Ph	10.5	58	85:15 (53)	99:1 (38)
rac-**38h**	*m*-Br	Me	Ph	Ph	14	55	91:9 (42)	99:1 (38)

rac-**38i**	*o*-Me	Me	Ph	Ph	10	53	77:23 (42)	79:21 (44)
rac-**38j**	H	Bn	Ph	Ph	4	59	84:16 (53)	99.5:0.5 (37)
rac-**38k**	H	$(CH_2)_2OBn$	Ph	Ph	6.5	51	93:7 (47)	93:7 (44)
rac-**38l**	H	*N*-pyrrolidinyl	Ph	Ph	5	57	79:21 (52)	89:11 (40)
rac-**38m**	H	*N*-morpholinyl	Ph	Ph	3.5	61	79:21 (55)	95:5 (37)
rac-**38n**	H	OMe	Ph	Ph	24	60	81:19 (55)	97:3 (37)
rac-**38o**	H	OPh	Ph	Ph	14	53	86:14 (48)	91:9 (44)
rac-**38p**	H	Me	*p*-$OMeC_6H_4$	*p*-$OMeC_6H_4$	8.5	51	89:11 (46)	95:5 (46)
rac-**38q**	H	Me	*n*-Bu	*p*-$OMeC_6H_4$	8.5	50	95:5 (46)	90:10 (46)
rac-**38r**	H	Me	*i*-Pr	*p*-$OMeC_6H_4$	8.5	43	94:6 (37)	82:18 (52)
rac-**38s**	H	Me	*n*-Bu	5-indolo	8.5	54	96:4 (48)	98:2 (43)

Much like their previous publication, this 2018 Cramer paper featured a large library of derivatives to emphasize the efficacy of their system. Varying the electronic and steric properties of both the alkyne and chiral phosphinamide led to moderate but consistent yields (36-55%) and enantioselectivities, in some cases exceeding 99:1. This included the use of various heterocycles and alkyl chains on both stating materials. The reaction was also performed on achiral diaryl phosphinamide **38t** to explore any possible regioselectivity for which ring results in the *benzo* fusion (Scheme 15). The authors found that there was an almost 1:1 distribution between the two possible products with an excellent overall yield for the transformation.

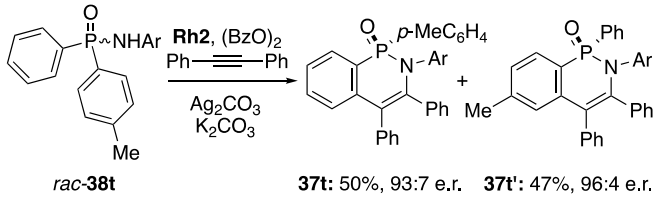

rac-**38t** **37t:** 50%, 93:7 e.r. **37t':** 47%, 96:4 e.r.

Scheme 15 Reactivity of bis-aryl functionalized chiral phosphinamide. Ar = 3,5-$(CF_3)_2C_6H_3$.

To investigate the application of this newly synthesized series as chiral phosphorus-based reagents for asymmetric catalysis, **37a** and **39** were added as a Lewis base (LB) to a reductive aldol condensation of chalcone **40** and benzaldehyde to furnish **41** (Scheme 16). Interestingly, the methyl-bearing **37a** gave not only a higher overall yield (95%) of product but also a dramatically improved enantioselectivity (96:4 e.r. of major diastereomer) compared to less selective **39**.

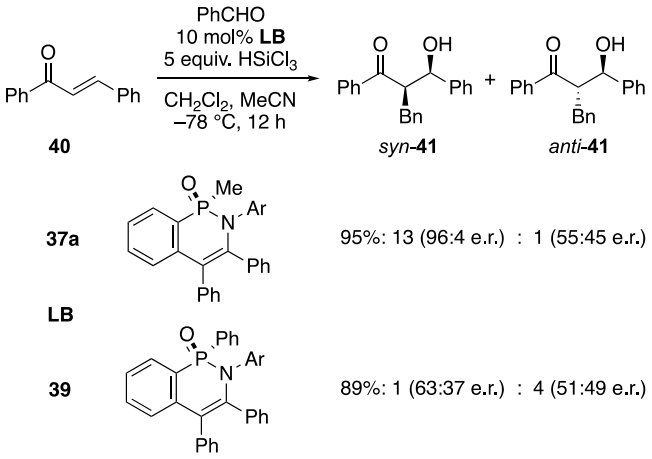

Scheme 16 Asymmetric reductive aldol condensation of enone **40** and benzaldehyde using chiral benzo[*c*]-1,2-dihydro-1,2λ^3-azaphosphinine additives as Lewis base (LB). Ar = 3,5-$(CF_3)_2C_6H_3$.

Continuing their investigation into asymmetric applications of their materials, the authors reduced **37a** from the P^V to P^{III} valence via thionation to **37a'** and reduction to **37a''**, which was then used as a ligand for asymmetric hydrogenation (Scheme 17). This hydrogenation reaction proceeded with quantitative yield and decent enantioselectivity, suggesting promising future applications for azaphosphinines in the field of organic catalysis.

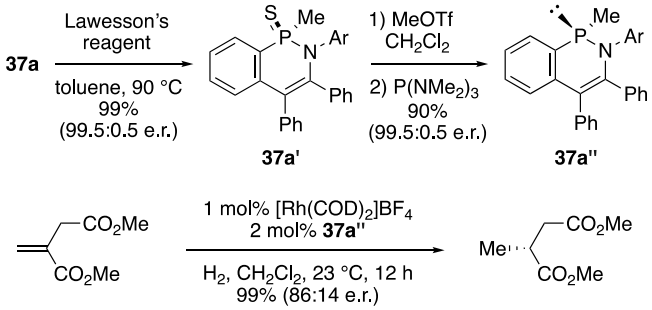

Scheme 17 Enantioselective reduction of **37a** and its use as a chiral ligand in an asymmetric hydrogenation reaction. Ar = 3,5-$(CF_3)_2C_6H_3$.

While these studies generated a large body of work that furthered the science of azaphosphinines considerably, the one potential drawback was the reliance on expensive Rh^I catalysts. In 2022, Shi and coworkers reported the design and application of a *in situ*-generated Co^{III} catalyst for the asymmetric heteroannulation of achiral phosphinamides **42** to benzo[*c*]-1,2-dihydro-1,2λ^5-azaphosphinine 2-oxides **43**.[59] Similar to Cramer's initial work, the early substrates are diphenylphosphinamides that rely on the enantiotopic aryl C–H bonds to generate a chiral intermediate.[57] Much of this work is dedicated to the logical design of an appropriate chiral ligand. Previous research suggested that monoanionic bidentate ligands were necessary for the *in situ*-generation of chiral Co^{III} active species.[60,61] After screening a number of ligands, the authors eventually decided upon salicyloxazoline (Salox) *(S)*-**L1**. This ligand, along with the $Co(OAc)_2•4H_2O$ precatalyst and $Mn(OAc)_2•4H_2O$ oxidant, were applied to many substrates

where both the achiral phosphinamide and alkyne were varied to form **43** (Scheme 18). In the case of every substrate, the aryl substituent is an 8-quinolinyl motif.

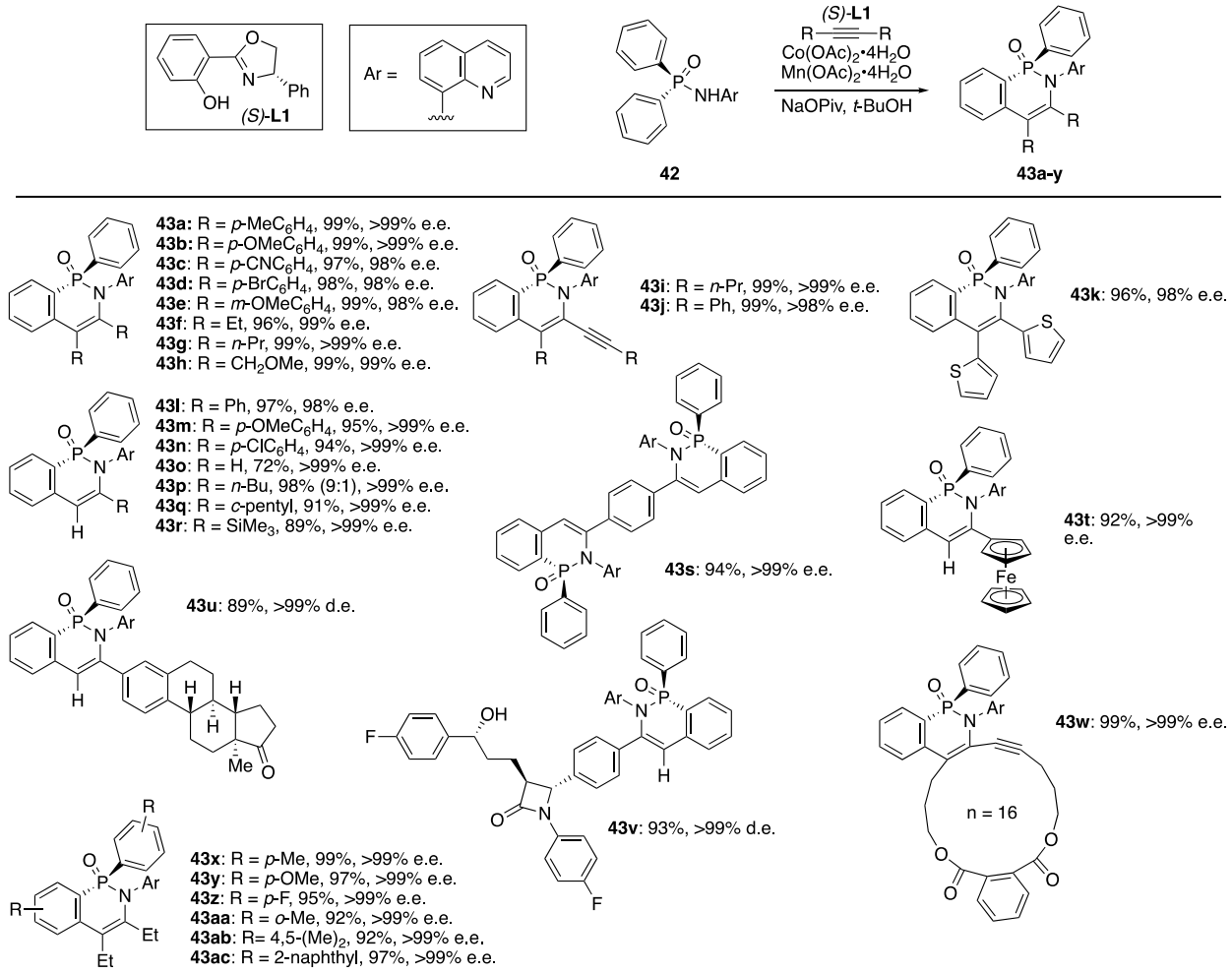

Scheme 18 Chiral C–H activation and heteroannulation using Co^{III} to afford **43**.

Shi and coworkers then performed a kinetic resolution experiment like Cramer, reacting a racemic mixture of compound **44** with phenylacetylene under conditions identical to the above trials (Scheme 19). The experimental results were excellent, with a near-quantitative overall yield and high enantioselectivity in forming just the (*S)*-enantiomer of the product **45** while ignoring the unreactive enantiomer of the starting phosphinamide (*R)*-**44**.

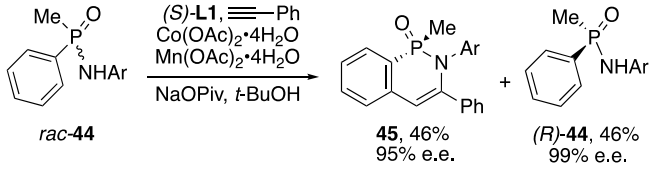

Scheme 19 Chiral resolution of phosphinamide **44** under standard reaction conditions. Ar = 8-quinolinyl.

Shi and coworkers also showed that the heteroannulation would proceed when the alkyne was replaced with a variety of allene coupling partners **46** (Scheme 20), affording **47** in good to excellent yields with high e.e. values.

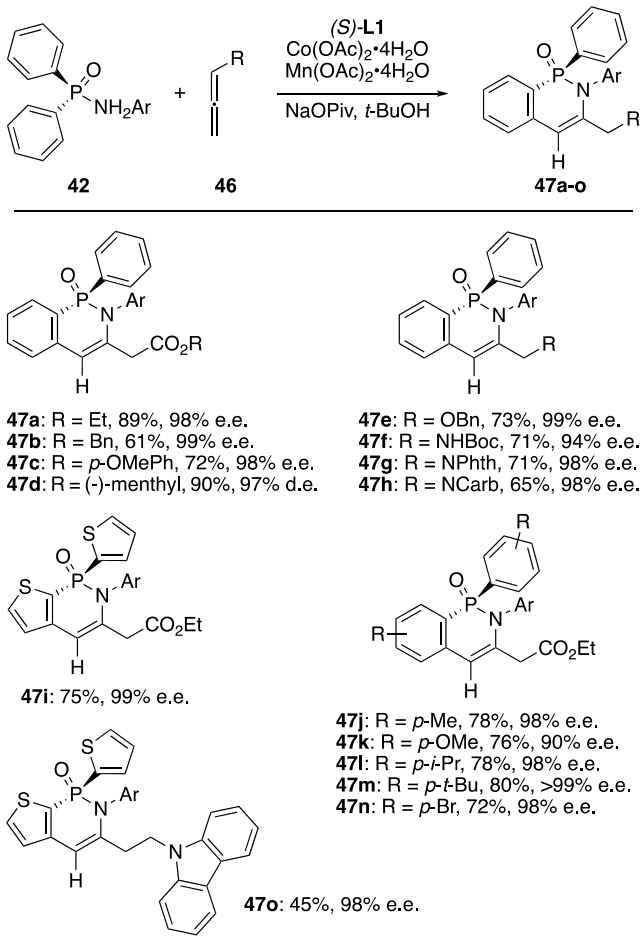

Scheme 20 Heteroannulation with allene coupling partners. Ar = 8-quinolinyl.

Very recently in 2023, Shi and coworkers reported similar transition-metal catalyzed [4 + 2] heteroannulation reactions on phosphanamines **48** and functionalized alkynes.[62] There are several important distinctions that separate this work from earlier publications. The design of the starting material is quite different, notably that the phosphorus atom of the phosphanamines is trivalent and is oxidized to pentavalence during the reaction. Secondly, the heteroannulation is conducted on *ortho*-halo-phosphanamines where the reactive bond is adjacent to the nitrogen instead of the phosphorus. This results in an inversion of the product atom geometry relative to the other species in similar publications. Although initially probed using tris(dibenzylideneacetone)dipalladium(0) (Pd_2dba_3) as the catalyst, screening studies revealed that $Ni(COD)_2$ gave dramatically improved yields. Further optimization of conditions showed that stoichiometric amounts of LiCl aided in the reduction of the Ni catalyst, and that elevated temperatures were required for optimal yield. The main body of explored substrates comprised of achiral phosphanamines with two identical alkyl or aryl substituents to furnish benzo[*e*]-1,2λ^5-azaphosphinines **49** (Scheme

21, top). The scope of functionalized alkynes includes not only aryl but also heteroaryl and alkyl substituents, indicating the wide degree of functional group tolerance. A dual heteroannulation was also conducted on **50** to furnish **51** with good to excellent yields (Scheme 21, bottom).

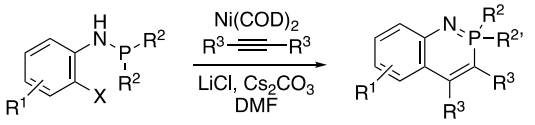

48 **49a-aj**

49a-o: R^2 = *t*-Bu, R^3 = Ph
49a: R^1 = H, 87%
49b: R^1 = *p*-Me, 69%
49c: R^1 = *m*-Me, 76%
49d: R^1 = 3,5-$(Me)_2$, 83%
49e: R^1 = *p*-*i*-Pr, 79%
49f: R^1 = *p*-*t*-Bu, 78%
49g: R^1 = *m*-OMe, 65%
49h: R^1 = *p*-F, 80%
49i: R^1 = 3-F, 4-Me, 81%
49j: R^1 = 3,4-F_2, 69%
49k: R^1 = *m*-Cl, 59%
49l: R^1 = *p*-OCF_3, 76%
49m: R^1 = *m*-CF_3, 87%
49n: R^1 = *p*-CN, 64%
49o: R^1 = *p*-COMe, 78%
49p-s: R^1 = H, R^3 = Ph
49p: R^2 = *i*-Pr, 87%
49q: R^2 = Cy, 82%
49r: R^2 = Ph, 63%
rac-**49s**: R^2 = Ph, $R^{2'}$ = *t*-Bu

49t-aj: R^1 = H, R^2 = *t*-Bu
49t: R^3 = *p*-MeC_6H_4, 78%
49u: R^3 = *m*-MeC_6H_4, 82%
49v: R^3 = *p*-*t*-BuC_6H_4, 87%
49w: R^3 = *p*-$OMeC_6H_4$, 71%
49x: R^3 = *p*-$SMeC_6H_4$, 80%
49y: R^3 = *p*-FC_6H_4, 90%
49z: R^3 = *p*-ClC_6H_4, 83%
49aa: R^3 = *m*-ClC_6H_4, 81%
49ab: R^3 = *p*-BrC_6H_4, 90%
49ac: R^3 = *p*-$CF_3C_6H_4$, 80%
49ad: R^3 = *p*-$OCF_3C_6H_4$, 89%
49ae: R^3 = *p*-$NH_2C_6H_4$, 46%
49af: R^3 = 2-thienyl, 33%
49ag: R^3 = 3-pyridyl, 57%
49ah: R^3 = Me, $R^{2'}$ = Ph, 71%
49ai: R^3 = *n*-Pr, $R^{2'}$ = Ph, 66%
49aj: R^3 = Et, 27%

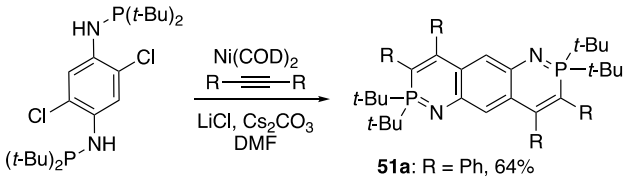

50

51a: R = Ph, 64%
51a: R = *p*-$OMeC_6H_4$, 84%
51a: R = *p*-FC_6H_4, 81%

Scheme 21 Ni^0-mediated heteroannulation to afford azaphosphinines **49** and **51**.

Shi and coworkers continued to explore the heteroannulation of *P*-stereogenic phosphanamines as well by protecting the P^{III} as borane complexes **52** and **53**. The starting materials were deprotected in situ and proceeded with moderate yields but excellent enantioselectivities for retention of the geometry of the chiral center in heterocycles **49s** and **49ak-an** (Scheme 22). Unlike most of the azaphosphinines covered in this review, this paper does provide analysis of the photophysical properties of the molecules. Density functional theory (DFT) provided the computed HOMO and LUMO energy levels of **49a**, which showed a clear distinction between HOMO and LUMO localization, with the HOMO predominantly on the benzo[*c*]azaphosphinine core while the LUMO is distributed across all the aromatic rings. This reasoning led to the conclusion that the LUMO and subsequent photophysical properties could be modulated through the identity of the aryl-substituent. Six heterocycles with varied aryl-substituents were measured for their emission in both solution and the solid state (Table 2). While the solution-state

quantum yields of the analyzed species were rather low (4%-13%), the solid-state quantum yields were comparatively quite high with **49y** reaching 90%.

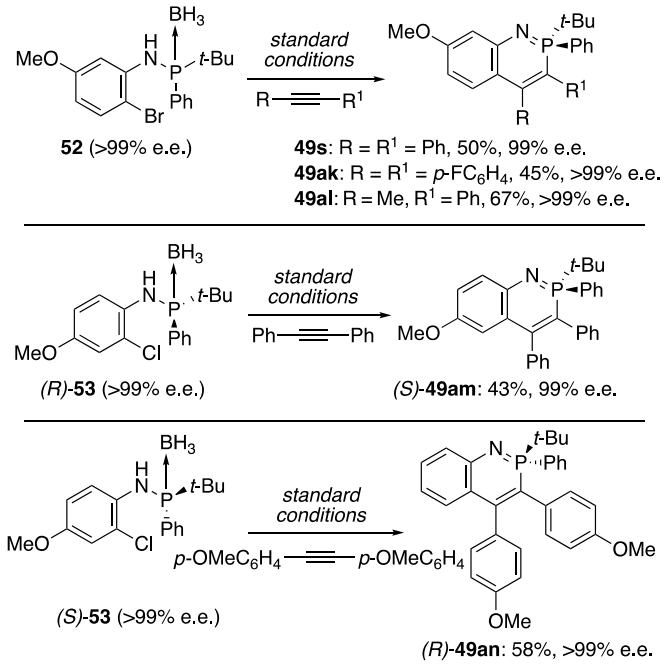

Scheme 22 Asymmetric [4 + 2] heteroannulation starting from chiral phosphanamines. Standard conditions of phosphanamine (1 equiv.), alkyne (2 equiv.), $Ni(COD)_2$ (10 mol%), LiCl (1 equiv.), Cs_2CO_3 (3 equiv.), DMF, 130 °C.

Table 2 Emission data for measured heterocycles **49**.

Substrate	Aryl group	λ_{em} (nm)[a,b]	ϕ (%)[b]	λ_{em} (nm)[a,c]	ϕ (%)[c]
49a	Ph	514	40	547	5
49t	*p*-MeC_6H_4	530	30	539	4
49w	*p*-$OMeC_6H_4$	518	11	536	4
49y	*p*-FC_6H_4	515	90	543	13
49ab	*p*-BrC_6H_4	561	66	560	7
49ac	*p*-$CF_3C_6H_4$	551	24	582	6

[a]Emission maxima upon excitation at maximum absorption wavelength. [b]Measured in solid state. [c]Measured in CH_2Cl_2.

Intramolecular cyclization reactions

Intermolecular heteroannulation reactions, particularly those catalyzed by transition metals, have the decided benefit of extremely varied substrate scopes and in many cases enantioselectivity. However, in terms of published methods, intramolecular cyclization reactions to form benzo[x]azaphosphinine systems remains the most popular. Like cycloaddition reactions, these intramolecular cyclizations are generally transition-metal free. Besides this, lack of reliance on an added alkyne allows for different substitutions made directly on the PN-heterocycle such as *O*- and *N*-substitutions, as well as fusion to larger conjugated systems. In 1966, a very early example of an azaphosphinine

synthesis from Shavel and coworkers was the intramolecular Bischler-Napieralski cyclization of indole derivative **54** via dichloro intermediate **55**, ultimately furnishing 1,2-dihydro-1,2λ^5-azaphosphinine 2-oxide **56** (Scheme 23).[63] Due to the time period, there is little analytical data for **56**, but it is one of the earliest examples of a PN-heterocycle prepared by an intramolecular route.

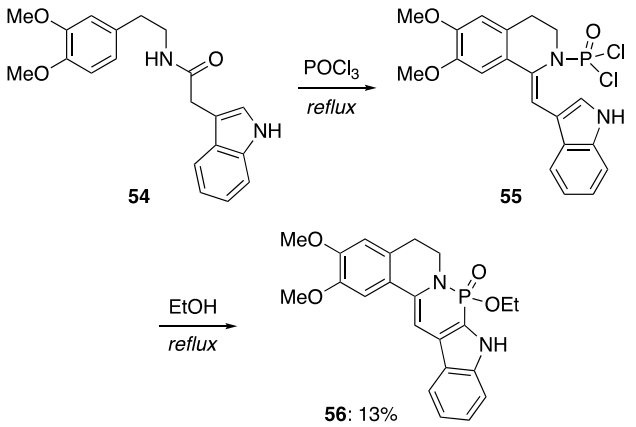

Scheme 23 Synthesis of indole-fused azaphosphinine 2-oxide **56**.

Twenty years later, Bourdieu and Foucaud reported in 1986 a concise synthesis to several 1,2-dihydro-1,2λ^3-azaphosphinines **57**.[33] This pathway was influenced by an earlier study from Nurtdinov et al. that prepared 2-oxo-1,2-azaphospholenes using dichlorophosphanes and *N*-butylimines.[64] In their adaption, Foucaud combined dichlorophenylphosphane with two equivalents of various alkyl imines **58** to furnish 1,2-dihydro-1,2λ^3-azaphosphinines **57** (Scheme 24). Several of these compounds featuring different alkyl substituents were synthesized in low to very good yields, with the corresponding azaphosphole generated as a side product. In a follow-up study the authors incorporated much larger number of *N*-alkylimines.[65] Overall, variation of chain length led to little discernable trend in the yields of the products.

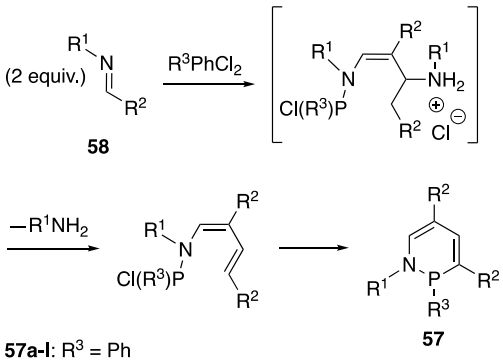

57a-l: R^3 = Ph
57a: R^1 = *t*-Bu, R^2 = Me, 64%
57b: R^1 = *i*-Bu, R^2 = Me, 5%
57c: R^1 = *t*-Oct, R^2 = Me, 70%
57d: R^1 = *i*-Pr, R^2 = Me, 42%
57e: R^1 = Bn, R^2 = Me, 25%
57f: R^1 = *n*-Bu, R^2 = Et, 6%
57g: R^1 = *t*-Bu, R^2 = Et, 60%
57h: R^1 = *i*-Bu, R^2 = Et, 8%
57i: R^1 = *t*-Bu, R^2 = *n*-Pr, 68%
57j: R^1 = *i*-Bu, R^2 = *n*-Pr, 10%
57k: R^1 = *t*-Bu, R^2 = *n*-Bu, 63%
57l: R^1 = *i*-Bu, R^2 = *n*-Bu, 8%
57m: R^1 = *t*-Bu, R^2 = Me, R^3 = Bn, *n.y.r.*
57n: R^1 = *t*-Bu, R^2 = Me, R^3 = OMe, *n.y.r.*

Scheme 24 Proposed pathway to 1,2-dihydro-1,2λ^3-azaphosphinines **57**. No yield reported (*n.y.r.*)

Bourdieu and Foucaud also performed several experiments with alternative phosphane and phosphinite reagents, namely $P(CH_2Ph)Cl_2$ and $P(OMe)Cl_2$, respectively; however, neither of the desired P^{III} heterocycles (**57m** and **57n**) were stable enough to be isolated and instead underwent oxidation in air to furnish the corresponding P^V oxo-compounds **57m'** and **57n'** (Scheme 25). Compound **57n** would also hydrolyze in the presence of acid to give **57n''**. Finally, the authors also showed how the P^{III} heterocycles could be intentionally oxidized to P^V using either H_2O_2 or S_8 to form the corresponding oxide **59** or sulfide **60** (Scheme 26).

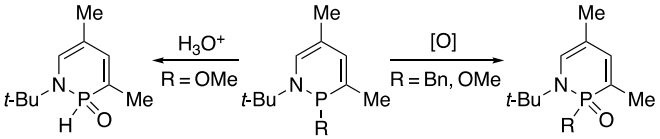

Scheme 25 Oxidation and hydrolysis of heterocycles **57m** and **57n**.

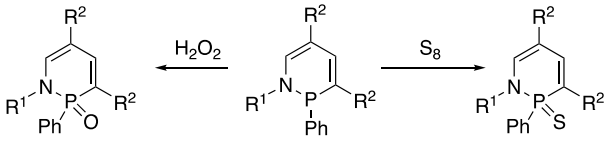

59a: R^1 = *t*-Bu, R^2 = Me, 83%
59b: R^1 = *i*-Bu, R^2 = Me, 78%
59c: R^1 = *t*-Oct, R^2 = Me, 86%
59d: R^1 = *i*-Pr, R^2 = Me, 75%
59e: R^1 = Bn, R^2 = Me, 70%
59f: R^1 = *n*-Bu, R^2 = Et, *n.y.r.*
59f: R^1 = *n*-Bu, R^2 = Et, *n.y.r.*
59g: R^1 = *t*-Bu, R^2 = Et, *n.y.r.*
59h: R^1 = *t*-Bu, R^2 = *n*-Pr, *n.y.r.*
59i: R^1 = *t*-Bu, R^2 = *n*-Bu, *n.y.r.*
60a: R^1 = *t*-Bu, R^2 = Me, 49%
60d: R^1 = *i*-Pr, R^2 = Me, 44%

Scheme 26 H_2O_2 and S_8 oxidations of azaphosphinines **57**.

A third paper from Bourdieu and Foucaud in 1987 rounded out the story by briefly describing a protocol for the conversion of the dihydro heterocycles to the corresponding fully conjugated azaphosphinine **61** (Scheme 27).[66] Pyrolysis of 1,2-dihydro-1,2λ^3-azaphosphinine **57c** at 600 °C thermolytically cleaved the substituents on both the 1 and 2 positions; however, product **61** was highly electrophilic and added a variety nucleophiles (water, isopropylamine, or methylmercaptan) across the reactive P=N bond, affording heterocycles **62**-**64**. Interestingly, both *P*-amino **63** and *P*-thio **64** also hydrolyzed to furnish **62** when exposed to water. No yields were reported for the reactions.

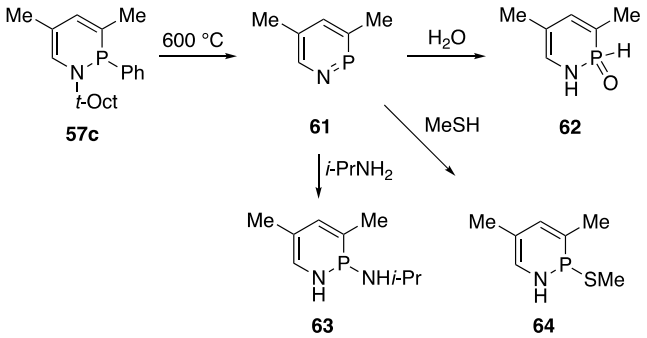

Scheme 27 Thermolytic synthesis of 1,2λ^3-azaphosphinine **61** and its dihydro products **62**-**64** from attack of various nucleophiles.

Also in 1987, Barluenga et al. published their work on the first example of benzo[*e*]-1,4-dihydro-4-oxo-1,2λ^5-azaphosphinines, which was achieved via intramolecular cyclization of *N*-aryl phosphazene (Scheme 28).[67] These imides were prepared via Staudinger reaction of methyl *o*-azidobenzoate **65** with various alkyldiphenylphosphanes. The phosphazenes were then cyclized with KH under mild temperatures to furnish the final heterocycles **66**. The authors found that the benzo[*e*]azaphosphinine resulting from a *P*-methylphosphazene was unstable and could not be isolated. Similar to previously discussed early works, this brief publication provides little-to-no subsequent analysis of the new compounds besides NMR chemical shifts. Despite that, the Barluenga study proved to be a key publication that opened the door for several additional reports to further develop the scaffold.

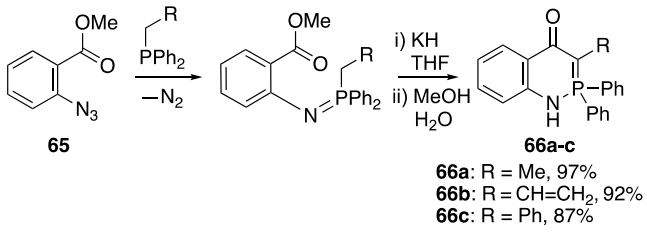

Scheme 28 Synthesis of benzo[*e*]-1,4-dihydro-1,2λ^5-azaphosphinines **66**.

In 1991, Bedel and Foucaud published the oxidation of their previously prepared 1,2-dihydro-1,2λ^3-azaphosphinines from P^{III} to P^V,[68] building upon the knowledge gained from their thermolysis of these heterocycles.[66] Methylation of azaphosphinines **57** generated *P*-methyl phosphonium salts **67**, which afforded **68** after thermolysis

at 210-230 °C (Scheme 29). This system was deprotonated under mildly basic conditions to furnish 1,2λ^5-azaphosphinines **69** in good-to-excellent yields. Upon exposure to air and/or water, the azaphosphinines slowly decomposed to give one equivalent of formamide and the corresponding phosphane oxide **70**.

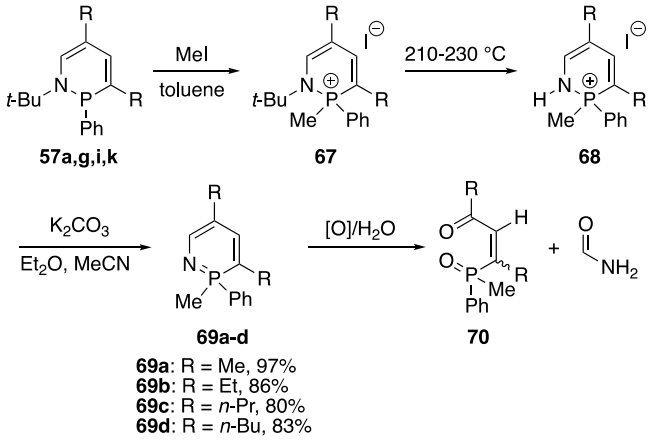

Scheme 29 Synthesis of 1,2λ^3-azaphosphinine **69** and subsequent hydrolysis/oxidation.

Fluck et al. published an entirely novel approach to the synthesis of 1,2λ^5-azaphosphinines in 1995, exploring the reactions between isothiocyanates **71** and 1,1,3,3-tetrakis(dimethylamino)-1λ^5,3λ^5-diphosphete **72** (Scheme 30).[69] Depending on the molar ratio of starting materials used, exotic azaphosphinine derivatives **73** are furnished. Despite not having an apparent application, this synthesis stands as a unique example of reactivity to obtain the typical azaphosphinine core. The resultant heavily substituted 1,2λ^5-azaphosphinines are notably stable with melting points near or at 200 °C.

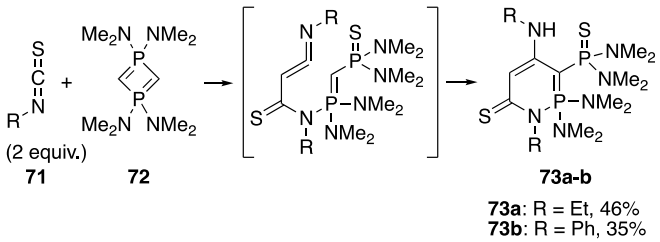

Scheme 30 Phosphete and isothiocyanate cyclization into azaphosphinine **73**.

The first example of benzo[*c*]-1,2-dihydro-1,2λ^5-azaphosphinine 2-oxides were published by Tang and Ding in 2006.[37] Their goal was to explore the azaphosphinine analogues of isoquinolin-1-ones, which they termed phosphaisoquinolin-1-ones. To generate these species, the authors first synthesized a library of *o*-(1-alkynyl)phenylphosphonamidate **74**. These were prepared in two steps by chlorinating the starting *o*-(1-alkynyl)phosphonic acid monoester with thionyl chloride and subsequently aminating with various primary amines. The phosphonamidates were then cyclized in a Pd-catalyzed reaction to yield **75** (Table 3). Because this was the first reported instance of the P^V–NH intramolecular heteroannulation, a variety of transition metals and temperatures

were investigated, revealing the use of $PdCl_2(MeCN)_2$ at 80 °C as optimal. Although, the reaction times varied from entry to entry, there was little notable effect on yield resulting from the R group identities. One noted exception was for **75k** where only 15% yield was isolated under normal optimized conditions, but the addition of a few drops of AcOH led to the dramatically improved yield of 65%. The authors proposed that this was a result of an external proton source aiding the cleavage of the vinylpalladium intermediate and regeneration of the $PdCl_2(MeCN)_2$. For these reactions only the six-membered product was generated, which is consistent with a 6-endo-dig cyclization. A potential explanation for the regioselectivity of cyclization is that the long C–P and P–N bonds would favor the transition state that leads into the six-membered product. The authors studied the antitumor properties of **75** in vitro, noting at high concentrations these species had very high inhibition ratios of A-549 lung cells in SRB (sulforhodamine B) assay; however, this inhibition fell off dramatically at lower concentrations, so further analysis is warranted.

Table 3 Substrate scope of cyclization of **74** to afford **75**.

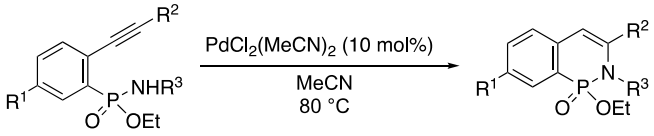

74 **75a-l**

R^1	R^2	R^3	Product	Yield [%]
H	Ph	Bn	**75a**	80
H	Ph	H	**75b**	68
H	Ph	*n*-Pr	**75c**	72
H	*n*-Bu	Bn	**75d**	87
Cl	Ph	Bn	**75e**	85
Cl	Ph	*n*-Pr	**75f**	67
Cl	*n*-Bu	Bn	**75g**	85
Cl	*p*-EtC_6H_4	Bn	**75h**	72
Cl	*p*-EtC_6H_4	*n*-Pr	**75i**	70
Cl	cyclopropyl	Bn	**75j**	90
Cl	CH_2OMe	*n*-Pr	**75k**	65
OMe	Ph	Bn	**75l**	79

In 2008, Ding and coworkers published a follow-up study that now included added allyl halide **76** in stoichiometric excess.[70] This reaction yielded the same benzo[c]1,2-dihydro-1,2λ^5-azaphosphinine scaffold as previously observed but with a 4-allyl substitution leading to series **77** (Table 4). A screen of reaction conditions showed that with excess methyloxirane the desired product **77** was formed in very good yield, with **75** generated in small amounts. Increasing the equivalents of both methyloxirane and allyl halide improved the yield of **77** and decreased formation of **75**. The reaction is decidedly robust with a large functional group tolerance and good yields. Much like the previous entry from Ding, it appears that the electron density of the phosphonamidate starting

material has little bearing on the yield of the product. This reaction also tolerates *N*-unsubstituted phosphonamidates, as is the case with **77b**. It is also worth noting that the reactivity of the system is selective for the allyl halide over the aryl halide even when both are the same (e.g., **77i-l**). The authors do note that the use of the substituted allyl chlorides (e.g., 3-chloro-1-butene) leads to an internal alkene in the final heterocycle with a consistent 77:23 distribution of *E* to *Z* isomers across all such products.

Table 4 Cyclization and subsequent allylation of give azaphosphinines **77**.

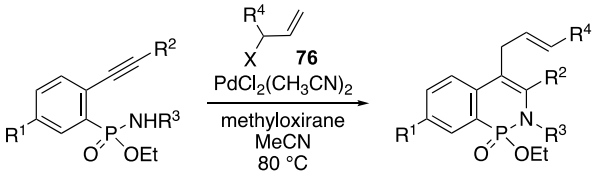

74 **77a-q**

R^1	R^2	R^3	R^4	X	Product	Yield [%]
H	Ph	Bn	H	Br	**77a**	90
H	Ph	H	H	Br	**77b**	69
Cl	Ph	Bn	H	Br	**77c**	92
Cl	Ph	*n*-Pr	H	Br	**77d**	87
Cl	*p*-EtC_6H_4	Bn	H	Br	**77e**	88
Cl	*n*-Bu	Bn	H	Br	**77f**	82
OMe	Ph	Bn	H	Br	**77g**	85
H	Ph	Bn	Me	Cl	**77h**	85[a]
H	*n*-Bu	Bn	Me	Cl	**77i**	78[a]
Cl	Ph	Bn	Me	Cl	**77j**	86[a]
Cl	Ph	*n*-Pr	Me	Cl	**77k**	81[a]
Cl	*p*-EtC_6H_4	*n*-Pr	Me	Cl	**77l**	83[a]
H	Ph	Ph	H	Br	**77m**	83
Cl	Ph	Ph	H	Br	**77n**	80
OMe	Ph	Ph	H	Br	**77o**	78
H	Ph	CH_2CO_2Et	H	Br	**77p**	82
Cl	Ph	CH_2CO_2Et	H	Br	**77q**	85

[a]Products isolated as (*E*/*Z*= 77:23).

As with their previous work, the authors also tested the biological properties of nine derivatives of **77**. At a concentration of 20 µg/mL, the enzyme Src homology 2-containing phosphatase-1 (SHP-1) inhibition ratios varied from 20.2% (**77a**) to 54.3% (**77i**). The heterocycles were then tested against melanin-concentrating hormone receptor-1 (MCH-1R) with IC_{50} values varying from 3.78 (**77d**) to 10.23 µmol (**77e**). The benzo[*c*]-4-allyl-1,2-dihydro-1,2λ^5-azaphosphinine 2-oxides showed no MCH-1R activities and are reported in the publication as the first example of using phosphorus analogues of heterocyclic natural products as MCH-1R inhibitors. An in-depth screen of a variety of antagonists of MCH-1R by Wang and coworkers in 2008[71] showed that of the derivatives of **75** and **77** tested, only

75a' (Cl on C(4)) showed significant binding affinity (K_i = 115.7 nmol/L) and potent antagonism (K_B = 23.8 nmol/L). The authors note that the benzo[*c*]-2-ethoxy-1,2λ^5-azaphosphinine 2-oxide core may prove to be a powerful motif in MCH-1R binding in the future despite being structurally quite different from previously found MCH-1R modulators.

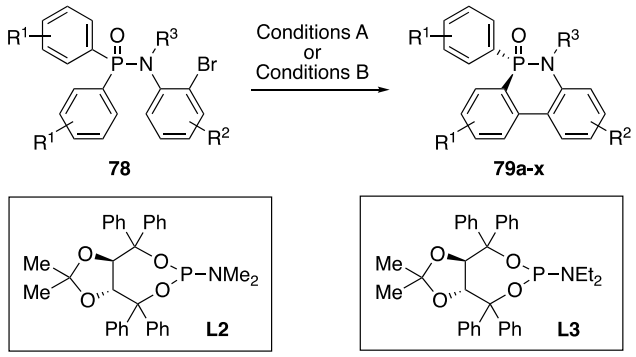

Conditions A (Duan)
79a-l: R^3 = Me
79a: R^1 = H, R^2 = H, 94%, 90% e.e.
79b: R^1 = H, R^2 = *p*-Me, 88%, 93% e.e
79c: R^1 = H, R^2 = *p*-OMe, 80%, 91% e.e
79d: R^1 = H, R^2 = *m*-F, 94%, 90% e.e
79e: R^1 = H, R^2 = *m*-CF_3, 92%, 92% e.e.
79f: R^1 = H, R^2 = *p*-Cl, 88%, 93% e.e.
79g: R^1 = *p*-OMe, R^2 = H, 88%, 89% e.e.
79h: R^1 = *p*-Cl, R^2 = H, 87%, 91% e.e.[a]
79i: R^1 = *p*-CF_3, R^2 = H, 91%, 91% e.e.[a]
79j: R^1 = *o*-Me, R^2 = H, 62%, 85% e.e.
79k: R^1 = 3,5-$(CF_3)_2$, R^2 = H, 79%, 83% e.e.
79l: R^1 = 3,5-$(CF_3)_2$, R^2 = *m*-Me, 58%, 86% e.e.
79m: R^1 = H, R^2 = H, R^3 = *p*-$OMeC_6H_4$, 81%, 91% e.e.

Conditions B (Ma)
79b: R^1 = H, R^2 = *p*-Me, 99%, 95% e.e.
79d: R^1 = H, R^2 = *m*-F, 99%, 95% e.e.
79e: R^1 = H, R^2 = *m*-CF_3, 99%, 95% e.e.
79f: R^1 = H, R^2 = *p*-Cl, 98%, 95% e.e.
79n-u: R^1 = H
79n: R^2 = H, R^3 = Et, 94%, 89% e.e.
79o: R^2 = H, R^3 = *n*-Bu, 61%, 88% e.e.
79p: R^2 = *m*-Me, R^3 = Me, 72%, 92% e.e.
79q: R^2 = *p*-*t*-Bu, R^3 = Me, 99%, 97% e.e.
79r: R^2 = *p*-Ph, R^3 = Me, 68%, 93% e.e.
79s: R^2 = *p*-CN, R^3 = Me, 64%, 96% e.e.
79t: R^2 = *p*-CF_3, R^3 = Me, 83%, 96% e.e.
79u: R^2 = H, R^3 = Bn, 12%, 92% e.e.
79v: R^1 = *p*-Ph, R^2 = H, R^3 = Me, 90%, 95% e.e.
79w: R^1 = *p*-Me, R^2 = H, R^3 = Me, 92%, 96% e.e.
79x: R^1 = *m*-OMe, R^2 = H, R^3 = Me, 54%, 91% e.e.

Scheme 31 Palladium catalyzed C–H activated heteroannulation to furnish chiral azaphosphinines **79**. Conditions A: $Pd(OAc)_2$ (5 mol%), **L2** (10 mol%), K_3PO_4 (1.5 equiv.), PivOH (30 mol%), toluene, 80 °C. Conditions B: $Pd(dba)_2$ (8 mol%), **L3** (10 mol%), Cs_2CO_3 (1.5 equiv.), PivOH, (40 mol%), hexanes, 60 °C. [a]Reaction performed at room temperature.

In 2015, Duan and coworkers and Ma and coworkers kicked off what would become a period of great activity for azaphosphinine chemistry.[72,73] The two groups submitted and published their papers within a week of one another and the content of both is very similar, with some identical derivatives being prepared. These works were conceptual continuations of the studies of not only Lee[57] and Cramer[38,58] but also the very early systems from

Dewar[47] and Campbell,[49] with the aim being the generation of chiral, dibenzo[*c*,*e*]1,2-dihydro-1,2λ^5-azaphosphinine 2-oxide species via transition-metal catalyzed C–H activation. Starting from achiral phosphinamide **78** (Scheme 31), one of the identical *P*-aryl substituents would be converted to a biphenyl derivative, generating a stereogenic phosphorus center. Interestingly, the two groups of authors screened the same exact pool of chiral phosphorus ligands and decided upon a ligand that only differed in chain length of the dialkylamino group. Whereas Duan used *N,N*-dimethyl ligand **L2**, Ma chose *N,N*-diethyl ligand **L3** and that their choices likely arise from the different reaction conditions, i.e., Conditions A (Duan) vs. Conditions B (Ma) in Scheme 31. Cyclization of a variety of achiral phosphinamide **78** furnished the corresponding dibenzo[*c*,*e*]1,2-dihydro-1,2λ^5-azaphosphinine **79** with both reactions showing excellent yields across the substrates studied. While the results suggest the conditions of Duan and coworkers were more consistent, Ma and coworkers used a wider substrate scope particularly in terms of *N*-substituents. Heterocycles **79b**, **79d**, **79e**, and **79f** were synthesized by both groups with Conditions B performing slightly better in the identical transformation.

Duan and coworkers also explored the generation of chiral phosphane oxides **80** from the P–N bond cleavage of **79** using MeLi, *i*-PrLi, and *t*-BuLi (Scheme 32). The former two yielded nearly racemic mixtures of the alkyl addition product, whereas the *t*-BuLi reaction resulted in a complex mixture of products that was not identified. This is a convenient route to chiral phosphane oxides that may find further use in catalysis.

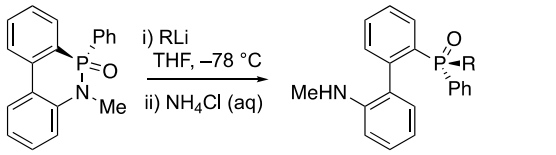

79a **80**

80a: R = Me, 73%, 1.3:1 atropisomers
80b: R = *i*-Pr, 59%, 2.2:1 atropisomers

Scheme 32 P–N bond cleavage to furnish chiral phosphane oxides **80**.

In early 2017, Yang and coworkers published their work on the transition-metal free *P*-stereogenic dibenzo[*c,e*]-1,2-dihydro-1,2λ^5-azaphosphinine derivatives **81** (Scheme 33).[74] In the aim of making the cyclization more economical, the authors decided to investigate the potential for transition-metal free oxidative C–H activation instead. An added benefit of this system would be stability under ambient atmosphere. After screening a variety of oxidants, the authors settled on hypervalent iodine species $PhI(OAc)_2$ with added I_2 in MeCN at 80 °C as the optimal conditions, which were applied to a library of phosphinamides **82** with various aryl and *N*-alkyl functional groups, giving the dibenzo[*c,e*]-8-iodo-1,2λ^5-azaphosphinine 2-oxides **81**. They found that the reaction proceeded better with less sterically demanding *N*-substituents, but having any *N*-alkyl group (46–78% yield) worked better than a hydrogen (20% yield). Electron-withdrawing R-groups (e.g., tosyl or pentafluorobenzene) resulted in C–H hydroxylation and instead gave **83** as product in moderate yields. In every case, excellent diastereoselectivities for the *P*-stereogenic center and the axial chirality of the aryl linking unit were obtained for **81** and **83**. It was also

observed that substitution of KBr for I_2 in the reaction furnished the corresponding 5'-bromo heterocycle but did not work with NaCl to yield the corresponding 5'-chloro species.

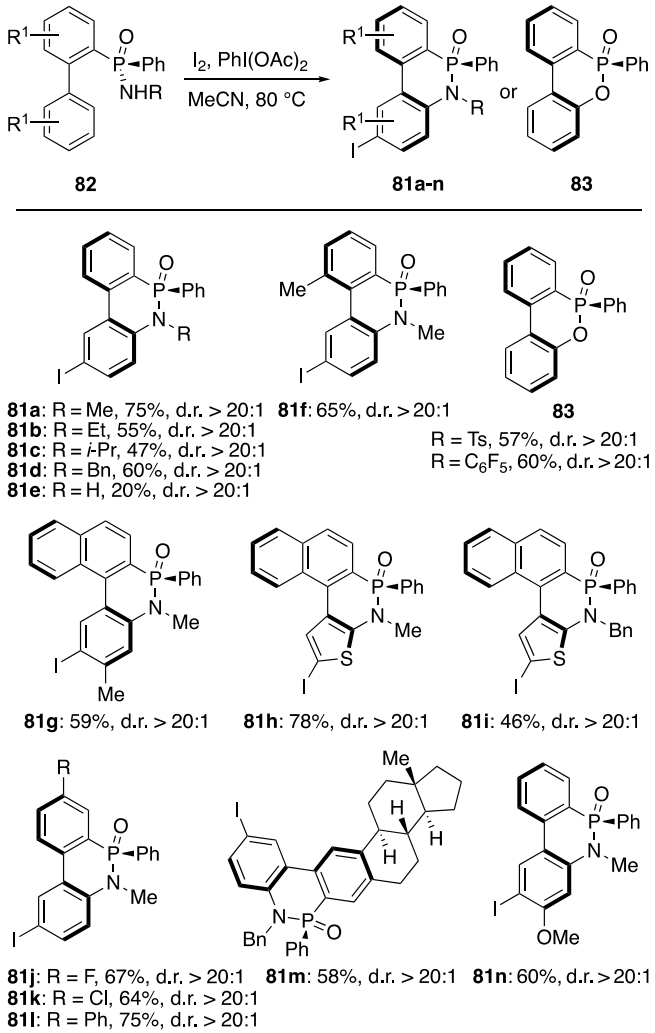

Scheme 33 Transition-metal free heteroannulation reaction to give azaphosphinines **81**.

To probe the mechanism of their hypervalent iodine-mediated heteroannulation, Yang and coworkers attempted the reaction in the presence of radical scavengers 2,2,6,6-tetramethylpiperidin-1-yl)oxyl (TEMPO) and butylated hydroxytoluene (BHT). The addition of either inhibited the reaction. Next, a noniodinated analogue **84** was reacted with $PhI(OAc)_2$ and I_2 under standard conditions and the corresponding product **81a** was isolated. This led the researchers to conclude that the iodination step occurs after the annulation. Their proposed radical mechanism for the transformation is shown in Scheme 34. The reaction is initiated by the homolytic cleavage of a weak N–I bond to generate a radical species, which is subsequently trapped by the nearby arene. This is rearomatized via $PhI(OAc)_2$ to give electron-rich **84**, which can rapidly iodinate to furnish the final heterocycle **81a**.

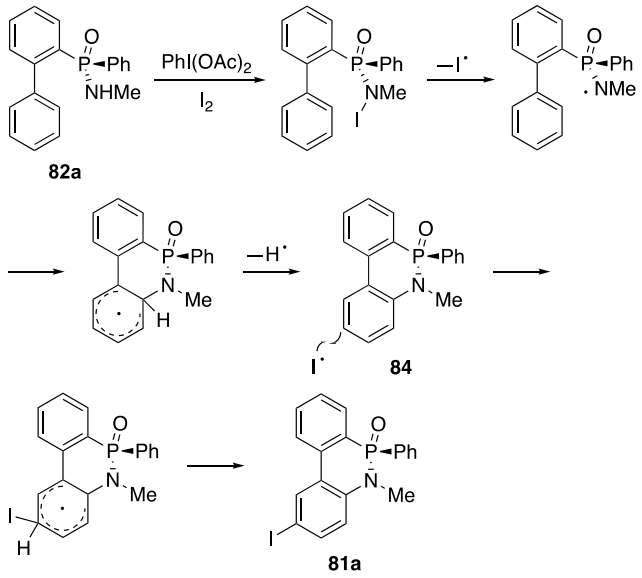

Scheme 34 Proposed mechanism for radical C–H activation heteroannulation and subsequent iodination.

Yang and coworkers showed that the aryl iodide generated during the heteroannulation could undergo typical cross-coupling reactions, providing examples of **81a** acting as a substrate in Heck, Suzuki-Miyaura, azidation, phosphination, and Cu(I)-catalyzed azide-alkyne cycloaddition (CuAAC) 'click' reactions in moderate to excellent yields and the typical high degree of diastereoselectivity. Finally, to prove the existence of the axial chirality component in their system, the P–N bond of **85** was selectively cleaved via addition of *n*-BuLi at –78 °C (Scheme 35). Once the rigidity of the aryl system was severed, racemization began, but at low temperatures the diastereomers **86** and **86'** were still detected, indicating axial chirality was preserved with a persistent *P*-stereogenic center. It was proposed that the inflexibility of the fully cyclized heterocycle retains the axial chirality under ambient conditions.

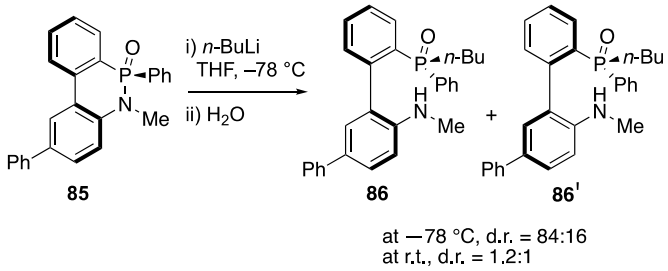

Scheme 35 Cleavage of P–N bond and racemization at different temperatures.

Han and coworkers published in 2017 a study that took a somewhat different approach to the dibenzo[*c,e*]-1,2-dihydro-1,2λ^5-azaphosphinine 2-oxide core.[75] As noted previously, the heteroannulation developed by Yang and coworkers did not tolerate electron-deficient *N*-protecting groups, the use of which resulted in oxygen substitution into the heterocycle. The authors proposed this lack of desired reactivity to be a result of difficulty in generating the necessary nitrogen radical. The Han study focused exclusively on the heteroannulation of *P*-stereogenic

phosphinamide **87** with a strongly electron-deficient *N*-pentafluorophenyl group (Scheme 36). To circumvent the issues found by Yang, the authors found an alternative method of radical oxidative heteroannulation using 2.2 equivalents of $Ce(NH_4)_2(NO_3)_6$ (CAN) at 40 °C to generate the desired heterocycles **88** in excellent yield with high enantiomeric excess, with several examples being prepared on the gram scale. At increased temperature and additional equivalents of CAN, they could also generate a nitrated analogue **89**, much in the same way Yang and coworkers iodinated their molecules. Both electron-rich and electron-deficient substituents were tolerated in the R^1 position; however, incorporating an electron-donating methoxy group into the R^2 position resulted in a high yield of the nitrated byproduct. This side reaction could be inhibited by addition of 10 equivalents of water to the reaction.

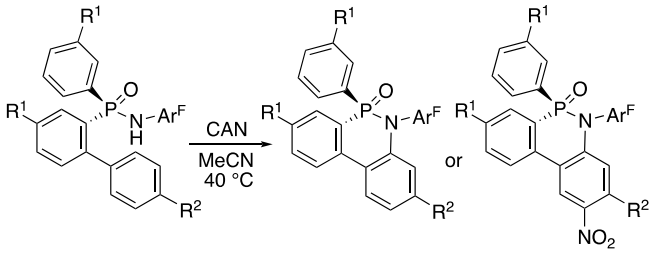

87 **88a-j** **89a,b**

88a-m, 89a-b: $Ar^F = C_6F_5$
88a: R^1 = Me, R^2 = Me, 93%, 97% e.e.
88b: R^1 = Me, R^2 = *t*-Bu, 91%, 94% e.e.
88c: R^1 = Me, R^2 = Br, 88%, 98% e.e.
88d: R^1 = Me, R^2 = CF_3, 83%, 85% e.e.
88e: R^1 = Me, R^2 = OMe, 63%, 91% e.e.[a]
88f: R^1 = *i*-Pr, R^2 = Me, 81%, 96% e.e.
88g: R^1 = H, R^2 = Me, 80%, 95% e.e.
88h: R^1 = OMe, R^2 = H, 93%, 87% e.e.
88i: R^1 = OMe, R^2 = Me, 93%, 85% e.e.
88j: R^1 = CF_3, R^2 = Me, 85%, 98% e.e.
89a: R^1 = Me, R^2 = Me, 65%, 99% e.e.[b]
89b: R^1 = Me, R^2 = OMe, 78%, 89% e.e.[c]

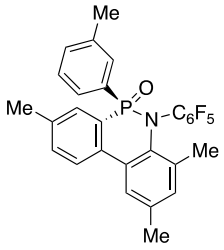

88k: 82%, 86% e.e.

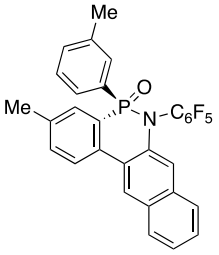

88l: 93%, 93% e.e.

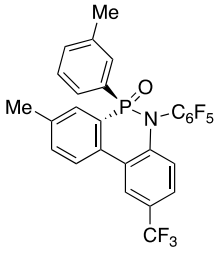

88m: 72%, 93% e.e.

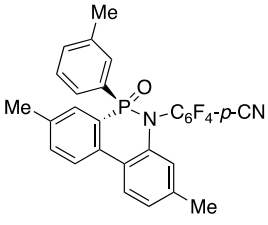

88n: 85%, 94% e.e.

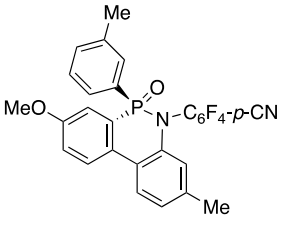

88o: 88%, 97% e.e.

Scheme 36 CAN-mediated heteroannulation to afford **88**. [a]10 equiv. of water added. [b]5 equiv. of CAN added and conducted at 60 °C. [c]Run for 2 h.

Further experiments were conducted examining the post-synthetic modifications available to the azaphosphinine core. In the interest of making *P*-stereogenic bidentate ligands (**90, 91**) for asymmetric catalysis, the P–N bond of **88a** could be cleaved by either LiMe or NaOMe (Scheme 37). Alternatively, conversion of **88a** to the sulfide **92** followed by treatment with MeOTf and then finally $P(NMe_2)_3$ gave the corresponding dibenzo[*c,e*]-1,2-dihydro-1,2λ^3-azaphosphinine, namely the P^{III} species **93**, in high overall yield.

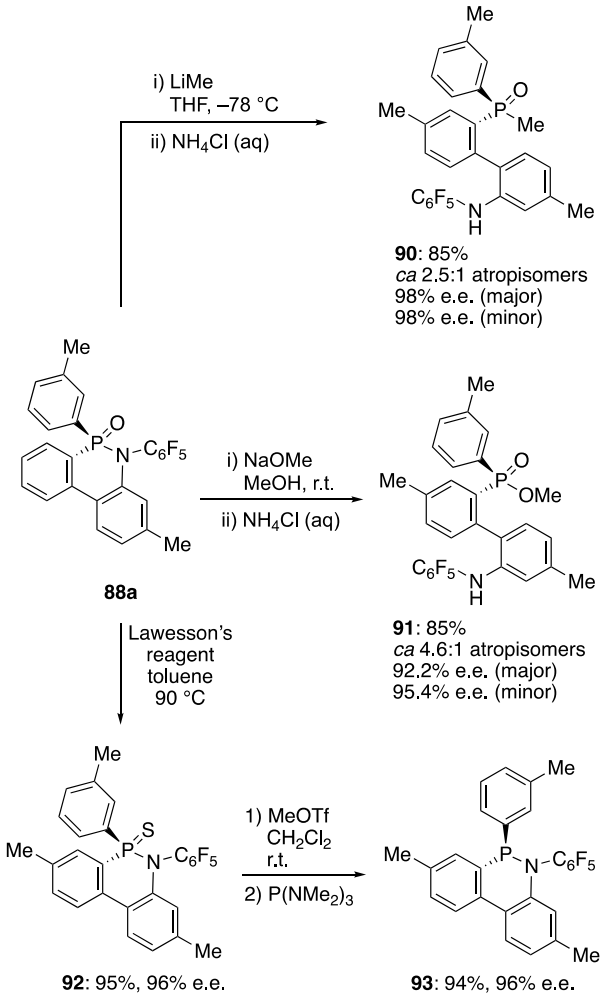

Scheme 37 Post-synthetic modification of **88a** to furnish chiral acyclic species **90** and **91**, and P^{III} species **93**.

Heterocycle **88a** could be used as a chiral LB catalyst in the condensation of enone **94** and benzaldehyde to furnish **95** (Scheme 38), similar to the reaction effected by Cramer in Scheme 16.[38] While the reaction proceeded in excellent yield, the diastereoselectivity and enantioselectivity were considerably lower than what was previously reported. Regardless, these experimental results in concert with those of Cramer heavily suggest such *P*-stereogenic species could find excellent application in asymmetric catalysis upon proper optimization.

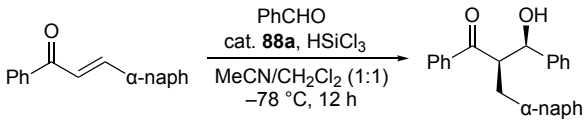

94 **95**: 94%
syn:anti = 83:17
60% e.e. for *syn* isomer

Scheme 38 Asymmetric catalyst **88a** used in condensation reaction.

In 2015, our lab published the first of over a dozen research articles on benzo[*e*]-1,2λ^5-azaphosphinines, benzo[*e*]-1,2-dihydro-1,2λ^5-azaphosphinine 2-oxides, and related fused systems. The team had been studying arylethynyl scaffolds as anion receptors when they serendipitously discovered[76] that *ortho*-ethynylanilines react with $P(OPh)_3$ in the presence of pyridine at elevated temperatures to affect a heteroannulation incorporating an equivalent of the phosphite (Table 5). This was an attractive discovery as it proved to be a robust and comparatively mild route to the benzo[*e*]-1,2λ^5-azaphosphinine core without the use of transition metals. The aniline starting materials **96** were also quite easy to diversify, with most being either commercially available or the products of one- or two-step Sonogashira cross-couplings. The direct result of the cyclization was the *P*-diphenoxy species **97**; however, these in general rapidly hydrolyzed to the corresponding dihydro molecules **98** either intentionally or during purification, depending on the derivative.

Table 5 Phosphite cyclization of *ortho*-ethynylanilines.

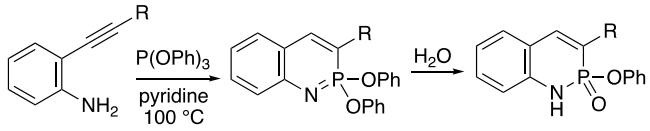

96 **97a-j** **98a-j**

R	Product	Yield **97** (%)	Yield **98** (%)
3,5-$(CF_3)_2C_6H_3$	**a**	__[a]	39
p-CNC_6H_4	**b**	54	79
p-$(CO_2Et)C_6H_4$	**c**	54	74
p-ClC_6H_4	**d**	__[a]	80
Ph	**e**	45	72
p-MeC_6H_4	**f**	63	82
p-$OMeC_6H_4$	**g**	56	66
p-$(NMe_2)C_6H_4$	**h**	68	__[a]
n-Pen	**i**	__[a]	73
2-pyridyl	**j**	71	31

[a]Not isolated.

Both azaphosphinines **97** and **98** display notable photophysical properties (Table 6). The authors comment that the emissive behavior is like that of the analogous carbostyril scaffold, with the key differences being an overall redder emission, stronger solvatochromism, and more acidic N–H bond. Deprotonating **98** with DBU resulted in a

strong bathochromic shift in emission of 22–124 nm. Following this initial publication, several more papers were published on the benzo[*e*]-fused scaffolds,[77–83] work that was summarized in an account in 2020.[39]

Table 6 Fluorescence properties of selected **97**, **98**, and deprotonated **98** in $CHCl_3$.

Cmpd	**97** λ_{em} (nm), Stokes shift (nm)	**98** λ_{em} (nm), Stokes shift (nm)	**98** + DBU λ_{em} (nm), Stokes shift (nm)
b	483, 83	430, 81, 4%[a]	554, 137, 41%[a]
c	473, 90	432, 81, 5%[a]	553, 151, 31%[a]
e	453, 80	418, 76	491, 127
f	450, 81	413, 72	482, 114
g	447, 78	410, 71	473, 107
j	467, 79	442, 79	514, 102

[a] Photoluminescent quantum yield; other molecules not measured.

The emissive data in Table 6 suggested that the photophysical properties of the resultant heterocycles are highly dependent on the electronic properties of the R-group. Knowing this, we broadened the substrate scope to include species with the group R^2 located para to the aniline nitrogen **99**, in turn yielding the more substituted series **100** (Scheme 39).[83] This facilitated a second handle with which to tune absorption and emission. It should be noted for nearly all subsequent studies that the pre-hydrolysis diphenoxy 'imidate' form **97** was not isolated, but rather all yields reflect both the cyclization and hydrolysis steps. There is no recognizable preference between R-groups in the yields, as both electron-rich and -deficient substituents result in modest to good yields (26–61%).

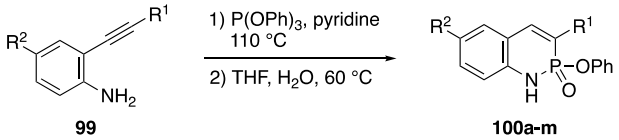

99 **100a-m**

100a: R^1 = *p*-CNC_6H_4, R^2 = CN, 26%
100b: R^1 = *p*-CNC_6H_4, R^2 = CF_3, 61%
100c: R^1 = *p*-CNC_6H_4, R^2 = Cl, 44%
100d: R^1 = *p*-CNC_6H_4, R^2 = *t*-Bu, 36%
100e: R^1 = *p*-$OMeC_6H_4$, R^2 = *t*-Bu, 44%
100f: R^1 = *p*-MeC_6H_4, R^2 = *t*-Bu, 50%
100g: R^1 = Ph, R^2 = *t*-Bu, 56%
100h: R^1 = 3,4-$(CN)_2C_6H_3$, R^2 = *t*-Bu, 34%
100i: R^1 = *p*-ClC_6H_4, R^2 = *t*-Bu, 60%
100j: R^1 = Ph, R^2 = CN, 42%
100k: R^1 = *p*-$OMeC_6H_4$, R^2 = CN, 30%
100l: R^1 = Ph, R^2 = CO_2Et, 55%
100m: R^1 = *p*-CNC_6H_4, R^2 = OEt, 54%

Scheme 39 Difunctionalized azaphosphinines **100**.

Compared to the series **98**, the addition of the second R-group added a new dimension to the understanding of how the electronic groups modulate the photophysics (Table 7), as donor and acceptor pairs typically resulted in redder absorption and emission. This effect was more prominent when the electron-withdrawing group was in the R^1-position and the electron-donating group was at R^2 (e.g., **100k** vs. **100m**).

Table 7 Photophysical properties of selected **100**.[a]

Cmpd	R^1	R^2	λ_{abs} (nm), ε (M^{-1} cm^{-1})	λ_{em} (nm), ϕ (%)[b]	Stokes shift (nm/cm^{-1})	Brightness (ε•ϕ)
100a	*p*-CNC_6H_4	CN	346, 12000	430, 18	84/5600	2160
100e	*p*-$OMeC_6H_4$	*t*-Bu	344, 16000	421, 6	77/5300	960
100f	*p*-MeC_6H_4	*t*-Bu	343, 14000	424, 8	81/5600	1120
100k	*p*-$OMeC_6H_4$	CN	345, 15000	471, 28	126/7800	4200
100m	*p*-CNC_6H_4	Oet	379, 25000	490, 24	111/6000	6000

[a]All values collected in $CHCl_3$ at room temperature. [b]Excited at 365 nm and collected using quinine sulfate (0.1 M H_2SO_4) standard.

Given the sensitivity of the photophysical properties to simple functional group substitutions, we next investigated the effect of arene backbone extension as well. These included heterocycles featuring pyreno[2,1-*e*]- **101**, naphtho[1,2-*e*]- **102**, naphtho[2,1-*e*]- **103**, and naphtho[2,3-*e*]- **104** fusion patterns (Scheme 40).[39,78–81]

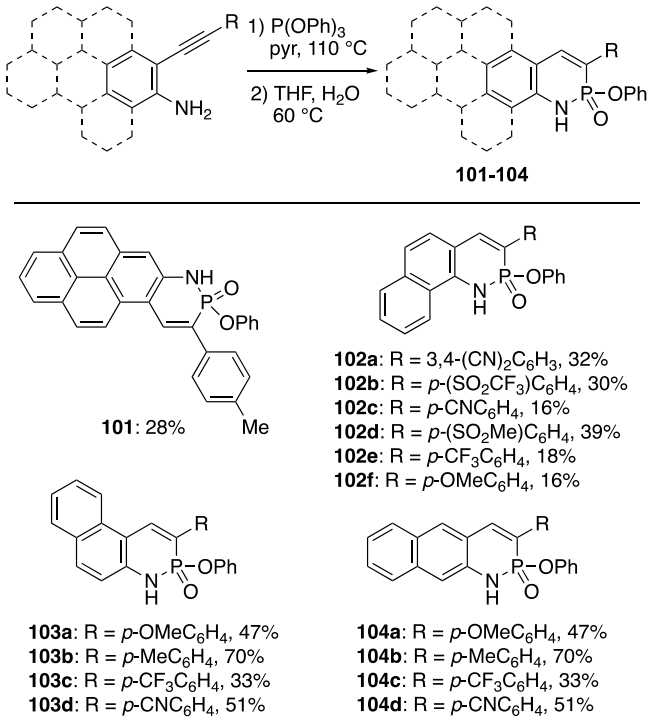

Scheme 40 Scope of arene-core extended azaphosphinines.

While simple modification of the aniline starting material could dramatically alter the final azaphosphinine topology, this did beg the question as to what impact, if any, would arise from alteration of the phosphorus substituent. By substituting $PhP(OPh)_2$ for $P(OPh)_3$, running the cyclization under the same conditions generated the analogous benzo[*e*]-1,2-dihydro-2-phenyl-1,2λ⁵-azaphosphinine 2-oxides **105** (Scheme 41).[77]

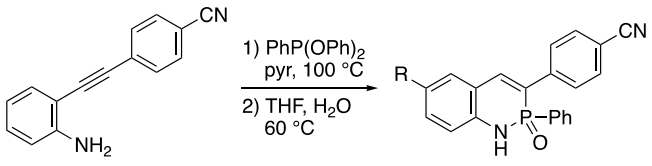

99 **105a-f**

105a: R = CN, 21% **105d**: R = H, 61%
105b: R = CF_3, 58% **105e**: R = *t*-Bu, 65%
105c: R = Cl, 31% **105f**: R = OEt, 31%

Scheme 41 *P*-phenyl substitution to afford azaphosphinines **105**.

In addition to P substitution, we explored the inclusion of the N atom in another ring to furnish heterocycles **106** (Scheme 42).[79] Ethynylpyrene **107**, the precursor of **101**, was cyclized using $PhP(OPh)_2$. The crude mixture was hydrolyzed and then iodinated under acidic conditions to give **108**, a *P*-phenyl analogue to **101**. Finally, Sonogashira cross-coupling followed by intramolecular cyclization of the alkyne with the NH group afforded π-extended and rigid **106** in good yields (63–87%).

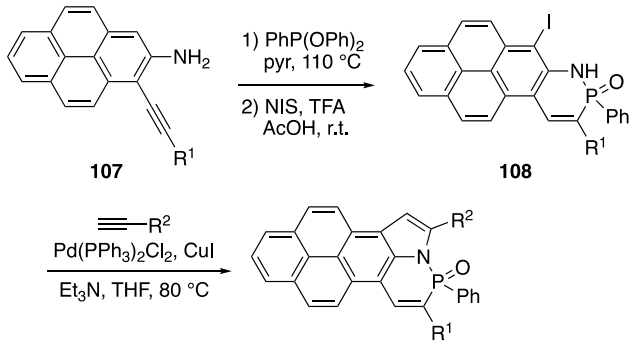

107 **108**

106a-d

106a: R^1 = *n*-Bu, R^2 = Ph, 87%
106b: R^1 = *n*-Bu, R^2 = *p*-$(NPh_2)C_6H_4$, 63%
106c: R^1 =. 3,5-$(CF_3)_2C_6H_3$, R^2 = Ph, 81%
106d: R^1 = 3,5-$(CF_3)_2C_6H_3$, R^2 = *p*-$(Ph_2N)C_6H_4$, 67%

Scheme 42 *P*-phenyl substituted PN-fused pyrenes **106**.

Comparison of the photophysical properties of the extended fused-arene core heterocycles (**101**–**104**) and the *P*-phenyl heterocycles **105** and **106** (Table 8) with those of **100** showed that the different families cover a wide range of values in all tabulated categories. As a result of the large linearly fused core, the naphtho[2,3-*e*]-fused **104** exhibit comparatively large absorption coefficients and red-shifted emissions; however, they also display quite low quantum yields, and as a result, possess consistently low brightness values. The two isomeric families of **102** and **103** display predictably similar absorption, emission, and Stokes shift values but deviate in terms of quantum yield. The 'bent-down' naphtho[1,2-*e*]-fused **102** family overall has a comparably high quantum yield with **102a** standing out dramatically at 93%. Conversely, the 'bent-up' naphtho[2,1-*e*]-fused **103** have significantly diminished quantum yield values that are comparable to the benzo-fused analogues **100**. Lastly, the *P*-phenyl derivatives **105** across the board are improvements over their *P*-phenoxy counterparts **100**. It is proposed that the enhancement of their quantum

yield and Stokes shift, as well as the overall red-shifting of emission, are all a result of the rigidification/reduced degrees of freedom of the scaffold and increased planarity of the aryl rings.

Table 8 Photophysical properties of selected heterocycles **101**–**106**[a]

Cmpd	λ_{abs} (nm), ε (M^{-1} cm^{-1})	λ_{em} (nm), ϕ (%)[b]	Stokes shift (nm/cm^{-1})	Brightness (ε•ϕ)
101	395, 26000	465, 70	70/3800	18000
102a	404, 12000	493, 93	89/4500	11000
102b	397, 5200	490, 80	93/4800	4100
103a	384, 13000	461, 12	77/4300	1600
103b	375, 9800	450, 10	75/4400	980
104a	339, 27000	464, 7	125/7900	1900
105a	348, 15000	447, 76	99/6400	11400
106b	431, 32000	551, 62	120/5100	20000
106d	437, 42000	622, 23	185/6800	9700

[a]Values collected in $CHCl_3$ at room temperature. [b]Excited at 365 nm and collected using a quinine sulfate (in 0.1 M H_2SO_4) standard.

The pyreno[2,1-*e*]- heterocycle **101** enjoys both a large quantum yield and absorption coefficient, resulting in one of the highest brightnesses of the data set. Despite this, the small Stokes shift value presents a potential issue with self-quenching and could be modulated with further functional group tuning, i.e., the **106** series. Among the azaphosphinines synthesized from our lab, compounds **106** stand in a league of their own for photophysical properties. While all of them exhibit comparatively high brightness and quantum yields, **106a** and **106d** exhibit the highest brightness value and most red-shifted emission tabulated, respectively. Fascinatingly, it was found that there was little-to-no charge transfer between excited pyrene units in mixtures of **106**, and the authors were able to show near-perfect solution-state white light emission in a mixture of **106a**, **106b**, and **106d**.[79]

One of the unique benefits of the heteroannulation reaction studied by our lab is the hydrogen-bond donating N–H motif resulting from the hydrolysis. Up until this point, nearly all azaphosphinine systems discussed contain either *N*-alkyl or *N*-aryl groups (e.g., **43**, **57**) or are sp^2 nitrogen centers with no possible proton (e.g., **49**, **97**). As previously noted, **98** can be deprotonated to dramatic effect in terms of heterocycle emission. However, we also performed extensive studies in using that site as a hydrogen-bond donor as generally the molecules form homodimers that are oriented in a head-to-tail fashion (Fig. 5), as the highly polarized phosphonyl acts as hydrogen bond acceptor to complement the N–H bond donor.

With exception of the **104** and **106**, we have assessed all their azaphosphinines for homodimerization strength (K_{dim}). The experiments are conducted via variable concentration (VC) ^1H and ^{31}P NMR experiments in water-saturated $CDCl_3$ at room temperature (Table 9). From the compiled data, it is noted that electron-deficient ring systems result in a higher dimerization constant (e.g., **100j**), as the N–H bond is being further polarized, which in turn generates a stronger hydrogen bond donor. For series **100**, the identity of the R^2 group on the fused benzene

core has a greater impact than the identity of the R^1 aryl substituent, which is thought to be a result of closer proximity to the hydrogen-bonding face. Lastly, the *P*-phenyl derivatives **105** consistently show lower dimerization values compared to their *P*-phenoxy **100** counterparts due to greater steric repulsion from proximity of the Ph group at the hydrogen-bonding face. Interestingly, X-ray crystallographic analysis of several dimers in the solid state mirror the solution data—those with the largest K_{dim} values exhibit the shortest intermolecular N•••O distances (e.g., 2.768(2) Å for **100j**), and those with small K_{dim} values exhibit the longest N•••O distances (e.g., 2.856(11) Å for **98g**) (Fig. 5).[83] In the solid state, nearly every heterocycle dimerizes as the *meso*-dimer with one *R*- and one *S*-enantiomer, although a few solid-state structures possess a polymeric zigzag ribbon structure (e.g., **100b**), likely due to steric issues within the structure.

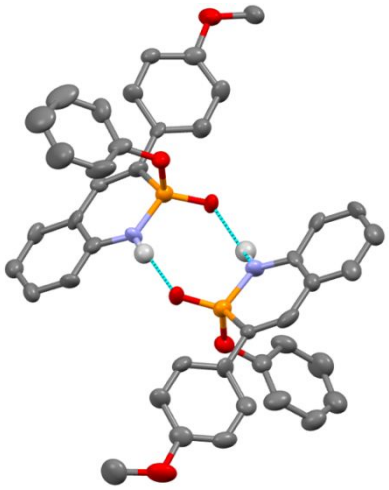

Fig 5. Representative *meso*-dimer of **98g**. Blue dashed lines represent hydrogen bonds between phosphonamidate moieties. Nonparticipating hydrogen atoms omitted for clarity.

Table 9 VC ^{1}H and ^{31}P NMR–measured dimerization constant for select azaphosphinines.

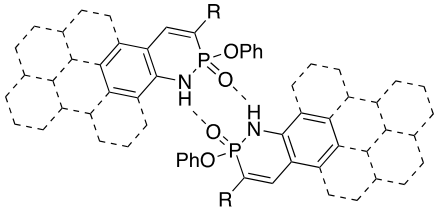

Heterocycle	K_{dim} (M^{-1}) [a]	Heterocycle	K_{dim} (M^{-1}) [a]
98e	62	**102b**	306
98g	56	**102e**	84
100b	293	**102f**	77
100j	525	**103a**	206
100l	200	**103b**	150
101	179	**105b**	82

[a]Values collected at room temperature in water saturated $CDCl_3$.

In 2020, our lab outlined a protocol for the thionation of the benzo[*e*]-fused systems using Lawesson's reagent (Scheme 43).[84] The reaction was conducted on both *P*-phenoxy **100** and *P*-phenyl **105**. Comparison of the photophysical properties of the thionated heterocycles **109** to the previously synthesized oxo-analogues (Table 10) showed that there was no apparent change to the absorption profiles upon thionation; however, it was noted that there was a substantial reduction in brightness values and a consistent ~20 nm redshift of emission, which was attributed to a lower S_1 excited state level resulting from the weaker P–S bond.

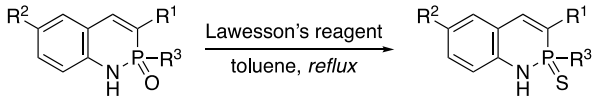

100, 105 **109a-f**

109a: R^1 = *p*-MeC_6H_4, R^2 = *t*-Bu, R^3 = OPh, 27%
109b: R^1 = *p*-CNC_6H_4, R^2 = H, R^3 = OPh, 60%
109c: R^1 = *p*-CNC_6H_4, R^2 = *t*-Bu, R^3 = OPh, 60%
109d: R^1 = *p*-CNC_6H_4, R^2 = H, R^3 = Ph, 59%
109e: R^1 = *p*-CNC_6H_4, R^2 = *t*-Bu, R^3 = Ph, 89%
109f: R^1 = *p*-CNC_6H_4, R^2 = CF_3, R^3 = Ph, 59%

Scheme 43 Lawesson's reagent-mediated thionation.

Table 10 Photophysical properties of selected **109**.[a]

Cmpd	λ_{abs} (nm), ε (M^{-1} cm^{-1})	λ_{em} (nm), ϕ (%)[b]	Stokes shift (nm/cm^{-1})	Brightness (ε•ϕ)
109a	348, 7180	444, 2	96, 6200	140
109b	352, 8600	462, 6	110, 6800	520
109e	373, 7950	492, 8	119, 6500	640
109f	357, 6840	466, 2	109, 6600	140

[a]Values collected in $CHCl_3$ at room temperature. [b]Excited at 365 nm and collected using a quinine sulfate (in 0.1 M H_2SO_4) standard.

Later entries on azaphosphinine chemistry from our lab focused primarily on the introduction of a second nitrogen atom in the fused ring. The pyrido[*e*]-1,2-dihydro-1,2λ^5-azaphosphinine 2-oxides were synthesized in a similar manner using aminopyridine substrates **110** in place of anilines (Scheme 44). The first of these reports focused on a family of pyrido[2,3-*e*]- fused heterocycles **111** that displayed unexpected tautomerization capabilities,[85] as X-ray crystallography revealed that **111a-d** underwent a prototropic tautomerization in the solid-state to assume the corresponding non-aromatic form **111'**. Only fluorinated **111e** did not undergo tautomerization in the solid state, which was attributed to the diminished basicity of the pyridyl nitrogen. Because of the regioselectivity of the alkylation from **111** to **112**, the quinoidal orientation of the core could be trapped, leading to stable samples that could be further analyzed in solution. A combination of photophysical, computational, and NMR experiments revealed that the tautomer only existed in the solid state, leading the authors to conclude that the heterocycles remained in their aromatic form in solution, regardless of environment, and tautomerized as a packing

effect. Greater intermolecular forces resulting from solidification promoted the tautomerization to **111'** to allow the heterocycles to arrange in long coordination polymer-like chain of head-to-tail self-association. Computed relative free energies indicated that there is a 6.3 kcal mol^{-1} stabilizing effect for the observed tautomerization when the azaphosphinines is protonated, indicating how a close-knit hydrogen-bonding network may shift the tautomeric preference.

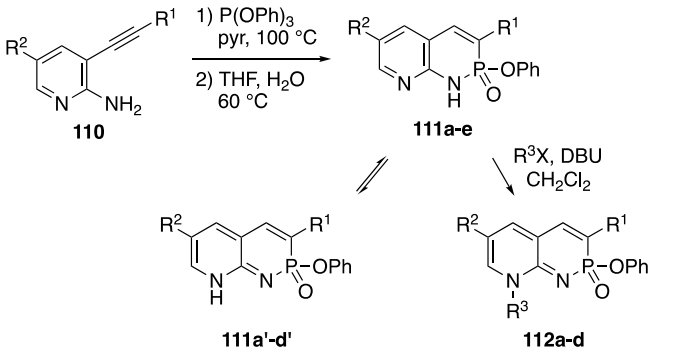

111a-d, 112a-d: R^2 = H
111a: R^1 = *p*-MeC_6H_4, 38%
111b: R^1 = *p*-$OMeC_6H_4$, 35%
111c: R^1 = *p*-$CF_3C_6H_4$, 38%
111d: R^1 = *p*-CNC_6H_4, 39%
111e: R^1 = *p*-MeC_6H_4, R^2 = F, 29%
112a: R^1 = *p*-MeC_6H_4, R^3 = Me, 20%
112b: R^1 = *p*-$CF_3C_6H_4$, R^3 = Me, 61%
112c: R^1 = *p*-CNC_6H_4, R^3 = CH_2CH_2OH, 39%
112d: R^1 = *p*-MeC_6H_4, R^2 = F, R^3 = Me, 41%

Scheme 44 Pyrido-fused azaphosphinines **111** and their trapped tautomeric forms **112.**

The second publication on pyrido[*e*]1,2λ^5-azaphosphinine 2-oxides focused on cyclization of 3-aminopyridines **113** to furnish pyrido[3,4-*e*]-1,2λ^5-azaphosphinine **114** and corresponding dihydro **115** (Scheme 45), molecules that possessed a donor-acceptor conjugated system through the azaphosphinine scaffold.[86] By orienting the pyridyl nitrogen via this fusion pattern, a linear conjugation network was established from the electron-withdrawing pyridine to the aryl substituent of the azaphosphinine ring. After preparing several derivatives of **114** and **115** with varying degrees of electron donation from group R, assessment of the optoelectronic properties (Table 11) showed the presence of a low energy absorption band. The absorption coefficient of this peak increased linearly with electron donation and was attributed to an internal charge transfer (ICT) band, which became the dominant transition in the strong donor-acceptor pairs **114d** and **115d**. As a result of this intense conjugation, these heterocycles became the model system for the azaphosphinine scaffold as a charge transfer system. The emission spectra of **114d** and **115d** exhibited intense solvatochromism of 63 and 52 nm, respectively, in solvents ranging from toluene to DMSO. The pair also displayed comparatively high quantum yields with **115d** reaching 90%, likely due to the rigidity of the scaffold in the quinoidal ICT state.

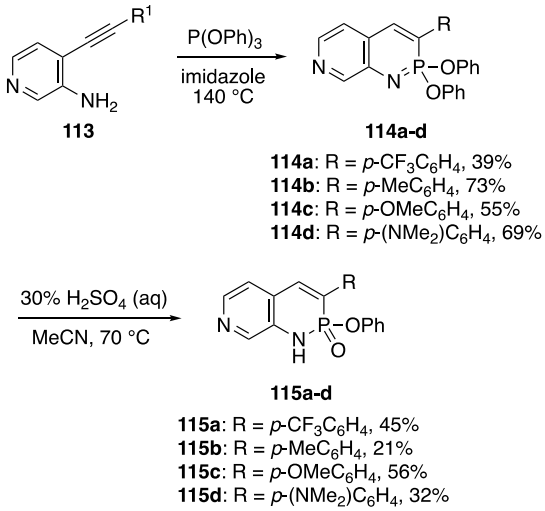

113 **114a-d**

114a: R = *p*-$CF_3C_6H_4$, 39%
114b: R = *p*-MeC_6H_4, 73%
114c: R = *p*-$OMeC_6H_4$, 55%
114d: R = *p*-$(NMe_2)C_6H_4$, 69%

115a-d

115a: R = *p*-$CF_3C_6H_4$, 45%
115b: R = *p*-MeC_6H_4, 21%
115c: R = *p*-$OMeC_6H_4$, 56%
115d: R = *p*-$(NMe_2)C_6H_4$, 32%

Scheme 45 Pyrido[3,4-*e*]-fused azaphosphinines.

Table 11 Photophysical properties of selected **114** and **115**.[a]

Cmpd	High-energy λ_{abs} (nm), ε (M^{-1} cm^{-1})	Low-energy λ_{abs} (nm), ε (M^{-1} cm^{-1})	λ_{em} (nm), ϕ (%)[b]	Stokes Shift (nm/cm^{-1})[c]
114a	295, 15800	390, 7200	475, 22	85, 4590
114b	310, 14000	385, 7700	459, 9	74, 4190
115c	331, 14000	351, 13400	415, 45	64, 4390
115d	330, 4500	405, 21000	489, 90	84, 4240

[a]Values collected in $CHCl_3$ at room temperature. [b]Excited at 365 nm and collected using standards of quinine sulfate (in 0.1 M H_2SO_4) and anthracene in EtOH. [c]Calculated from low-energy ICT band.

In 2019, our lab took advantage of the hydrogen-bond donating and accepting ability of **100** by incorporating an azaphosphinine group into a supramolecular receptor for binding hydrogen sulfate (HSO_4^-).[82] HSO_4^- is typically seen as a contaminant in agricultural and industrial fields.[87] Oxoanions in general make poor guests in anion host-guest complexes because of their mix of hydrogen-bond acceptors and donors as well as relatively oblong or tetrahedral geometries when compared to more spherical guests like halides. The nonplanar alignment of the hydrogen-bond accepting P=O and hydrogen bond donating N–H provides a unique and complementary pocket for the non-spherical HSO_4^- anion. In this instance a stronger host-guest interaction results when compared to a more planar receptor such as an analogous bis-urea species.[88–91] To prepare this new host, **100d** was iodinated to yield **100d'** (Scheme 43). This was attached to one of two aryl-ethynyl arms (**116**) via Sonogashira cross-coupling followed by urea formation to ultimately generate receptors **117**. This receptor class not only recognized HSO_4^- selectively over all other competing anions (Table 12) but could also be recycled for further use by washing the host-guest complex in aqueous media. This high level of selectivity for the HSO_4^- anion (~40:1 for **117b**) results not only from the tetrahedral phosphorus center but also the mix of hydrogen bond donors and acceptors in the azaphosphinine core that maps ideally to the mix of donors and acceptors in HSO_4^-.

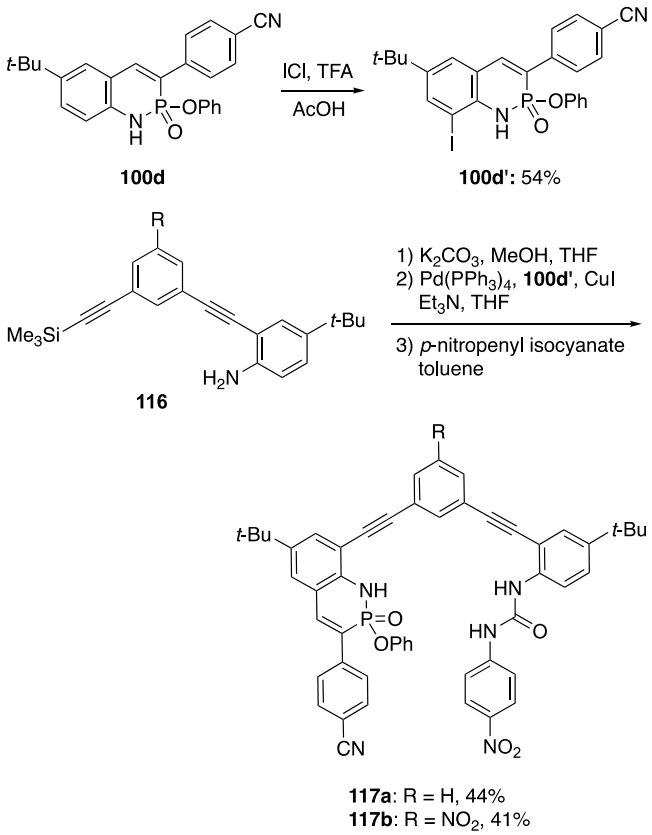

Scheme 46 Synthesis of azaphosphinine-based anion receptors **117**.

Table 12 Association constants[a] (K_a, M^{-1}) of receptors **117** with various anions in 10 vol% DMSO-d_6/$CDCl_3$ at room temperature.

Anion	**117a**	Relative Affinity[b]	**117b**	Relative Affinity[c]
HSO_4^-	1420 (1480)	1	9600 (10500)	1
NO_3^-	40 (30)	0.028	105 (100)	0.011
Cl^-	200	0.14	260	0.027
Br^-	30	0.021	75	0.008
I^-	—[d]	0	20	0.002
ClO_4^-	—[d]	0	—[d]	0

[a]1:1 binding fit. All reported association constants represent the average value from triplicate titrations. The values derived from ^{31}P NMR titrations are given in parentheses. Uncertainties less than 15%. All anions used as TBA salts. [b]Relative to the ^1H NMR titration derived K_a of **117a**•HSO_4^-. [c]Relative to the ^1H NMR titration derived K_a of **117b**•HSO_4^-. [d]No binding or too weak to be quantified.

Very recently, our lab published work describing the application of benzo[*e*]-1,2-dihydro-1,2λ^5-azaphosphinine 2-oxides for cellular imaging.[92] Use in cellular imaging is often a long-term goal for small molecule fluorophores. While this field is typically dominated by more traditional dyes (e.g., coumarins, xanthenes, cyanines etc.),[93–95] we envisioned the easily functionalized and emissive azaphosphinines our lab has developed as promising candidates as well. Initial studies proved that **118** (Fig. 6) was not only cell permeable at 0.5% DMSO in water but also maintained

its weak emission (λ_{em} = 452 nm, ϕ = 23%) inside HeLa cells. Encouraged by this initial result, we developed successive generations **119** and **120**. Molecule **119** introduced both *N*-methyl substitution, which decreased pH sensitivity, and an aryl ester functional handle, which redshifted the emission (λ_{em} = 499 nm, ϕ = 23%). Cytotoxicity measurements taken of **119** in HeLa cells suggested negligible cytotoxicity after 30 min in concentrations up to 150 μM. The next iteration of the initial cell dyes, **120**, was designed with the addition of a morpholine appendage for sub-cellular targeting, as the morpholine group is commonly used for lysosome targeting due to its basic nature.[96] While **120** had almost the exact same emission as **119**, the quantum yield was significantly higher (λ_{em} = 500 nm, ϕ = 50%). To test specific subcellular localization of **120**, three different concentrations (1, 3, and 5 μM) were co-incubated with 50 nM LysoTracker Deep Red in HeLa cells. The colocalization fidelity was measured using the Pearson correlation coefficient, revealing moderate colocalization for the three concentrations with Pearson coefficients of 0.49, 0.61, and 0.65 respectively. The success of this experiment was showing the cell permeability, lack of cytotoxicity, and broad pH stability range in the azaphosphinine core, suggesting future work could be done to further optimize successive generations of azaphosphinine dyes with subcellular targeting capabilities.

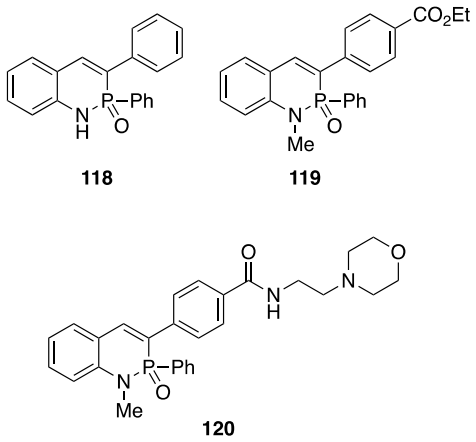

Fig. 6 Benzo[*e*]-1,2-dihydro-1,2λ^5-azaphosphinine 2-oxide cellular imaging dyes.

In 2021 Park and coworkers disclosed the preparation of a highly substituted benzo[*e*]-1,2λ^3-azaphosphinine following a similar synthetic thread to previous publications, cyclizing *o*-(phenylethynyl)aniline **96e** with phenylphosphonyl dichloride ($PhPOCl_2$) under basic conditions at extremely high temperature (Scheme 47).[97] After screening a variety of bases, using 0.5 equivalents of DBU in 1,2,4-trichlorobenzene (TCB) furnished the desired product **121** good yield. Installation of two more phenyl substituents via Chan-Lam and Suzuki cross-coupling reactions gave **122** and **123**, respectively. Finally, to reduce the system from P^V to P^{III}, **123** was first thionated with Lawesson's reagent leading to **124** and then lastly methylated with MeOTf followed by $P(NMe_2)_3$ yielding **125**. Unlike its carbocyclic analogue tetraphenylnaphthalene (TPN), X-ray crystallographic analysis of **125** showed all four phenyl substituents were perpendicular to the core, indicating poor conjugation through the whole system; nonetheless, cyclic voltammetry of **125** revealed a diminished HOMO-LUMO energy gap compared to TPN (2.75 vs 3.83 eV).

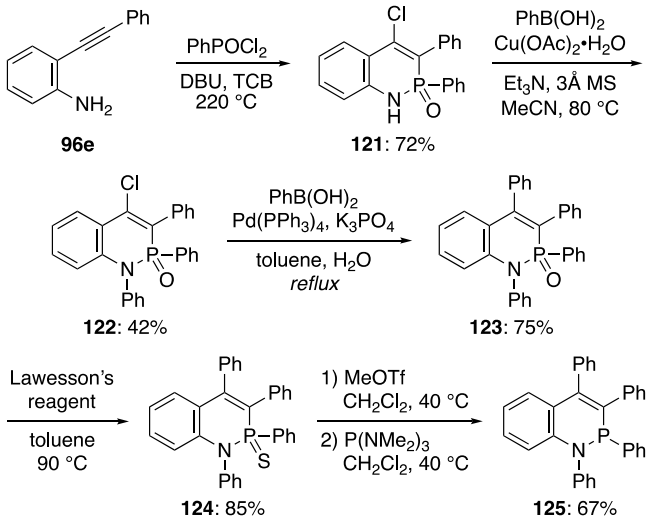

Scheme 47 Synthesis of azaphosphinine **125**.

A recent addition to this field comes from Deng et al. in 2022, which took a new approach to the Pd-catalyzed route to dibenzo[*c*,*e*]-1,2λ^5-azaphosphinines.[98] Instead of the typical approach, which until this point has involved P^V starting materials that are then incorporated into the final azaphosphinine, this publication used P^{III} phosphanamines **126**. Much like the similar work from Shi and coworkers[62] published in 2023, the trivalent phosphorus starting materials are oxidized to the pentavalent state during the heteroannulation. However, unlike Shi and coworkers the reaction explored in this work did not involve any intermolecular condensations or additions to furnish the final azaphosphinines. Instead, halide functional handles on the biphenyl substituent of the phosphanamines were used to close the azaphosphinine ring and generate a series of dibenzo[*c*,*e*]-1,2λ^5-azaphosphinines **127** (Scheme 48). In terms of substrate scope, Deng et al. first explored achiral phosphanamines with identical *P*-substituents. They synthesized a wide library of **127** containing functional groups of varying electronic character in the biphenyl backbone (**127a**-**w**) including alkenyl, alkynyl, heteroaromatic, and acene fusions. Despite the wide variety of biphenyl substituents, the only derivative that saw a drop in yield from the usual 68–92% range was the binapthyl derivative **127ai**. Next, several P-substituents were tried (**127w**–**aa**). It was noted that less sterically hindered groups such as cyclohexyl or *i*-Pr resulted in diminished yields.

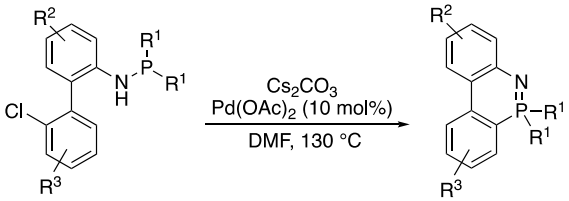

126 **127**

127a-v: R^1 = *t*-Bu
127a: R^2 = *m*-Me, R^3 = H, 79%
127b: R^2 = *p*-Me, R^3 = H, 85%
127c: R^2 = H, R^3 = *p*-Me, 86%
127d: R^2 = H, R^3 = *m*-Me, 68%
127e: R^2 = *p*-*i*-Pr, R^3 = H, 88%
127f: R^2 = *p*-*t*-Bu, R^3 = H, 79%
127g: R^2 = *p*-OMe, R^3 = H, 92%
127h: R^2 = H, R^3 = *p*-OMe, 72%
127i: R^2 = *p*-F, R^3 = H, 90%
127j: R^2 = H, R^3 = *m*-F, 81%
127k: R^2 = H, R^3 = *o*-F, 72%
127l: R^2 = 3,4-$(F)_2$, R^3 = H, 91%
127m: R^2 = *m*-Cl, R^3 = H, 86%
127n: R^2 = *p*-Cl, R^3 = H, 85%
127o: R^2 = H, R^3 = *p*-Cl, 72%
127p: R^2 = H, R^3 = *m*-Cl, 87%
127q: R^2 = *p*-OCF_3, R^3 = H, 98%
127r: R^2 = H, R^3 = *m*-CF_3, 89%
127s: R^2 = *p*-CN, R^3 = H, 82%
127t: R^2 = *p*-CO_2Et, R^3 = H, 85%
127u: R^2 = *p*-Ph, R^3 = H, 89%
127v: R^2 = *p*-$(NPh)_2$, R^3 = H, 69%
127w-aa: R^2 = R^3 = H
127w: R^1 = Cy, 25%
127x: R^1 = *i*-Pr, 56%
127y: R^1 = Ad, 70%
127z: R^1 = Ph, 64%
127aa: R^1 = 1-naphthyl, 83%

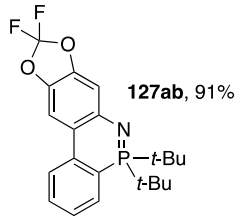

127ab, 91%

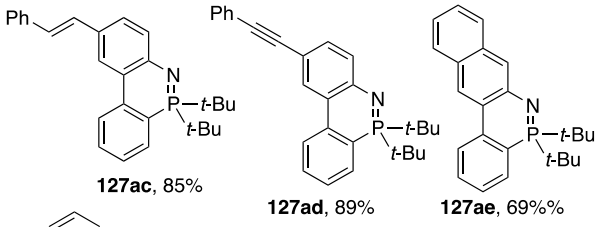

127ac, 85% **127ad**, 89% **127ae**, 69%%

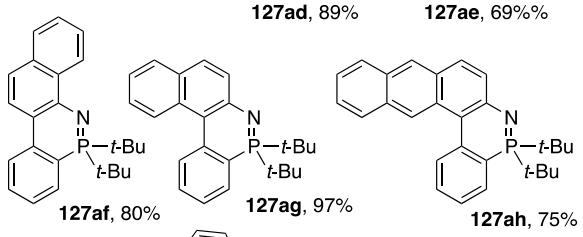

127af, 80% **127ag**, 97% **127ah**, 75%

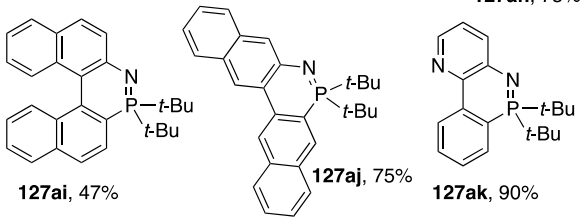

127ai, 47% **127aj**, 75% **127ak**, 90%

Scheme 48 Pd-catalyzed heteroannulation of achiral phosphanamines **126** to furnish dibenzo[*c*,*e*]-1,2λ^5-azaphosphinines **127**.

Next, Deng et al. decided to investigate the stereospecificity in their heteroannulation. First a library of chiral phosphanamines were isolated via HPLC, then these enantioenriched starting materials were protected by complexing with borane to furnish **128**. These chiral complexes were then subjected to the same heteroannulation conditions developed previously to ultimately yield **129** (Scheme 49). In almost every substrate used, the chiral

heteroannulation resulted in an excellent e.e. of >99%. The extremely high and consistent stereoretention in such a comparatively simple system is very promising for future directions. Retention of stereocenters when converting directly from an acyclic to cyclic phosphorus species is a useful tool in the development of targeted phosphorus heterocycles, azaphosphinine or otherwise.

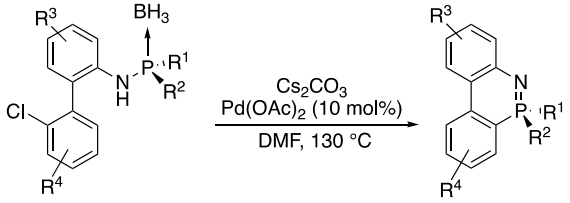

128 **129**

129a-c: R^1 = Ph, R^2 = *t*-Bu
129a: R^3 = R^4 = H, 85%, 99% e.e.
129b: R^3 = R^4 = *p*-OMe, 69%, >99% e.e.
129c: R^4 = *p*-F, R^4 = H, 58%, 99% e.e.
129d-g: R^3 = R^4 = H
129d: R^1 = Ph, R^2 = Cy, 81%, >99% e.e.
129e: R^1 = Ph, R^2 = *i*-Pr, 87%, >99% e.e.
129f: R^1 = *o*-MeC_6H_4, R^2 = *t*-Bu, 72%, >99% e.e.
129g: R^1 = Cy, R^2 = *t*-Bu, 61%, 84% e.e.

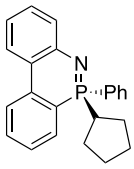

129h, 77%, >99% e.e.

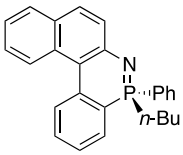

129i, 93%, >99% e.e.

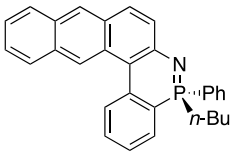

129j, 83%, >99% e.e.

Scheme 49 Retention of stereogenic P-center in heteroannulation of phosphanamine **128**.

Deng et al. continue to note that **127** are quite emissive and display both solution and solid-state fluorescence with high quantum yields, with **127s** especially exhibiting 77% in CH_2Cl_2. Due to the range of λ_{em} in **127**, the authors calculated the frontier molecular orbitals of their dibenzo[*c*,*e*]-1,2λ^5-azaphosphinines scaffold to determine what regions made the highest contributions to the HOMO and LUMO. Interestingly, it was found that C(2), located *para* to the nitrogen atom made the highest contribution to the HOMO and none to the LUMO. Conversely, C(9) located *para* to the phosphorus provided the opposite effect. The consequence of these contributions is represented in the photophysical properties of **127s** vs **127r**. In the former, the electron-withdrawing nitrile lowers the energy of the HOMO, blueshifting the emission (450 nm), while the energy of the LUMO is lowered in the latter due to the trifluoromethyl substituent, leading to a redder emission (505 nm).

1,3-Azaphosphinines

Heteroatom Exchange

1,3-Azaphosphinines are significantly less studied than their 1,2-azaphosphinine counterparts, yet there are still several papers exploring their preparation and post-synthetic modification.[99] A vast majority of the methods used to prepare the 1,3λ^3-azaphosphinine motif begin with a nitrogen-containing heterocycle to which a phosphorus atom is then added. One of the most direct and earliest examples of this was shown by Märkl and Dorfmeister in 1987.[100] Building off work forming 1,3-azaphospholes, they converted a series of triaryl-1,3-azapyrilium tetrafluoroborate salts **130** into the respective 1,3λ^3-azaphosphinine products **131** in the presence of tris(trimethysilyl)phosphane in modest yields (Scheme 50).[101,102]

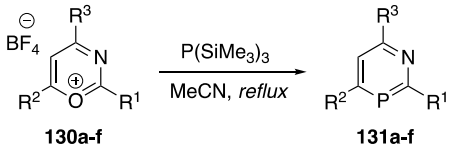

130a-f **131a-f**

131a: $R^1 = R^2 = R^3$ = Ph, 26%
131b: R^1 = *p*-MeC_6H_4, $R^2 = R^3$ = Ph, 21%
131c: $R^1 = R^2$ = Ph, R^3 = *p*-MeC_6H_4, 18%
131d: $R^1 = R^3$ = Ph, R^2 = *p*-MeC_6H_4, 20%
131e: R^1 = *p*-ClC_6H_4, $R^2 = R^3$ = Ph, 24%
131f: R^1 = *p*-ClC_6H_4, R^2 = Ph, R^3 = *p*-MeC_6H_4, 26%

Scheme 50 Conversion of azapyrilium tetrafluoroborate salts to 1,3λ^3-azaphosphinines **131**.

Treating the 2,4,6-triphenyl derivative **131a** with phenyl lithium added a phenyl group to the phosphorus center to afford phosphinyl anion **132**, and subsequent protonation by water gave non-aromatic 2,3-dihydro-1,3λ^3-azaphosphinine **133** (Scheme 51). Alternatively, **131a** could react as a diene in a [4 + 2] cycloaddition with either DMAD or methyl propiolate followed by cycloreversion to extrude benzonitrile, forming phosphinines **134a** or **134b**, respectively, in good yields.

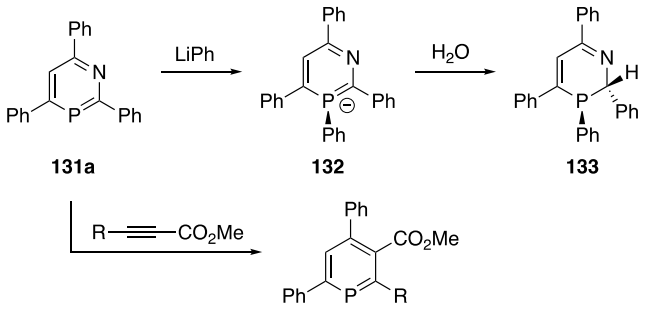

131a **132** **133**

134
134a: R = CO_2Me, 64%
134b: R = H, 76%

Scheme 51 Probing the reactivity of azaphosphinine **131a**.

Pericyclic / Cycloadditions

About the same time as Märkl's study, Appel et al. showed, also in 1987, that reaction of *α*-pyrone analogue **135** with two different phosphaalkynes resulted in formation of 1,3λ^3-azaphosphinines **136** (Scheme 52)[103] via Diels-Alder

reaction and subsequent evolution of CO_2 gas. Yields were not reported for this reaction. While a brief study, it laid the groundwork for many future works by proving that the 1,3λ^3-azaphosphinine moiety can be synthesized, isolated, and spectroscopically characterized. Specifically, several examples follow the cycloaddition/cycloreversion method instead of the above-mentioned heteroatom exchange, likely owing to synthetic flexibility.

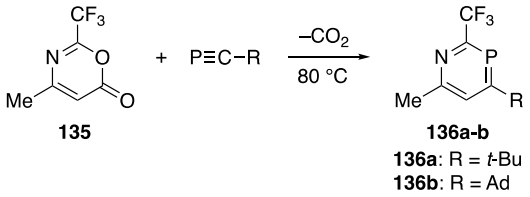

135 **136a-b**
136a: R = *t*-Bu
136b: R = Ad

Scheme 52 Diels-Alder route to 1,3λ^3-azaphosphinines **136**.

In 1988, Regitz and coworkers explored the reactivity of tri-*tert*-butylazete **137** and showed the molecule could undergo [4+2] cyclization with (2,2-dimethylpropylidyne)phosphane to generate Dewar benzene-like **138** in very good yield (Scheme 53).[104] The authors then explored the reactivity of **138** upon exposure to heat and light, which isomerized to form prismane **139** and 1,3λ^3-azaphosphinine **140**, respectively. Interestingly, prismane **139** slowly rearranged to 1,4λ^3-azaphosphinine **141** at room temperature, which could then be irradiated to form azaphosphabenzvalene **142** that also aromatizes to **140** upon heating.[105] These unusual transformations all resemble those observed for the purely hydrocarbon benzene valence isomers $(CH)_6$.[106]

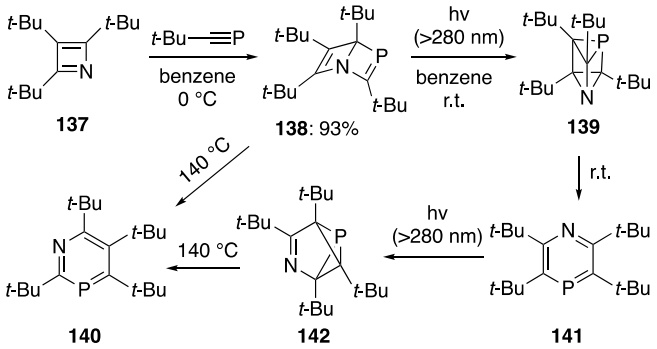

137 **138**: 93% **139**

140 **142** **141**

Scheme 53 Complex synthetic pathway leading to either 1,3λ^3- or 1,4λ^3-azaphosphinines.

The next entry into the family of 1,3-azaphosphinines came in 1989, where Appel and Poppe expanded upon their initial work with oxazinone **135** by performing a cycloaddition with an *N*-silyl-phosphaalkyne to produce intermediate **143**, which then extruded CO_2 gas to afford 4-silylamino-1,3λ^3-azaphosphinine **144** (Scheme 54).[107] Subsequent hydrolysis afforded the final heterocycle **145** in moderate yield.

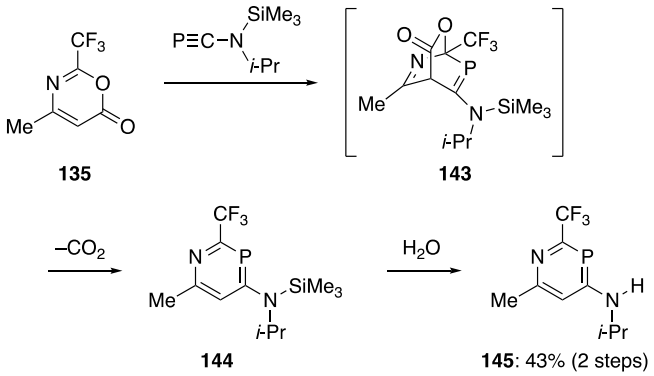

Scheme 54 Diels-Alder mediated synthesis of amine-bearing 1,3λ^3-azaphosphinine **145**.

Next, in 1991, Märkl and Dörges showed that 1,5,3-diazaphosphinines **146** undergo [4 + 2] cycloaddition with internal alkynes to first form bicyclic structures **147** before undergoing cycloreversion to extrude benzonitrile and form 1,3λ^3-azaphosphinines **148** (Scheme 55).[108]

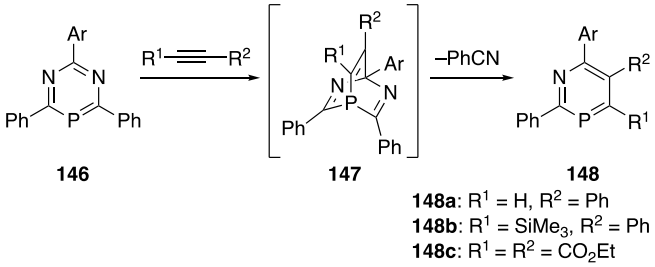

Scheme 55 Consecutive cycloaddition / cycloreversion pathway to furnish heavily substituted 1,3λ^3-azaphosphinines **148**. No yields reported for **148**.

This reaction can be repeated with another equivalent of internal alkyne to extrude another equivalent of benzonitrile to afford phosphinine **149** (Scheme 56), for which no yields were reported.[53,109–110] Interestingly, when treated instead with a phosphalkyne, 1,3λ^3-azaphosphinines instead form an azaphosphabarrelene **150**.

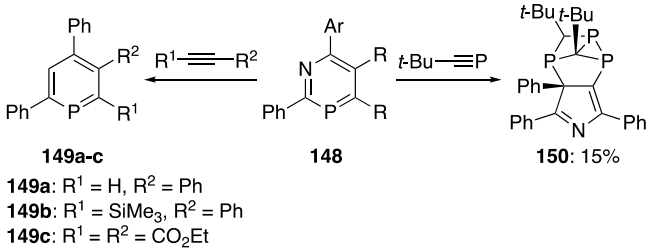

Scheme 56 Post-synthetic modification of **148** to either phosphinine **149** (left) or azaphosphabarrelene **150** (right).

In 1986, the first example of a 1,3λ^5-azaphosphinine was prepared by Galishev et al.[111] They first reacted imidoyl chloride **151** with diethyl(phenylethynyl)phosphonite to give zwitterion **152**, which then intramolecularly cyclized to form **153** (Scheme 57).

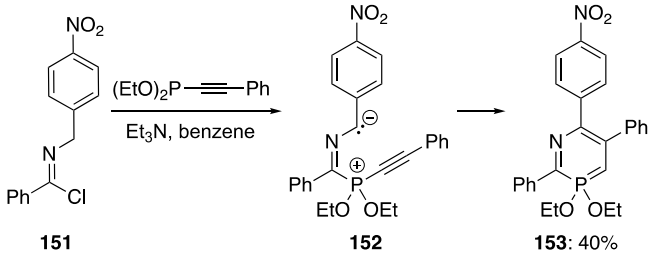

Scheme 57 Generation of heavily substituted **153** via zwitterionic intermediate.

While studying the synthesis of similar 1,3λ^5-azaphosphinines, the Märkl team reported that 1,3λ^3-azaphosphinine **131a** can be oxidized to the corresponding 1,3λ^5-azaphosphinine **154** upon treatment with diazoalkanes in alcohol solutions, adding both an alkyl group and a methoxy group in the process (Scheme 58). When run in ether rather than alcohol, however, the "dimeric" polycycle **155** was formed.[112]

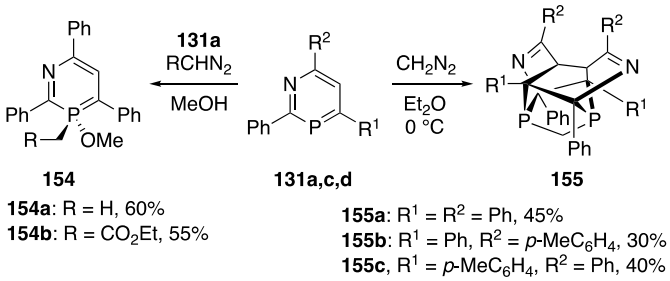

Scheme 58 Oxidation of **131** to P^V heterocycle **154** (left) or conversion to polycyclic **155** (right).

In 1999, Le Floch and co-workers performed a computational study exploring a series of nitrogen and phosphorus heterocycles to better understand their structure and reactivity.[113] This paper was a follow-up to previously published results that showed the 1,3,2-diazaphosphinine and 1,2-azaphosphinines reacted much more quickly with alkynes than their 1,3,5-diazaphophinine and 1,3-azaphosphinine counterparts, respectively, due to increased dipolar characteristics.[53,114] In this computational study, they concluded that the 1,3λ^3-azaphosphinine scaffold was both planar and weakly aromatic, showing decreased shortening of the P–N double bond on average compared to the double bonds in pyridine or the double bond in phosphinine. They also determined the internal bond angles for the C–P–C, P–C–N, and C–N–C bond angles were 98.0°, 129.3°, and 120.1°, respectively. This C–P–C angle is significantly smaller than the C–N–C bond angle in pyridine (117.1°), which is likely the result of the longer P–C bonds. Also, increased s-character in the P lone pair that leads to more p-character in the P–C bonds since P is a higher Z (and more electropositive) element than N.

In 2018, Hansmann developed a novel inverse electron demand hetero-Diels-Alder reaction to form 1,3λ^3- and 1,4λ^3-azaphosphinines from several 1,2,4-triazine starting materials **156** (Scheme 59).[115] This was achieved at 90 °C through the use of sodium phosphaethynolate (NaOCP) and subsequent loss of N_2 gas to drive the reaction. The

substituent groups on the starting triazine led to a dramatic difference in the ratio of formation of the 1,3λ^3-azaphosphinine **157** compared to the competing 1,4λ^3-derivative **158**. For instance, placement of phenyl rings in the 5- and 6-positions as well as either a phenyl or *p*-trifluoromethylphenyl group in the 3-position leads to formation of the 1,3λ^3-azaphosphinine derivative **157** in a 1:4 ratio to the 1,4λ^3-azaphosphinine **158** (Scheme 59). This ratio was determined through examination of the ^{31}P NMR spectrum and comparison to predicted values determined through DFT; however, the computed thermodynamic stabilities of the two scaffolds were very close, with the 1,3λ^3-derivative favored by 1.7 kcal mol^{-1}, suggesting that the mechanism of formation likely leads to this discrepancy.

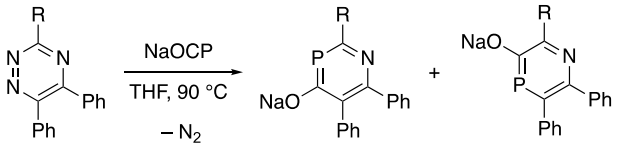

Scheme 59 Conversion of triazine **149** to mixture of corresponding 1,3λ^{3-} and 1,4λ^3-azaphosphinines.

To further examine the directing effects of the substituent groups, 2-pyridyl groups were introduced as ion tethers in multiple positions on triazene **156c-e**, resulting in dramatic shifts in the ratios of **157c-e** to **158c-e** (Scheme 60). In the 3-position, the 2-pyridyl on triazene **156** leads to a 1:15 ratio of 1,3λ^3-azaphosphinine **157c-d** to 1,4-azaphosphinine **158c-d** upon treatment with NaOCP at 60 °C. This was true when starting with either diphenyltriazene **156c** or with dimethyltriazene **156d**. When starting with triazene **156e** at room temperature, however, only 1,4λ^3-azaphosphinine **158e** was formed.

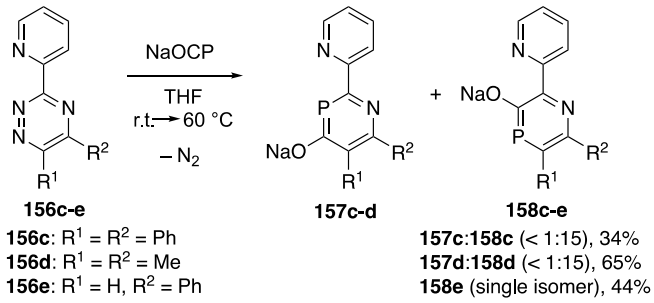

Scheme 60 Use of 2-pyridyl directing group to dramatically favor 1,4λ^3 product **158**.

With the 2-pyridyl group on both the 5- and 6-positions and a phenyl group in the 2-position on triazene **156f**, treatment with NaOCP at 60 °C gave a 4:1 ratio of 1,3λ^3-azaphosphonine **157f** to 1,4λ^3-azaphosphinine **158f** (Scheme 61), likely due to the directing nature of the pyridyl groups. Interestingly, when running the same reaction in the presence of 15-crown-5, a reversed trend of 1:2.5 **157f:158f** was observed, supporting the idea that the Na$^+$ ion plays a large directing role in the product ratio. To further favor the 1,3λ^3-azaphosphinine product **157g**, the reaction was run with a hydrogen in place of the phenyl group, which led to a 15:1 **157g**:**158g** ratio in good yields.

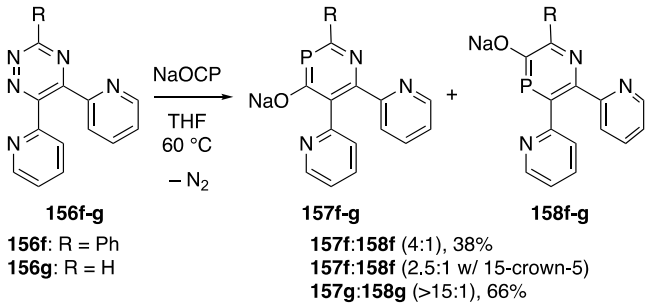

Scheme 61 Reversed trend in selectivity for azaphosphinine isomer based on substitution pattern of starting triazine **156**.

Lastly, when starting from 1,2,3-triazene **159** and treating it with NaOCP at –78 °C in THF, the sodium salt of 1,3λ^3-azaphosphinine 2-oxide **160** was solely formed (Scheme 62), confirming the versatility of this synthetic route.

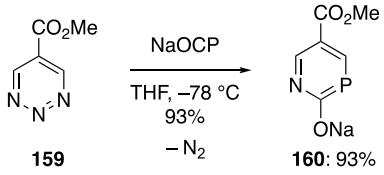

Scheme 62 Use of 1,2,3-triazine **159** to give exclusively 1,3λ^3 product **160**.

Intramolecular cyclization reactions

In 2018, Mathey and coworkers explored a more conjugated system containing the 1,3-azaphosphinine moiety.[116] Bromination of **161** with *N*-bromosuccinimide (NBS) afforded indole **162**, which was then protected as the dimethoxy acetal **163** (Scheme 63). Lithiation and subsequent addition to *P*-cyano-3,4-dimethylphosphole gave phosphorus- and nitrogen-containing structure **164**. The phosphole ring then underwent a [4 + 2] cycloaddition with N-phenylsuccinimide to first furnish **165**, which upon treatment with $AlCl_3$ gave *P*-chloro intermediate **166**. Elimination of HCl with 1,4-diazabicyclo[2.2.2]octane (DABCO) afforded 1,3λ^3-azaphosphinine **167** in a good yield. Alternatively, reaction of **166** with Et_2NH and then S_8 gave thionated 1,3λ^3-azaphosphinine 3-sulfide **168** in excellent yield.

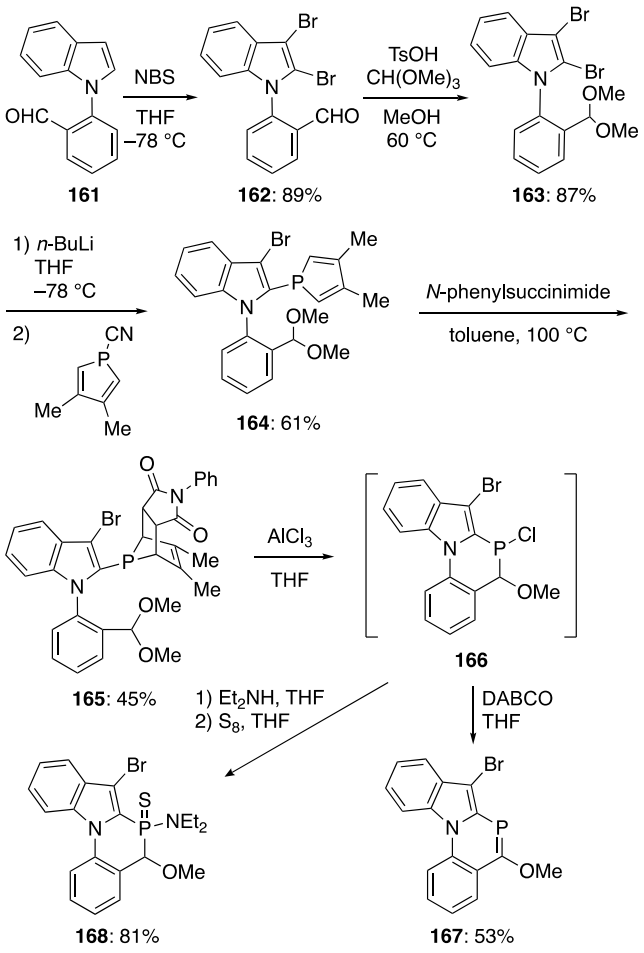

Scheme 63 Synthetic pathway to π-extended 1,3λ^3 azaphosphinine **167** and corresponding 1,3λ^5 azaphosphinine sulfide **168**.

To explore the reactivity of π-extended **167**, heating in MeOH at 60 °C gave dimethoxy product **169** in very good yield (Scheme 64). Additionally, the phosphorus-containing double bond could undergo a Diels-Alder reaction with 2,3-dimethyl-1,3-butadiene in toluene at 100 °C to furnish heterocycle **170**, which could be oxidized with H_2O_2 to afford the respective 1,3λ^5-heterocycle **171** in excellent yield.

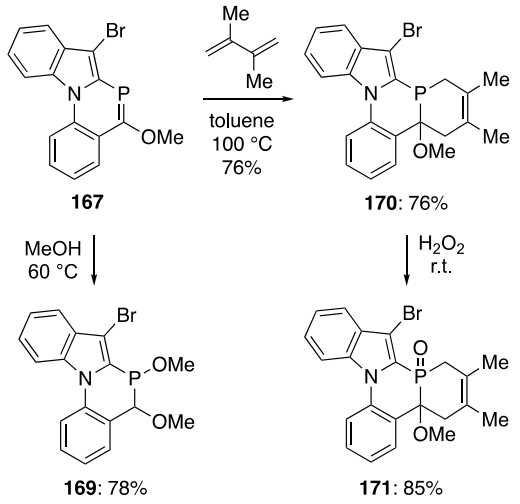

Scheme 64 Synthesis of dimethoxy **169** (left) and consecutive Diels-Alder/oxidation to give product **171** (right).

1,4-Azaphosphinines

Bis-β-ketophosphane oxide cyclization

One of the earliest examples of a 1,4-dihydro-1,4λ^5-azaphosphinine 4-oxide comes from Aguiar and coworkers in 1971.[36] Unlike most early publications in this review, their synthesis was not primarily concerned with just pushing the bounds of novel heteroaromatics, but rather, designing new bioactive species. Starting from (diethynyl)phenylphosphane oxides **172**, conjugate addition of butylamine followed by hydrolysis afforded the corresponding bis-β-keto-phosphane oxides **173** (Scheme 65). Lastly, **173** were cyclized with ammonium carbonate to furnish the desired dihydro product **174**. As apparent from the next few entries in this review, this particular technique of synthesizing an azaphosphinine scaffold was extremely influential and facilitates much of the early work performed on the 1,4-isomer.

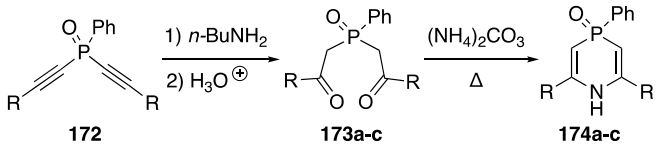

172 **173a-c** **174a-c**

173a: R = Ph, 67% **174a**: R = Ph, 60%
173b: R = *t*-Bu, 78% **174b**: R = *t*-Bu, 62%
173c: R = *n*-Pr, 85% **174c**: R = *n*-Pr, 56%

Scheme 65 Synthesis of 1,4-dihydro-1,4λ^5-azaphosphinine 4-oxide **174**.

The earliest published example of any non-fused, aromatic λ^3-azaphosphinine came from Märkl and Matthes in 1972.[32] The initial interest for this system arose from curiosity surrounding previously synthesized azaarsine heterocycles. Their synthetic approach involved thermolyzing a dihydro precursor to the fully aromatized system (Scheme 66). The success of this technique led to it being used later in some of the other early syntheses of 1,4λ^3-azaphosphinines.[66,68] The first four steps of their syntheses are directly analogous to that of Aguiar et al. but use a

suitable 'leaving group' (*t*-Bu) instead of a Ph ring. Bis(phenylethynyl)-*t*-butylphosphane **175** was oxidized and the water formally added to the alkynes to give bis-β-keto-phosphane oxide **176**. This was cyclized with ammonium carbonate and reduced to P^{III} with phenylsilane to afford **177**, which lastly was thermolyzed to furnish the desired 2,6-diphenyl-1,4λ^3-azaphosphinine **178**.

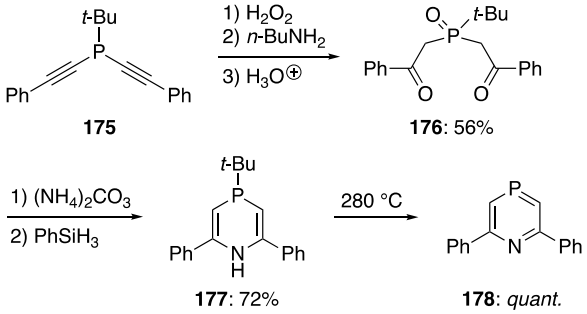

Scheme 66 Synthesis of 2,6-diphenyl-1,4λ^3-azaphosphinine **178**.

Like prior azaphosphinine examples, the differences in the heteroatom electronegativity meant that **178** was quite electrophilic (Scheme 67). Several dihydro products (**177**, **179, 180**) could be synthesized through the attack of various nucleophiles at the phosphorus center, followed by either protonation or methylation to afford the secondary or tertiary amino species, respectively.

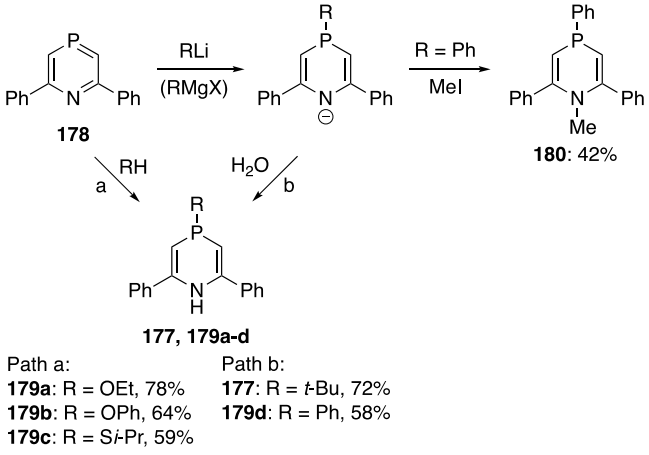

Scheme 67 Dihydro-products resulting from attack of various nucleophiles.

Also in 1972, Mebazaa and Simalty were developing their synthesis of the first non-fused 1,4λ^5-azaphosphinine, a pathway that would become standard for nearly a decade in the development of such species (Scheme 68).[117] Starting from phosphonium pyran salt **181**, hydrolysis furnished bis-β-keto-phosphane oxide **182**. Analogous to the previous two 1,4-azaphosphinine syntheses, **182** was cyclized with ammonium acetate to yield **183**.[32,36] Anion exchange gave the perchlorate salt **183'**, which was subsequently deprotonated with NaH to furnish 2,4,4,6-tetraphenyl-1,4λ^5-azaphosphinine **184**. While the exact method of anion exchange was not reported in the paper, a

similar publication from the same authors used sodium perchlorate;[118] no product yields were reported for either. The authors make the case for the aromaticity of their target **184** through the UV-Vis spectra and its dramatic change upon protonation. However, through the modern perspective noted at the beginning of this review, while there may be a degree of delocalization via the ylidic nature of **184**, there is no "aromaticity" as one would typically define it.

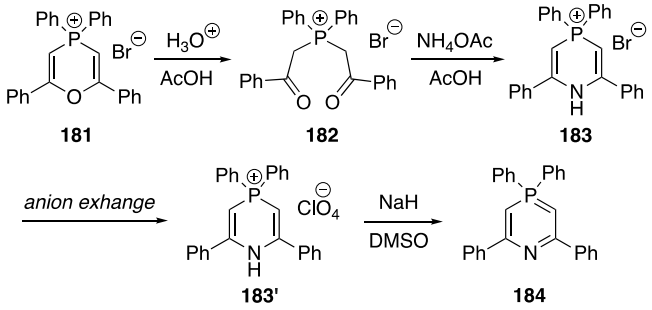

Scheme 68 Synthesis of 2,4,4,6-tetraphenyl-1,4λ^5-azaphosphinine **184**.

In 1984, Quin et al. expanded upon the synthetic pathway initially developed by Aguiar.[36,119] They had been examining methods of converting phospholene oxides **185** into bis-β-ketophosphane oxides **173a** and **186** via ozonolysis (Scheme 69).[120] Their alternative approach to generating the acyclic starting material of the 1,4-dihydro-1,4λ^5-azaphosphinine 4-oxide scaffold **174a** and **187** facilitated novel functional groups and substitution patterns. While their substrate scope was primarily limited to phenyl and methyl groups, they were able to furnish heterocycles with only one substituent α to the nitrogen atom, which was not achievable with previous symmetric bis-β-keto-phosphane oxides. While there was limited analytical data provided for the compounds, the ^{13}C NMR spectra showed a strong upfield shift (91–93 ppm) of the olefinic carbon β to the nitrogen atom, suggesting a transfer of electron density from the nitrogen atom to this carbon similar to enamines.

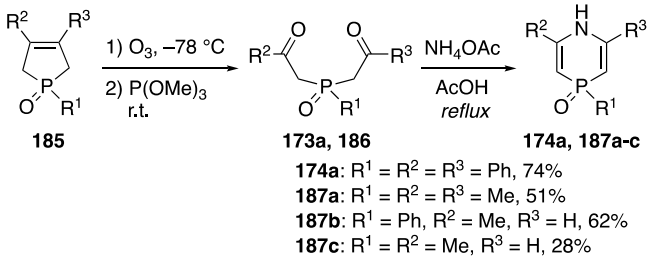

Scheme 69 Ozonolysis-based approach to 1,4-dihydro-1,4λ^5-azaphosphinine 4-oxides **174a** and **187**.

By 1990, Quin and Marsi published a more comprehensive work on phosphorus heterocycles derived from more exotic bis-β-keto-phosphane oxides **188** and **189** (Scheme 70).[121] While many of these species do not fit the scope of this review, there were a few interesting examples that explore the possibilities of extension via saturated ring fusion such as **190** and **191**.

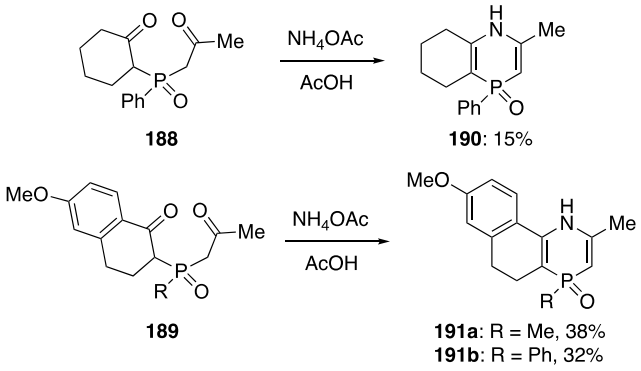

Scheme 70 Additional examples of ring-fused 1,4-dihydro-1,4λ^5-azaphosphinine 4-oxides.

Pericyclic/Cycloaddition Reactions

Work from Barluenga et al. began to emerge around this time that was focused on developing alternative pathways to 1,4-azaphosphinines. Some of the limitations of the aforementioned bis-β-keto-phosphane oxides were i) a lack of functionalization at the 3- and 5-positions and ii) the harsh conditions required to reduce the phosphorus atom from P^V to P^{III}.[122] A popular technique in the early days of 1,2-azaphosphinine chemistry, Barluenga used cycloaddition/electrocyclization reactions to his advantage. Starting from previously described phosphazene **192** (Scheme 71),[35] reaction with DMAD proceeded through a [2+2] cycloaddition/4π-electron ring-opening to furnish acyclic intermediate **193** (where R^1 = H), which upon further heating yielded azaphosphinine **194** after loss of an equivalent of aniline. If R^1 was an alkyl substituent, the reaction furnished **194** directly, likely proceeding via the same mechanism with the corresponding derivatives of **193** being too reactive to isolate.

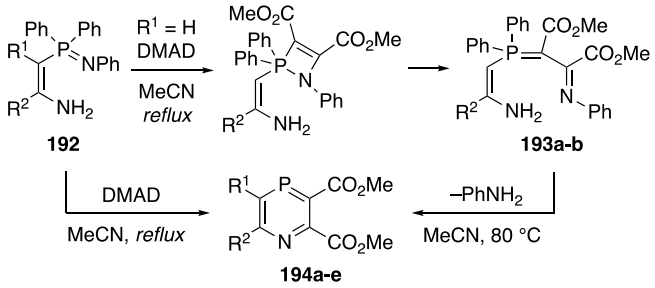

193a-b, 194a-b: R^1 = H
193a: R^2 = *p*-MeC_6H_4, 86%
193b: R^2 = Cy, 82%
194a: R^2 = *p*-MeC_6H_4, 80%
194b: R^2 = Cy, 77%
194c: R^1 = Me, R^2 = *p*-MeC_6H_4, 76%
194d: R^1 = $CH_2CH{=}CH_2$, R^2 = *p*-MeC_6H_4, 79%
194e: R^1 = Bn, R^2 = Cy, 78%

Scheme 71 Synthesis of azaphosphinines **194**.

Barluenga et al. soon departed from the cycloadditions route and instead examined the reactivity of 2-aza-1,3-dienes, which were gaining popularity in Diels-Alder type reactions.[123] The authors hypothesized that these 2-aza-

1,3-dienes could also be employed as nucleophiles in cyclization reactions using suitable electrophiles. Reacting several 2-aza-1,3-dienes **195** with dichlorophenylphosphane led to a mild, one-pot synthesis of the corresponding tetrasubstituted 1,4-dihydro-1,4λ^5-azaphosphinine 4-oxides **196** (Scheme 72). The authors could trap trivalent **197** by removing *in situ*-generated HCl with Et_3N, and subsequently showed that **197** could be oxidized to either oxide **196** or sulfide **198** with H_2O_2 or S_8, respectively.

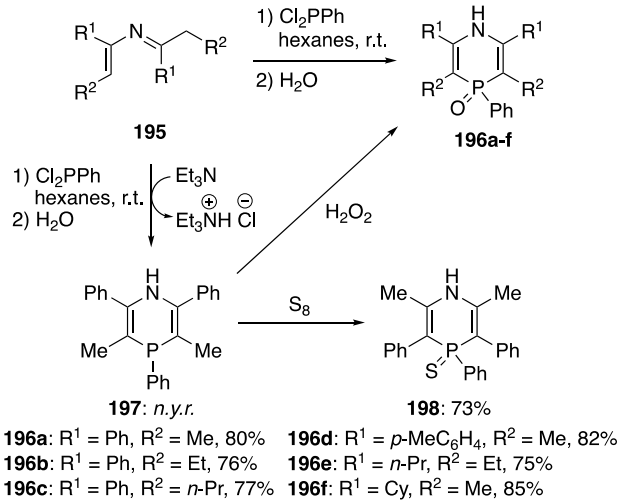

Scheme 72 One-pot cyclization to form 1,4-dihydro-1,4λ^5-azaphosphinines **196**.

Barluenga et al. also showed that substituting phosphorus trichloride for dichlorophenylphosphane in the cyclization could furnish **196'** (Scheme 73).

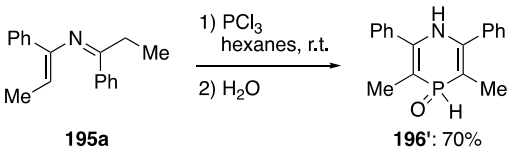

Scheme 73 Synthesis of secondary 1,4λ^5-azaphosphinine 4-oxide **196'**.

Barluenga et al. returned to the cycloaddition route in a 1990 publication concerning the synthesis of 2-oxo-1,4λ^5-azaphosphinines.[124] Just prior to this report, the same authors had described a method for formation of conjugated phosphonium ylides using phosphazenes and DMAD, then subsequently converting them to phosphole derivatives.[125] The reaction between one of the two alkyne diesters, DMAD or diethyl acetylenedicarboxylate (DEAD), and the *N*-alkoxycarbonylphosphazene **199** is proposed to proceed via [2 + 2] cycloaddition and subsequent electrocyclic ring opening to yield the conjugated phosphonium ylides **200** (Scheme 74). This is a similar process to the group's earlier work on formally conjugated 1,4λ^3-azaphosphinines.[122] However, for these derivatives the *N*-alkoxycarbonyl functionality served as an electrophile, in which deprotonation of the CH_2 unit next to P and cyclocondensation ultimately furnished azaphosphinines **201** in excellent yields.

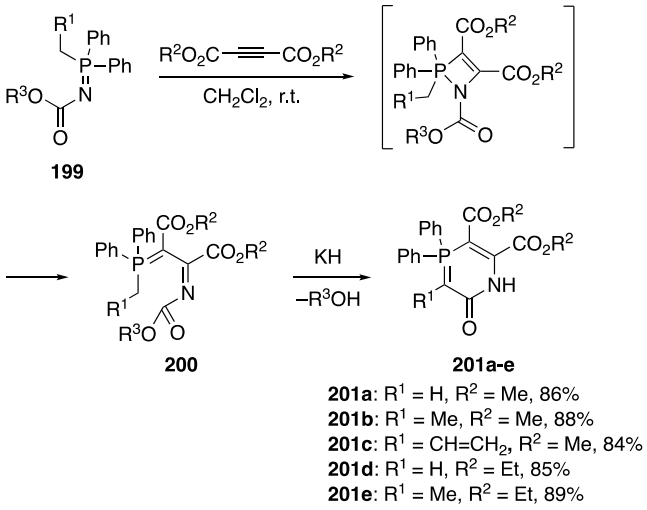

Scheme 74 Cycloaddition/intramolecular cyclization route to 2-oxo-1,4λ^5-azaphosphinines **201**. R^3 is either Me or Et.

In 2011, Alajarin et al. reinvestigated generating azaphosphinine scaffolds from phosphazene-alkyne cycloaddition.[126] Unlike previous works that used diester-functionalized alkynes, this study involved *in situ*-generated benzyne derivatives. The reaction of phosphazenes **202** with various *o*-trimethylsilylphenyl triflates **203** furnished the saturated benzo[*b*]-tetrahydro-1,4-azaphosphonium triflate **204** via the cycloaddition/electrocyclization mechanism proposed in Scheme 75. While the authors do generate several derivatives of this species, the saturated nature of the azaphosphinine ring puts it beyond the scope of this review aside from this single mention.

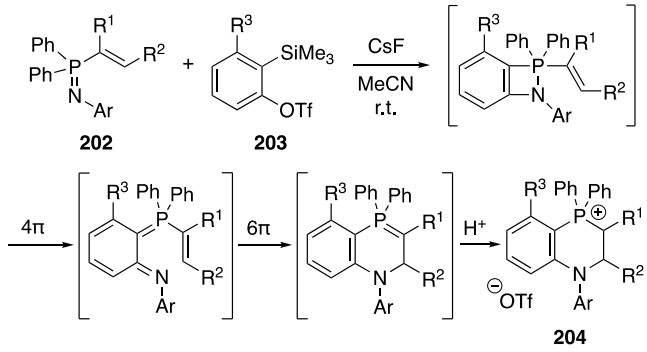

Scheme 75 Proposed general mechanism to generate tetrahydro species **204**.

Importantly, Alajarin et al. applied the reaction strategy outlined in Scheme 75 to several *P*-alkynyl-λ^5-phosphazenes **205** and produced the corresponding benzo[*b*]-1,4-dihydro-1,4-azaphosphininium triflates **206** (Scheme 76). The proposed mechanism is believed to be the same for both **204** and **206**. One could imagine if an unprotected nitrogen atom could survive this synthesis, the whole ring system could be deprotonated with strong base like the synthesis by Mebazaa and Simalty.[117]

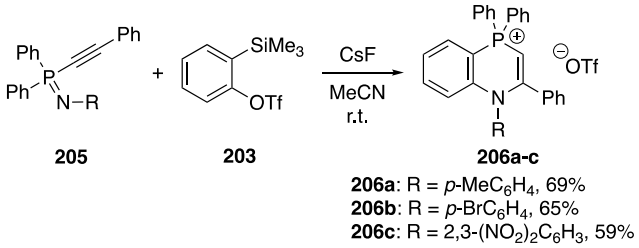

Scheme 76 Phosphazene **205** heteroannulation with benzyne to give azaphosphinines **206**.

A very unusual contribution came from Bertrand and coworkers describing the use of a benzo-λ^5-phosphete for the synthesis of a benzo[*b*]-1,4λ^5-azaphosphinine **207** (Scheme 77).[127] Fused 1,4-azaphosphinines of any valence are extremely rare in the literature, and this novel approach took advantage of an even less-common substrate. This work hinges on the unusual stability of phosphetes. When fused to a benzene ring, phosphete ring **208** becomes highly reactive and sensitive to oxygen and moisture, likely due to the lengthened P–C bonds. This high reactivity gave rise to the unexpected formation of the benzo[*b*]-1,4λ^5-azaphosphinine **207** in excellent yield when reacted with acetonitrile, the structure of which was supported by spectroscopic analysis. This substitution pattern is unexpected because it must arise from cycloaddition of the C–C bond of the 4-membered ring in **208** with acetonitrile, rather than the expected cycloaddition with the P–C bond.

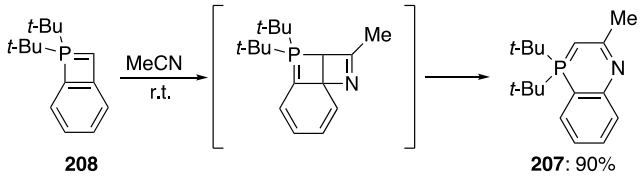

Scheme 77 Phosphete route to benzo[*b*]-1,4λ^5-azaphosphinine **207**.

As is the case with the other azaphosphinine isomers, more modern research gravitates toward transition-metal catalyzed reactions. Accordingly, in 2002 Leung and coworkers published their work on the Pd-catalyzed synthesis of 1,2,4,6-tetraphenyl-1,4-dihydro-1,4λ^3-azaphosphinine **209** (Scheme 78).[128] The primary benefit of this approach is the simplicity and one-pot nature of the reaction. Whereas no reactivity occurred between bis(phenylethynyl)phenyl phosphane **210** and aniline alone, addition of $PdCl_2(MeCN)_2$ allowed the reaction to proceed forming stable monomeric **211** and dimeric **212** azaphosphinine complexes with Pd that were confirmed via X-ray crystallography. This is an interesting and more modern take on the 1,4-dihydro-1,4λ^3-azaphosphinines synthesized by Märkl and Matthes where the multistep oxidation and heteroannulation is replaced by a single catalytic step.[32] The azaphosphinine ring could subsequently be liberated with the addition of KCN, affording **209**. The authors note that the geometry and bond lengths of the nitrogen atom in both cases are that of sp^2 hybridization, indicating delocalization around the azaphosphinine ring. The low-field NMR shift of the azaphosphinine proton signal (δ 7.73) suggests the presence of aromaticity within the λ^3-azaphosphinine ring.

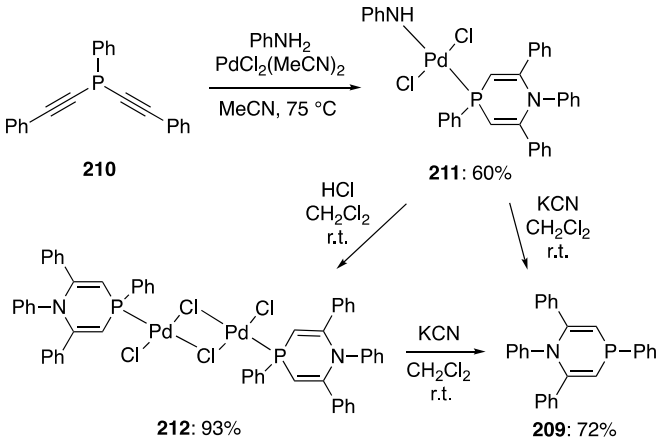

Scheme 78 Pd-catalyzed heteroannulation to give 1,2,4,6-tetraphenyl-1,4-dihydro-1,4λ^3-azaphosphinine **209**.

In 2015, Duan, Mathey and coworkers followed up on the efforts of both Alajarin and Leung to develop new routes to both benzo[*b*]-1,4-dihydro-1,4-azaphosphonium triflates and a transition metal catalyzed dimeric azaphosphonium species.[126,128,129] *o*-Diarylphosphinoaryl isocyanides **213** are first methylated with MeOTf to give **214**, which are then treated with *t*-BuOK base and then triflic acid to yield azaphosphonium triflates **215** (Scheme 79). The proposed mechanism of this latter transformation involves deprotonation to form an ylidic species that undergoes [2 + 2] cycloadditon with the *o*-isocyanide moiety; a hydrogen shift, cycloreversion, and protonation complete the transformation. These salts are directly analogous to those prepared by Leung and coworkers but without a *N*-atom substituent, as well as less substitution on the azaphosphininium ring itself.

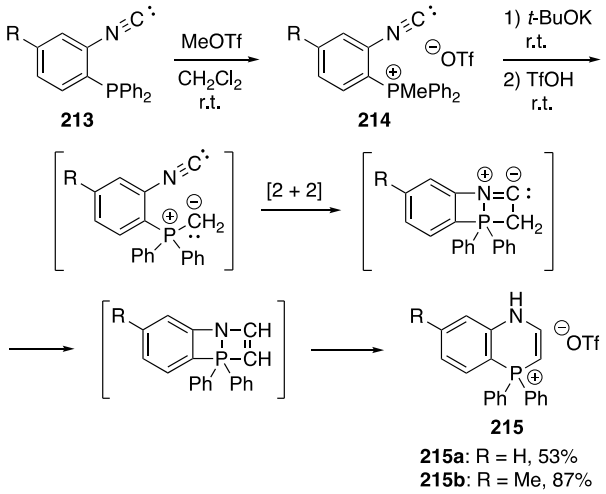

Scheme 79 Intramolecular cyclization of *o*-diarylphosphinoaryl isocyanide ylides.

Conversely, when **213a** is subjected to room temperature conditions in the presence of $NiCl_2$ an entirely different process occurs. Stable dicationic species **216** is the only isolable product of the reaction (Scheme 80). The

authors note the mechanism of formation is not clear, and only provide NMR and X-ray crystallographic data in terms of analysis. Although the yield is omitted, this fused azaphosphininium species is quite novel in its chemistry and again begs the question if a strong base is used, would the heterocycle convert to the neutral 1,4λ^5-azaphosphinine like those of Mebazaa and Simalty?[117]

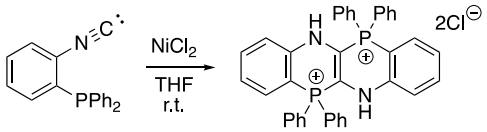

213a **216**

Scheme 80 Cyclization of isocyanide **213a** into dicationic **216**.

Comparing electronic properties of the azaphosphinine isomers

With such varied examples of azaphosphinines across several isomers and valences, it becomes easy to lose track of the exhibited properties, namely aromaticity, of each heterocycle. Only azaphosphinine compounds with an endocyclic P^{III}=X double bond are formally aromatic. In this state the rings are analogous to both pyridine and phosphinine, the single heteroatom-containing nitrogen and phosphorus analogues. As noted earlier, the computational work from Le Floch and co-workers in 1999 sought to compare the aromaticities of 1,2λ^3- and 1,3λ^3-azaphosphinines not only to each other but also to pyridine and phosphinine.[113] This work compared Nucleus Independent Chemical Shift (NICS) values (Table 13, left), computed bond lengths, and computed bond angles. In the NICS calculations, negative values denote aromaticity. From these data there is a clear distinction between the aromaticities of the 1,2λ^3- and 1,3λ^3- isomers, with both being less aromatic than the single heteroatom species. The authors ascribe this difference to the dramatically different electronegativities of the nitrogen and phosphorus atoms, which cause more π-electron localization when the two are directly bonded. Interestingly, it is also noted that even though the 1,3λ^3-isomer is more aromatic, it is also less stable. While it is typically thought that increased aromaticity should lead to higher stabilities, this suggests that the opposite is true for these molecules. Upon further study of the molecular orbitals through NBO analysis, it was found that the placement of heteroatoms within the 1,3-azaphosphinine and 1,3,2-diazaphosphinine leads to electron distribution which limits electronic delocalization within the ring. This is rationalized computationally by calculating the [1,4] P–C$_4$ dipole in the 1,2λ^3-isomer as well as qualified by experimental observations made in a previous publication from this group.[53]

In 2018, Elguero et al. published a computational study that calculated the NICS values for a large number of P–N heterocycles including several theoretical species such as the parent 1,2λ^3, 1,3λ^3, and 1,4λ^3-azaphosphinines (Table 13, right).[131] The small differences in NICS values between the two studies are likely due to different levels of theory and different scanning distances used above the theoretical ring (0.5 vs. 1.0 Å). Regardless, both data sets follow the same basic trend of aromaticity in the azaphosphinine derivatives, with the later work by Elguero et al. suggesting that 1,4λ^3-azaphosphinine would be the most aromatic, rivaling that of phosphinine. Both studies include the benzene, pyridine, and phosphinine as reference values to their computations.

Table 13 Computed NICS values of relevant heterocycles computed by Le Floch (left) and Elguero (right)

Compound	NICS(0.5) (ppm)[a]	NICS(1) (ppm)[b]
benzene	–11.5	–10.2
pyridine	–10.6	–10.2
phosphinine	–10.2	–9.7
1,2λ^3-azaphosphinine	–8.9	–9.2
1,3λ^3-azaphosphinine	–9.3	–9.6
1,4λ^3-azaphosphinine	—	–9.7
1,3,2λ^3-diazaphosphinine	–7.5	–8.5

[a]Computed 0.5 Å above ring centers at GIAO-SCF/6-31+G*//B3LYP/6-31G* level. [b]Computed 1 Å above ring center at B3LYP 6-311++G/d,p level.

By comparison, pentavalent azaphosphinine rings cannot be described as aromatic. Modern computational and experimental work into the nature of pentavalent phosphorus indicate that the bonds are almost entirely ionic in nature. Due to the readily available electron density that is transferred to electronegative substituents (e.g., N, O), a considerable amount of donation then occurs in the form of negative hyperconjugation. While this effect is in essence the distribution of electron density to adjacent bonds, it does not constitute aromaticity as the delocalization is not global and cannot pass through the phosphorus atom. Despite the P^V azaphosphinine rings themselves failing to meet the criteria of aromaticity, most compounds discussed in this review still exhibit some local aromaticity. This is due to fusion of the azaphosphinine ring to aromatic species such as benzene, naphthalene, or pyridine.

There is no published computational work that assesses the electronics and localized charge in P^V azaphosphinines. However, using ^{1}H and ^{31}P NMR we can speculate on the effect of different azaphosphinine characteristics. Properties such as endo- vs. exocyclic double bonds and the relative position of the two pnictogen atoms on the ring will of course result in changes to the electronic character of the complex system. ^{1}H and ^{31}P NMR data for selected azaphosphinines are described in Table 14. **61**, **131b**, and **178** represent the 1,2λ^3, 1,3λ^3, and 1,4λ^3 isomers respectively. As expected, all the proton signals for the three P^{III} azaphosphinines are at an appropriately deshielded chemical shift for aromatic species. Comparison of **178** to its P^V counterparts **174a** and **184** directly demonstrates this loss of aromaticity in the same proton signal. H(3/5) of **178** undergoes a dramatic upfield shift to 5.62 and 5.10 ppm in **174a** and **184**, respectively.

The notably different ^{1}H NMR chemical shifts of **16b** does well to illustrate the ylidic nature of the P^V azaphosphinine ring, in which the 2, 4, and 6 positions of the ring will distribute a negative charge. One could imagine much of this electron density would rest on the electronegative nitrogen atom,; however, H(5) of this ring still experiences a shielding effect causing the ^{1}H NMR signal to appear at 6.06 ppm. Comparison of compounds **97f** and hydrolysis product **98f** leads to a commonly observed change in the ^{31}P NMR spectra. As a greater number of electronegative substituents are bonded to the pentavalent phosphorus, the chemical shift becomes more like that

of phosphonium compounds, emphasizing the lack of electron density on the phosphorus. This effect is also directly observed in the analogous example of **174a** and **184**.

Table 14 Comparison of selected ^{1}H and ^{31}P NMR chemical shifts across selected azaphosphinine systems

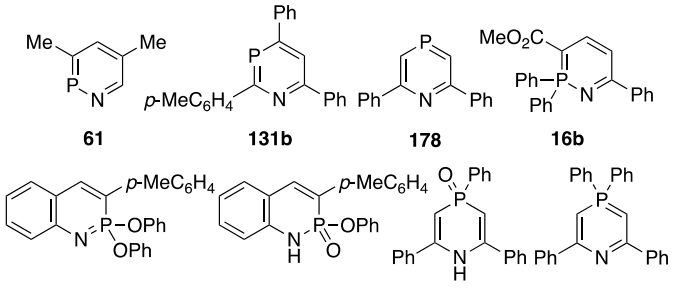

Cmpd	^{1}H NMR δ [ppm] (m, Hz)[a]	^{31}P NMR δ [ppm] (m, Hz)[a,b]
61	9.11 (H6), 7.58 (H4)	263.3
131b	8.10 (H5, d, 5.23)	161.3
178	8.66 (H3/5, d, 18)	–245.5 (t, 18)
16b	8.04 (H4), 6.06 (H5)	23.6
97f	8.07 (H4, d, 41.2)	25.68 (d, 41.2)
98f	7.57 (H4, d, 40.5)	11.15 (d, 40.5)
174a	5.62 (H3, d, 6)	–8.7
184	5.10 (H3, d, 12)	–1.5

[a]Values collected in $CDCl_3$ at room temperature. [b]Measured against H_3PO_4 standard.

Conclusions

As detailed in this review, azaphosphinines can assume three regioisomeric geometries (1,2- vs. 1,3- vs. 1,4-) with two different valences of the phosphorus center (P^{III} vs. P^{V}). Because of the disparity in stabilities of the isomers, there is a notable difference in the amount of research published on each. The 1,2-isomers of both valences are by far the most studied, and an abundance of reaction pathways can be used to prepare them. A vast majority of the known azaphosphinine structures were prepared simply as experimental curiosities, i.e., can they be made? Recent efforts over the last decade by several groups have nonetheless demonstrated that these unique heterocycles can be used in a wide variety of applications, such as a chiral catalyst for stereospecific transformations, as a hydrogen bond donor and acceptor motif in anion receptors, as a fluorophore in cellular imaging, and as a potential pharmacophore in medical chemistry. Azaphosphinines also serve as an interesting model in how we define heteroaromatic structures. While λ^3-azaphosphinines are aromatic, λ^5-azaphosphinines most certainly are not. Nonetheless, the unique properties specific to systems containing both phosphorus and nitrogen atoms combine regions of local aromaticity with regions of unique electronic complexity. These recent studies only scratch the surface of the vast future potential uses of azaphosphinines. We for one are excited to see how this field continues to blossom over the next 10-20 years.

Acknowledgements

This research has been supported by the US National Science Foundation (CHE-1607214 and 2107425 to MMH and DWJ). This work was also supported by the Bradshaw and Holzapfel Research Professorship in Transformational Science and Mathematics to DWJ.

Glossary of abbreviations

Ad	1-adamantyl
BHT	butylated hydroxytoluene
CAN	$Ce^{IV}(NH_4)_2(NO_3)_6$
Cp	η^5-cyclopentadienyl
Cp*	η^5-pentamethylcyclopentadienyl
CuACC	Copper-catalyzed azide-alkyne cycloaddition
Cy	cyclohexyl
DABCO	1,4-diazabicyclo[2.2.2]octane
DBU	1,8-diazabicyclo[5.4.0]undec-7-ene
DCE	1,2-dichloroethane
DEAD	diethyl acetylenedicarboxylate
DMAD	dimethyl acetylenedicarboxylate
ICT	internal charge transfer
LB	Lewis base
MCH-1R	melanin-concentrating hormone receptor 1
NaOCP	sodium phosphaethynolate
NBO	natural bond order
NBS	*N*-bromosuccinimide
NICS	nucleus independent chemical shift
N.Y.R.	No yield reported
Pd_2dba_3	tris(dibenzylideneacetone)dipalladium(0)
Salox	salicyloxazoline
SHP-1	Src homology 2-containing phosphatase-1
SRB	sulforhodamine B
TCB	1,2,4-trichlorobenzene
TPN	tetraphenylnaphthalene
VC	variable concentration

References

1 G. Brugnatelli, *G. Fis. Chim. Storia Nat. Med. Ed Arti*, 1818, **1**, 117–129.
2 E. Kabir and M. Uzzaman, *Results Chem.*, 2022, **4**, 100606.
3 F. Ullah, S. Ullah, M. F. A. Khan, M. Mustaqeem, R. N. Paracha, M. F. Rehman, F. Kanwal, S. S. Hassan and S. Bungau, *Molecules*, 2022, **27**, 6631–6649.
4 J. Jampilek, *Molecules*, 2019, **24**, 3839–3843.
5 O. Ostroverkhova, *Chem. Rev.*, 2016, **116**, 13279–13412.
6 M. M. Heravi and V. Zadsirjan, *RSC Adv.*, 2020, **10**, 44247–44311.
7 S. S. M. Fernandes, M. C. R. Castro, D. Ivanou, A. Mendes and M. M. M. Raposo, *Coatings*, 2022, **12**, 34–46.
8 S. Kumar, *J. Heterocycl. Chem.*, 2019, **56**, 1168–1230.
9 R. Iftikhar, F. Z. Khan and N. Naeem, *Mol. Divers.*, 2023, DOI:10.1007/s11030-022-10597-0.
10 E. Peris, *Chem. Rev.*, 2018, **118**, 9988–10031.
11 S. C. Sau, P. K. Hota, S. K. Mandal, M. Soleilhavoup and G. Bertrand, *Chem. Soc. Rev.*, 2020, **49**, 1233–1252.
12 K. Mezgebe and E. Mulugeta, *RSC Adv.*, 2022, **12**, 25932–25946.
13 C. Reus and T. Baumgartner, *Dalton Trans.*, 2016, **45**, 1850–1855.
14 T. Baumgartner, *Acc. Chem. Res.*, 2014, **47**, 1613–1622.
15 M. Stolar and T. Baumgartner, *Chem. – Asian J.*, 2014, **9**, 1212–1225.
16 X. He and T. Baumgartner, *RSC Adv.*, 2013, **3**, 11334–11350.
17 T. Baumgartner and R. Réau, *Chem. Rev.*, 2006, **106**, 4681–4727.
18 X.-D. Jiang, J. Zhao, D. Xi, H. Yu, J. Guan, S. Li, C.-L. Sun and L.-J. Xiao, *Chem. – Eur. J.*, 2015, **21**, 6079–6082.
19 C. Müller, Z. Freixa, M. Lutz, A. L. Spek, D. Vogt and P. W. N. M. van Leeuwen, *Organometallics*, 2008, **27**, 834–838.
20 C. Müller, E. A. Pidko, M. Lutz, A. L. Spek and D. Vogt, *Chem. – Eur. J.*, 2008, **14**, 8803–8807.
21 A. Fukazawa, S. Suda, M. Taki, E. Yamaguchi, M. Grzybowski, Y. Sato, T. Higashiyama and S. Yamaguchi, *Chem. Commun.*, 2016, **52**, 1120–1123.
22 V. Jancik, F. Cortés-Guzmán, R. Herbst-Irmer and D. Matínez-Otero, *Chem. – Eur. J.*, 2017, **23**, 6964–6968.
23 A. B. Chaplin, J. A. Harrison and P. J. Dyson, *Inorg. Chem.*, 2005, **44**, 8407–8417.
24 S. S. Krishnamurthy, *Phosphorus Sulfur Silicon Relat. Elem.*, 1994, **87**, 101–111.
25 J. Liebig, *Justus Liebigs Ann. Chem.*, 1834, **11**, 139–150.
26 P. v. R. Schleyer and A. J. Kos, *Tetrahedron*, 1983, **39**, 1141–1150.
27 K. Dimroth, *Acc. Chem. Res.*, 1982, **15**, 58–64.
28 T. Delouche, E. Caytan, M. Cordier, T. Roisnel, G. Taupier, Y. Molard, N. Vanthuyne, B. Le Guennic, M. Hissler, D. Jacquemin and P.-A. Bouit, *Angew. Chem. Int. Ed.*, 2022, **61**, e202205548.
29 C. Müller, D. Wasserberg, J. J. M. Weemers, E. A. Pidko, S. Hoffmann, M. Lutz, A. L. Spek, S. C. J. Meskers, R. A. J. Janssen, R. A. van Santen and D. Vogt, *Chem. – Eur. J.*, 2007, **13**, 4548–4559.
30 D. G. Gilheany, *Chem. Rev.*, 1994, **94**, 1339–1374.
31 A. Schenk and A. Michaelis, *Ber. Dtsch. Chem. Ges.*, 1888, **21**, 1497–1504.
32 G. Märkl and D. Matthes, *Angew. Chem. Int Ed. Engl.*, 1972, **11**, 1019–1020.
33 C. Bourdieu and A. Foucaud, *Tetrahedron Lett.*, 1986, **27**, 4725–4726.
34 T. Kobayashi and M. Nitta, *Chem. Lett.*, 1985, **14**, 1459–1462.
35 J. Barluenga, F. Lopez and F. Palacios, *J. Chem. Res. Synposes*, 1985, **7**, 221.

36 J. C. Williams, J. A. Kuczkowski, N. A. Portnoyz, K. S. Yong, J. D. Wander and A. M. Aguiar, *Tetrahedron Lett.*, 1971, **12**, 4749–4752.

37 W. Tang and Y.-X. Ding, *J. Org. Chem.*, 2006, **71**, 8489–8492.

38 Y. Sun and N. Cramer, *Chem. Sci.*, 2018, **9**, 2981–2985.

39 J. P. Bard, D. W. Johnson and M. M. Haley, *Synlett*, 2020, **31**, 1862–1877.

40 T. Eicher, S. Hauptmann, and A. Speicher, *The Chemistry of Heterocycles*, John Wiley & Sons, Ltd, 2nd edn., 2003, vol. 1, ch. 2, pp. 5–16.

41 M. Häring, *Helv. Chim. Acta*, 1960, **43**, 1826–1840.

42 A. I. Bokanov and B. I. Stepanov, *Russ. Chem. Rev.*, 1977, **46**, 855–860.

43 L. D. Freedman and H. S. Freeman, *Chem. Rev.*, 1987, **87**, 289–306.

44 J. J. Skolimowski, L. D. Quin and A. N. Hughes, *J. Org. Chem.*, 1989, **54**, 3493–3496.

45 Y. Zhi-Gang and Z. De-Feng, *Chin. J. Chem.*, 2010, **21**, 71–78.

46 W. Ye, X. Li, B. Ding, C. Wang, M. Shrestha, X. Ma, Y. Chen and H. Tian, *J. Org. Chem.*, 2020, **85**, 3879–3886.

47 M. J. S. Dewar and V. P. Kubba, *J. Am. Chem. Soc.*, 1960, **82**, 5685–5688.

48 M. J. S. Dewar, V. P. Kubba and R. Pettit, *J. Chem. Soc. Resumed*, 1958, 3073–3076.

49 I. G. M. Campbell and J. K. Way, *J. Chem. Soc.*, 1960, 5034–5041.

50 H. Yamamoto, T. Kobayashi and M. Nitta, *Heterocycles*, 1998, **48**, 1903–1915.

51 J. M. Alvarez-Gutirrez and F. López-Ortiz, *Tetrahedron Lett.*, 1996, **37**, 2841–2844.

52 N. Avarvari, P. Le Floch and F. Mathey, *J. Am. Chem. Soc.*, 1996, **118**, 11978–11979.

53 G. Märkl, S. Dietl, M. L. Ziegler and B. Nuber, *Angew. Chem. Int. Ed. Engl.*, 1988, **27**, 389–391.

54 N. Avarvari, P. Le Floch, L. Ricard and F. Mathey, *Organometallics*, 1997, **16**, 4089–4098.

55 U. Rhörig, N. Mézailles, N. Maigrot, L. Ricard, F. Mathey and P. Le Floch, *Eur. J. Inorg. Chem.*, **2000**, 2565–2571.

56 D. Zhao, C. Nimphius, M. Lindale and F. Glorius, *Org. Lett.*, 2013, **15**, 4504–4507.

57 S. Park, B. Seo, S. Shin, J.-Y. Son and P. H. Lee, *Chem. Commun.*, 2013, **49**, 8671–8673.

58 Y. Sun and N. Cramer, *Angew. Chem. Int. Ed.*, 2017, **56**, 364–367.

59 Q. Yao, J. Chen, H. Song, F. Huang and B. Shi, *Angew. Chem. Int. Ed.*, 2022, **61**, e202202892.

60 V. G. Zaitsev, D. Shabashov and O. Daugulis, *J. Am. Chem. Soc.*, 2005, **127**, 13154–13155.

61 L. Zeng, S. Tang, D. Wang, Y. Deng, J.-L. Chen, J.-F. Lee and A. Lei, *Org. Lett.*, 2017, **19**, 2170–2173.

62 R. Huang, M. Wang, H. Deng, J. Xu, H. Yan, Y. Zhao and Z. Shi, *Sci. Adv.*, 2023, **9**, eade8638.

63 G. C. Morrison, R. O. Waite and J. Shavel, *J. Heterocycl. Chem.*, 1966, **3**, 540–540.

64 S. Kh. Nurtdinov, I. V. Tsivunina, V. I. Savran, N. M. Ismagilova, T. V. Zykova and V. S. Tsivunin, *Zh. Obshch. Khim.*, 1981, **51**, 1549.

65 W. H.-L. Wai Tan, C. Bourdieu and A. Foucaud, *Tetrahedron*, 1990, **46**, 6715–6730.

66 C. Bourdieu and A. Foucaud, *Tetrahedron Lett.*, 1987, **28**, 4673–4674.

67 J. Barluenga, F. Lopez and F. Palacios, *Tetrahedron Lett.*, 1987, **28**, 4327–4328.

68 C. Bedel and A. Foucaud, *Tetrahedron Lett.*, 1991, **32**, 2619–2620.

69 E. Fluck, F. Rosche, G. Heckmann and F. Weller, *Heteroat. Chem.*, 1995, **6**, 355–363.

70 W. Tang, Y. Ding and Y.-X. Ding, *Tetrahedron*, 2008, **64**, 10507-10511.

71 J.-H. Yan, Q.-Y. Li, J. Boutin, M. P. Renard, Y.-X. Ding, X.-J. Hao, W.-M. Zhao and M.-W. Wang, *Acta. Pharmacol. Sin.*, 2008, **6**, 752–758.

72 Z.-Q. Lin, W.-Z. Wang, S.-B. Yan and W.-L. Duan, *Angew. Chem. Int. Ed.*, 2015, **54**, 6265–6269.

73 L. Liu, A.-A. Zhang, Y. Wang, F. Zhang, Z. Zuo, W.-X. Zhao, C.-L. Feng and W. Ma, *Org. Lett.*, 2015, **17**, 2046–2049.

74 Y.-N. Ma, X. Zhang and S. Yang, *Chem. – Eur. J.*, 2017, **23**, 3007–3011.

75 Y.-H. Chen, X.-L. Qin and F.-S. Han, *Chem. Commun.*, 2017, **53**, 5826–5829.

76 C. L. Vonnegut, A. M. Shonkwiler, M. M. Khalifa, L. N. Zakharov, D. W. Johnson and M. M. Haley, *Angew. Chem. Int. Ed.*, 2015, **54**, 13318–13322.

77 J. P. Bard, H. J. Bates, C.-L. Deng, L. N. Zakharov, D. W. Johnson and M. M. Haley, *J. Org. Chem.*, 2020, **85**, 85–91.

78 J. P. Bard, J. L. Mancuso, C.-L. Deng, L. N. Zakharov, D. W. Johnson and M. M. Haley, *Supramol. Chem.*, 2020, **32**, 49–55.

79 C.-L. Deng, J. P. Bard, L. N. Zakharov, D. W. Johnson and M. M. Haley, *Org. Lett.*, 2019, **21**, 6427–6431.

80 C.-L. Deng, J. P. Bard, L. N. Zakharov, D. W. Johnson and M. M. Haley, *J. Org. Chem.*, 2019, **84**, 8131–8139.

81 N. A. Takaesu, E. Ohta, L. N. Zakharov, D. W. Johnson and M. M. Haley, *Organometallics*, 2017, **36**, 2491–2493.

82 C.-L. Deng, J. P. Bard, J. A. Lohrman, J. E. Barker, L. N. Zakharov, D. W. Johnson and M. M. Haley, *Angew. Chem. Int. Ed.*, 2019, **58**, 3934–3938.

83 J. P. Bard, C.-L. Deng, H. C. Richardson, J. M. Odulio, J. E. Barker, L. N. Zakharov, P. H.-Y. Cheong, D. W. Johnson and M. M. Haley, *Org. Chem. Front.*, 2019, **6**, 1257–1265.

84 J. P. Bard, J. N. McNeill, G. I. Warren, L. N. Zakharov, D. W. Johnson and M. M. Haley, *Isr. J. Chem.*, 2021, **61**, 217–221.

85 J. N. McNeill, L. J. Karas, J. P. Bard, K. Fabrizio, L. N. Zakharov, S. N. MacMillan, C. K. Brozek, J. I. Wu, D. W. Johnson and M. M. Haley, *Chem. – Eur. J.*, 2022, **28**, e202200472.

86 J. N. McNeill, M. A. Kascoutas, L. J. Karas, L. N. Zakharov, J. I. Wu, D. W. Johnson and M. M. Haley, *Chem. – Eur. J.*, 2023, **29**, e202203918.

87 T. J. Grahame and R. B. Schlesinger, *Inhalation Toxicol.*, 2005, **17**, 15–27.

88 H. A. Fargher, N. Lau, L. N. Zakharov, M. M. Haley, D. W. Johnson and M. D. Pluth, *Chem. Sci.*, 2019, **10**, 67–72.

89 B. W. Tresca, A. C. Brueckner, M. M. Haley, P. H.-Y. Cheong and D. W. Johnson, *J. Am. Chem. Soc.*, 2017, **139**, 3962–3965.

90 M. D. Hartle, R. J. Hansen, B. W. Tresca, S. S. Prakel, L. N. Zakharov, M. M. Haley, M. D. Pluth and D. W. Johnson, *Angew. Chem. Int. Ed.*, 2016, **55**, 11480–11484.

91 B. W. Tresca, R. J. Hansen, C. V. Chau, B. P. Hay, L. N. Zakharov, M. M. Haley and D. W. Johnson, *J. Am. Chem. Soc.*, 2015, **137**, 14959–14967.

92 J. P. Bard, S. G. Bolton, H. J. Howard, J. N. McNeill, T. P. de Faria, L. N. Zakharov, D. W. Johnson, M. D. Pluth and M. M. Haley, *J. Org. Chem*., 2023, DOI: 10.1021/acs.joc.3c01927.

93 G. Signore, R. Nifosì, L. Albertazzi, B. Storti and R. Bizzarri, *J. Am. Chem. Soc.*, 2010, **132**, 1276–1288.

94 G. Niu, W. Liu, B. Zhou, H. Xiao, H. Zhang, J. Wu, J. Ge and P. Wang, *J. Org. Chem.*, 2016, **81**, 7393–7399.

95 D. Aristova, R. Selin, H. S. Heil, V. Kosach, Y. Slominsky, S. Yarmoluk, V. Pekhnyo, V. Kovalska, R. Henriques, A. Mokhir and S. Chernii, *ACS Omega*, 2022, **7**, 47734–47746.

96 Z. Li, J. Zou, and X. Chen, *Adv. Mater.*, 2022, **35**, 2209529.

97 J. Park, S. J. Kim, H. Kwon, E. Jin, K. Yoon, H. Kim, S. Shadman, W. Choe, J. Kim and Y. S. Park, *Chem. Commun.*, 2021, **57**, 12147–12150.

98 H. Deng, M. Wang, Y. Liang, X. Chen, T. Wang, J. J. Wong, Y. Zhao, K. N. Houk and Z. Shi, *Chem*, 2022, **8**, 569–579.

99 G. Märkl and P. Kreitmeier, in *Phosphorus-Carbon Heterocyclic Chemistry*, ed François Mathey, Elsevier Science, Amsterdam, 1st edn, 2001, Ch. 5.3, pp 535-630.

100 G. Märkl and G. Dorfmeister, *Tetrahedron Lett.*, 1987, **28**, 1093–1096.

101 G. Märki and S. Pflaum, *Tetrahedron Lett.*, 1986, **27**, 4415–4418.

102 G. Märkl and G. Dorfmeister, *Tetrahedron Lett.*, 1986, **27**, 4419–4422.

103 R. Appel, M. Groβe-bley, H. Souady and W. Steglich, *Phosphorus Sulfur Relat. Elem.*, 1987, **30**, 757–757.

104 U. J. Vogelbacher, M. Ledermann, T. Schach, G. Michels, U. Hees and M. Regitz, *Angew. Chem. Int. Ed. Engl.*, 1988, **27**, 272–274.

105 M. Regitz, O. J. Scherer and R. Appel, *Multiple bonds and low coordination in phosphorus chemistry*, G. Thieme Verlag; Thieme Medical Publishers, Stuttgart, New York, 1990.

106 I. Gutman and J. H. Potgieter, *J. Chem. Educ.*, 1994, **71**, 222–224.

107 R. Appel and M. Poppe, *Angew. Chem. Int. Ed. Engl.*, 1989, **28**, 53–54.

108 G. Märkl and C. Dörges, *Angew. Chem. Int. Ed. Engl.*, 1991, **30**, 106–107.

109 G. Märkl, C. Dörges, T. Riedl, F.-G. Klärner and C. Lodwig, *Tetrahedron Lett.*, 1990, **31**, 4589.

110 G. Märkl and S. Dorsch, *Tetrahedron Lett.*, 1995, **36**, 3839–3842.

111 V. A. Galishev, V. N. Sakharov, T. S. Dolgushina, L. Tamm and A. A. Petrov, *Zh. Obshc. Khim.*, 1986, **56**, 1661–1663.

112 G. Märkl, Ch. Dörges, H. Nöth and K. Polborn, *Tetrahedron Lett.*, 1990, **31**, 6999–7002.

113 G. Frison, A. Sevin, N. Avarvari, F. Mathey and P. Le Floch, *J. Org. Chem.*, 1999, **64**, 5524–5529.

114 K. Karaghiosoff, H. Klehr and A. Schmidpeter, *Chem. Ber.*, 1986, **119**, 410–419.

115 M. M. Hansmann, *Chem. – Eur. J.*, 2018, **24**, 11573–11577.

116 H. Huang, Z. Wei, J. Hou, R. Wang, G. Tao, M. Wang, Z. Duan and F. Mathey, *Eur. J. Org. Chem.*, **2018**, 2863–2869.

117 M. Habib Mebazaa and M. Simalty, *Tetrahedron Lett.*, 1972, **13**, 4363–4366.

118 M. Simalty and H. Chahine, *Bull. Soc. Chim.*, 1968, **12**, 4938–4943.

119 L. D. Quin, C. C. Henderson, N. S. Rao and J. C. Kisalus, *Synthesis*, 1984, **1984**, 1074–1075.

120 L. D. Quin and J. C. Kisalus, *Phosphorus Sulfur Relat. Elem.*, 1985, **22**, 35–39.

121 L. D. Quin and B. G. Marsi, *Heteroat. Chem.*, 1990, **1**, 93–107.

122 J. Barluenga, F. Lopez and F. Palacios, *J. Chem Soc., Chem. Commun.*, 1985, 1681–1682.

123 J. Barluenga, F. Palacios, F. J. González and S. Fustero, *J. Chem. Soc., Chem. Commun.*, 1988, 1596–1597.

124 J. Barluenga, F. López and F. Palacios, *J. Organomet. Chem.*, 1990, **382**, 61–67.

125 J. Barluenga, F. López and F. Palacios, *J. Chem. Soc. Chem. Commun.*, 1986, 1574–1575.

126 M. Alajarin, C. Lopez-Leonardo, R. Raja and R.-A. Orenes, *Org. Lett.*, 2011, **13**, 5668–5671.

127 U. Heim, H. Pritzkow, U. Fleischer, H. Grützmacher, M. Sanchez, R. Réau and G. Bertrand, *Chem. – Eur. J.*, 1996, **2**, 68–74.

128 X. Liu, T. K. W. Ong, S. Selvaratnam, J. J. Vittal, A. J. P. White, D. J. Williams and P.-H. Leung, *J. Organomet. Chem.*, 2002, **643–644**, 4–11.

129 L. Zhang, W. Yu, C. Liu, Y. Xu, Z. Duan and F. Mathey, *Organometallics*, 2015, **34**, 5697–5702.

130 Z. Chen, C. S. Wannere, C. Corminboeuf, R. Puchta and P. v. R. Schleyer, *Chem. Rev.*, 2005, **105**, 3842–3888.

131 E. Elguero, I. Alkorta and J. Elguero, *Heteroatom. Chem.*, 2018, **29**, e21441.